

https://dspace.org/

The occurrence of the pegmatites of the Mbeta area, Lower Gwanda greenstone belt in Matabeleland South Province, Zimbabwe

Musinga, Rutendo A

2021

https://hdl.handle.net/10539/33143

Downloaded from a DSpace repository. https://dspace.org/

The occurrence of the pegmatites of the Mbeta area, Lower Gwanda greenstone belt in Matabeleland South Province, Zimbabwe

By

RUTENDO A MUSINGA

1833726

A Research Report submitted in partial fulfilment of the requirements for the degree

MSc: Economic Geology

Department of Geosciences

Faculty of Science

Supervisor: Prof Judith Kinnaird

Prof Paul NEX

School of Geosciences

University of Witwatersrand

October 2021

DECLARATION

I, Rutendo Amanda Musinga, student number 1833726, do hereby declare this research is my original work and that to my best knowledge and belief, it has not been previously in its entirely or in part been submitted and is not currently being submitted either in whole or in part at any university for a degree or diploma, and that all references are acknowledged. It is being submitted for the Degree of Master in Science by Coursework and Research Report to the University of the Witwatersrand, Johannesburg, South Africa.

SIGNED on this ____**5th** _____ day of _____**October**_____ **2021**



_____

Rutendo A Musinga

ABSTRACT

The study aimed to use geological and geochemical approaches to understand the occurrence of pegmatites in the Mbeta area. Several methodologies including field mapping, laboratory work (thin section microscope studies, modal mineralogy composition analysis), X-RAY Fluorescence (XRF) and X-RAY Diffraction (XRD) analysis were used to carry out the study.

The pegmatites are hosted in the Archaean Lower Gwanda greenstone belt which consists of metamorphosed and deformed mafic volcanics with lenses of intrusive serpentinite, near its regional contact with basement granites and gneisses. The mapping of the area showed that the greenstones are well exposed, consisting of finely textured epidiorites and amphibolites. Exposures of contacts in surface workings show the greenstone are fractured and schistose with a regional strike of $N80^0E$ and dip towards the south at around 45^0.

A swarm of approximately parallel coarsely-crystalline pegmatite veins and dykes occur in the area. They are hosted in a zone of apparent shearing measuring more than 400m in width and traceable along strike for a distance of at least 1.8km. The main pegmatite, which has been extensively trenched, dips either steeply towards the southeast or near vertical and strikes $N70^0E$.

The petrographic studies show that the Mbeta pegmatites are dominated by quartz, albite-plagioclase, muscovite and minor rutile, topaz, lepidolite and garnets.

Modal mineralogy studies indicate the main framework grains are subhedral crystals of quartz and albite-plagioclase comprising ~70-90%, muscovite mica constitutes 5-20% while lepidolite forms 1-5% of the samples and accessory minerals such as rutile and topaz constituted less than 4%. The apparent lack of K-Feldspar as indicated by modal and quantitative XRD analyses is confirmed by the very low K_2O contents (<1%, corrected for the presence of micas) in most samples. Consequently the Mbeta albite pegmatites cannot be crystallised conventional granitic melts and have been explained as formed by secondary replacement by sodic fluids or preferential release of K in a separate fluid phase at a very late stage of pegmatite consolidation. Albitisation is a common feature in rare element enriched pegmatites, with Bikita being a prime example.

It is concluded that while the pegmatites of the Mbeta area only constitute a minor lepidolite resource its economic significance is still yet to be fully ascertained. The albite rich nature of the Mbeta pegmatites resemble those hosting the main Li ore deposits at Bikita and thus suggest some similarities.



ACKNOWLEDGEMENTS

"For I know the plans that I have for you, plans not to harm you, plans to prosper you, plans to give you a hope and a future," says the Lord in Jeremiah 29 v11.

I would like to thank the Almighty God for bringing me this far. My special thanks to my project supervisors Professor Judith Kinnaird and Professor Paul NEX (University of the Witwatersrand) for their guidance in carrying out this project. The countless hours you spent going through my work and corrections and your availability is very much appreciated.

I would like to extend my profound gratitude to all the staff at Ministry of Mines and Mining Development, Department of Geological Survey and Midlands State University Colleagues who chipped in with vital information, advice and assistance.

My heartfelt appreciations to my family especially my children Kyle and Kevin for the understanding, encouragement and support throughout the duration of my degree and carrying out this project. I could not do it alone without my love, my late husband Alfred, MHSRIP, who assisted me in GIS work and gave me strength and support.

Contents

ABSTRACT ii
ACKNOWLEDGEMENTS iii
CHAPTER 1 1
INTRODUCTION 1
1.1 Background Information 1
1.2 Location 2
1.3 Regional Geology 3
1.4 Local Geology 3
1.5 Project Justification 5
1.6 Problem Statement 6
1.7 Aims and Objectives 6
1.8 Methodology 6
CHAPTER 2 8
LITERATURE REVIEW 8
2.1 Definition of Pegmatites 8
2.2 Origin 8
2.3 Classification of Pegmatites 9
2.4 Types of Pegmatites 13
2.5 Age Distribution 16
2.6 Mineralogy of Pegmatites 17
2.7 Genetic Model 18
2.8 Pegmatite Exploration 19
2.9 Case Studies 19
2.10 Conclusions from the review 22
CHAPTER 3 23
METHODOLOGY 23
3.1 Introduction 23
3.2 Field mapping 26
3.3 Sample preparation and XRD analysis 26
3.4 X-Ray Fluorescence (XRF) analysis 27

3.5 Petrographic analysis 27
3.6 Modal mineral composition analysis (point counting) 27
CHAPTER 4 29
FIELD MAPPING 29
4.1 Introduction 29
4.2 Geology 29
CHAPTER 5 36
PETROGRAPHY 36
5.1 Introduction 36
5.2 Modal Composition Analysis 36
5.3 Petrographic descriptions 38
Quartz 39
Albite 40
Muscovite 41
Lepidolite 42
Garnet 42
Topaz 43
Rutile 43
5.4 Mineralogy using X-Ray Diffraction (XRD) analysis 44
5.5 X-RAY Fluorescence (XRF) analysis 45
CHAPTER 6 48
DISCUSSION 48
6.1 Introduction 48
6.2 Mineralogy 49
6.2.1 Significance of Albite 49
6.3 Economic Aspect 51
CHAPTER 7 54
CONCLUSIONS AND RECOMMENDATIONS 54
REFERENCES 55
APPENDIX A 59
APPENDIX B 65
APPENDIX C 71

WITS
UNIVERSITY

List of Figures

Figure 1. 1: *Map showing the pegmatite deposits in Zimbabwe. (Zimbabwe Geological Survey, Mukandi, M.A., 2009)* _____ *1*
Figure 1. 2: *Mbeta Project Location Map. (Adapted from Google Map).* _____ *3*
Figure 1. 3: *Mbeta photo showing boundary permits, geological contacts and the location of the historical lithium pegmatite workings and associated photo lineament. (Adapted from the ASX Announcement Report. Burns, 2018)* _____ *4*
Figure 1. 4: *Photographs showing the exposed pegmatites at Mbeta. (A) Moderately dipping pegmatite exposed in the floor of a historical pit. (B) Stockpiled lepidolite-bearing pegmatite. (Adapted from the ASX Announcement Report. Burns, 2018)* _____ *5*

Figure 2. 1: *Image showing the graphic texture of pegmatites (Harraz and Aly, 2004).* _____ *8*
Figure 2. 2: *Zoning structure in pegmatites (Steiner, 2019).* _____ *15*
Figure 2. 3: *Regional zoning in fertile granites and pegmatites (from Cerny, 1991b): (a) regional zoning of a fertile granite (outwardly fractionated) with an aureole of exterior lithium pegmatites; (b) schematic representation of regional zoning in a cogenetic parent granite + pegmatite group. Pegmatites increase in degree of evolution with increasing distance from the parent granite.* _____ *16*

Figure 3. 1: *Mbeta Base map showing the Mbeta pits, dump and the greenstone granite contact.* _____ *24*
Figure 3. 2: *Image of MB02A showing point counting of minerals (Qz) quartz, (Plag) plagioclase/ albite, (Mus) muscovite and (Gnt) garnets.* _____ *28*

Figure 4. 1: *Google Earth extract showing the exact localities where samples were collected at Mbeta.* _____ *29*
Figure 4. 2: *Image showing the greenstone walls and the massive feldspar outcrops within pegmatite from the Main Pit at Mbeta.* _____ *30*
Figure 4. 3: *Image showing the massive lepidolite exposure in the main pit. (GPS location: 35K 682449E 7644906N).* _____ *31*
Figure 4. 4: *Geological map of the Main Pit showing the lepidolite bearing pegmatite intruding into the greenstone.* _____ *32*
Figure 4. 5: *Image of sample showing the topaz with bluish quartz from the western pit but it gives a true representation of how the topaz occurs in the Mbeta pits. Sample number MB03. (GPS Location: 35K 679529 E 7644 816N).* _____ *33*
Figure 4. 6: *Sharp contact of quartz to the greenstones at the Western pit at Mbeta. (GPS location: 35K 679463E 7644826N).* _____ *34*
Figure 4. 7: *Image showing the core of feldspar with minor quartz and lepidolite sharp contact with the greenstone. (GPS location: 35K 679463E 7644826N).* _____ *35*

Figure 5. 1: *The graphical representative of the modal composition analysis of the Mbeta samples.* _____ *38*
Figure 5. 2: *Image showing the scanned thin sections of MB08 (western pit). (A) Is a plane polarised light showing quartz grains. (B) Is in cross polarised light showing the even granular texture of the grains.* _____ *39*
Figure 5. 3: *Image showing the scanned thin section image that is rich in plagioclase, muscovite and quartz in thin section in MB01 (western pit). (A) Plane- polarised light (B) Cross- polarised light.* _____ *40*

Figure 5. 4: *Image of MB02A (collected from the western pit) showing albite exhibiting a wide range in grain size, shape, as well as skeletal and graphic intergrowths. (A) Plane polarised light (B) Cross- polarised light. Garnet also occurs in this sample and a grain showing isotropism is labelled.* _____ *41*
Figure 5. 5: *Image showing scanned thin sections that include muscovite in MB04. (A) Plane polarised light. Note that muscovite is restricted to a massive lens at the top of the photo. (B) Cross- polarised light.* _____ *42*
Figure 5. 6: *Image showing scanned thin sections with large crystals of topaz in MB06 (main pit) in XPL.* ____ *43*
Figure 5. 7: *Consolidated XRD scans of the Mbeta samples together with reference diffractogram of the principal minerals.*_____ *46*

Figure 6. 1: *Modified Mbeta photo showing boundary of mineral licences in which the samples were collected from, geological contacts and the location of the historical lithium pegmatite workings and associated photo lineament. (Adapted from the ASX Announcement Report. Burns, 2018)* _____ *48*
Figure 6. 2: *Sample (MB07) from the main pit showing greenish tinted muscovite and K-feldspar. (GPS location: 35K 682438E 7644906N)*_____ *49*
Figure 6. 3: *Manipulation of the modal, XRD and XRF tables, together with data from the Bikita literature. The data as a ternary plot showing the Ab rich nature of Mbeta compared with published data from Bikita and other sites in Zimbabwe.*_____ *50*

Figure A. 1: *Image (MB01) showing oxidised outcrop from Western Pit. (GPS Location: 35K 679502E 7644801)* _____ *59*
Figure A. 2: *Image (MB02) showing fresh sample of pegmatite from the Western pit (GPS Location: 35K 679463E 7644826N)* _____ *59*
Figure A. 3: *Image (MB03) showing lepidolite from the Western pit. The lepidolite sample exhibits greenish micas. (GPS Location: 35K 679529 E 7644 816N).* _____ *60*
Figure A. 4: *Image (MB04) showing the contact of the pegmatite zone and the greenschist zone in the western pit. (GPS Location: 35K 679595E 7644924N).*_____ *60*
Figure A. 5: *Image (MB05) showing the lepidolite sample from the northern pit. (GPS Location: 35K 683167E 7645983N).* _____ *61*
Figure A. 6: *Image (MB06) showing a lepidolite sample from the main pit. (GPS Location: 35K 682449E 7644906N).* _____ *61*
Figure A. 7: *Image (MB07) showing a pegmatite sample with greenish micas from the main pit. (GPS Location: 35K 682438E 7644906N).* _____ *62*
Figure A. 8: *Image (MB08) showing the quartz core from the northern pit. (GPS Location: 35K 679562E 7644921N).* _____ *62*
Figure A. 9: *Image (MB09) showing the lepidolite quartz contact from the western pit (GPS Location: 35K 679567E 7644921N).*_____ *63*
Figure A. 10: *Image (MB10) showing the green schist host rock form the western pit. (GPS Location: 35K 679595E 7644924N)* _____ *63*
Figure A. 11: *Image (MB11) showing sands from the dump north of the northern pits.*_____ *64*

Figure B. 1: *Sample number MB01.* _____ *65*
Figure B. 2: *Sample number MB02A and MB02B* _____ *65*
Figure B. 3: *Sample number MB03.* _____ *66*
Figure B. 4: *Sample number MB04.* _____ *66*

Figure B. 5: *Sample number MB05A and MB05B.* 67
Figure B. 6: *Sample number MB06.* 67
Figure B. 7: *Sample number MB07.* 68
Figure B. 8: *Sample number MB08.* 68
Figure B. 9: *Sample number MB09.* 69
Figure B. 10: *Sample number MB10.* 70

Figure C. 1: *MB01 scanned image of the thin section in (PPL) plane polarised light to the left and (XPL) cross polarised light to the right.* 71
Figure C. 2: *MB02A scanned image of the thin section in (PPL) plane polarised light to the left and (XPL) cross polarised light to the right.* 72
Figure C. 3: *MB02B scanned image of the thin section in (PPL) plane polarised light to the left and (XPL) cross polarised light to the right.* 73
Figure C. 4: *MB03 scanned image of the thin section in (PPL) plane polarised light to the left and (XPL) cross polarised light to the right.* 74
Figure C. 5: *MB04 scanned image of the thin section in (PPL) plane polarised light to the left and (XPL) cross polarised light to the right.* 75
Figure C. 6: *MB05A scanned image of the thin section in (PPL) plane polarised light to the left and (XPL) cross polarised light to the right.* 76
Figure C. 7: *MB05B scanned image of the thin section in (PPL) plane polarised light to the left and (XPL) cross polarised light to the right.* 77
Figure C. 8: *MB06 scanned image of the thin section in (PPL) plane polarised light to the left and (XPL) cross polarised light to the right.* 78
Figure C. 9: *MB07 scanned image of the thin section in (PPL) plane polarised light to the left and (XPL) cross polarised light to the right.* 79
Figure C. 10: *MB08 scanned image of the thin section in (PPL) plane polarised light to the left and (XPL) cross polarised light to the right.* 80
Figure C. 11: *MB09 scanned image of the thin section in (PPL) plane polarised light to the left and (XPL) cross polarised light to the right.* 81

List of Tables

Table 2. 1: *Four main categories of pegmatite classification were identified that were based on the depth of formation. (Cerny, 1991a)* 11
Table 2. 2: *The four classes of granitic pegmatites showing environment of formation, metamorphic facies, relationship to parent granites and their likely economic minerals. (Cerny, 1991a, 1991b).* 12
Table 2. 3: *Relationship between the Cerny's (1991a) pegmatite classes, families, types and subtypes related to LCT and NYF families.* 13
Table 2. 4: *Table showing the mineral compositions of typical pegmatite zones (Simmons, 2007).* 15
Table 2. 5: *Economic rare minerals of pegmatites (London, 2008).* 17

Table 3. 1: *Table showing the rock samples collected from the main, western and northern pits at Mbeta.* 25

Table 5. 1: *Point counting was undertaken on 11 samples and this table shows the actual grains of minerals counted.* 36
Table 5. 2: *Table showing modal composition expressed as a percentage from the results of point counting.* 37
Table 5. 3: *Percentage mineralogical abundances (%) of the Mbeta Pegmatites by XRD.* 45
Table 5. 4: *Table showing the major element (wt. % oxides) analysis of the Mbeta pegmatites.* 47

Table 6. 1: *Table showing analyses and assays by Jan de Poorter (Goldberg, 1963).* 52
Table 6. 2: *Table showing analysis by Booth, Garnett and Blair (Goldberg, 1963).* 52
Table 6. 3: *Table showing analysis by Messrs, Poote Minerals, Philadelphia, on a sample of 115.5 tonnes* 52
Table 6. 4*: Table showing analysis by Messrs, Poote Minerals, Philadelphia on three samples.* 52
Table 6. 5: *Table showing analysis by Messrs, Poote Minerals, Philadelphia on a sample of 115.5 tonnes.* 52
Table 6. 6: *Analyses by Daniel Griffiths, London, Bennedict Kitto and Sons (Goldberg, 1963).* 53
Table 6. 7: *Results of the chemical analyses on bulk samples at Mbeta in May 1995. (Dube, 1995).* 53

WITS UNIVERSITY

CHAPTER 1

INTRODUCTION

1.1 Background Information

The major lithium-bearing pegmatites in Zimbabwe are found at Bikita in the Masvingo Province. Some pegmatite bodies in Zimbabwe also occur at Hwange, Goromonzi, Fort Rixon, Chegutu, Harare, Mt Darwin, Odzi, Mudzi and Gwanda as shown in Figures 1.1 and 1.2.

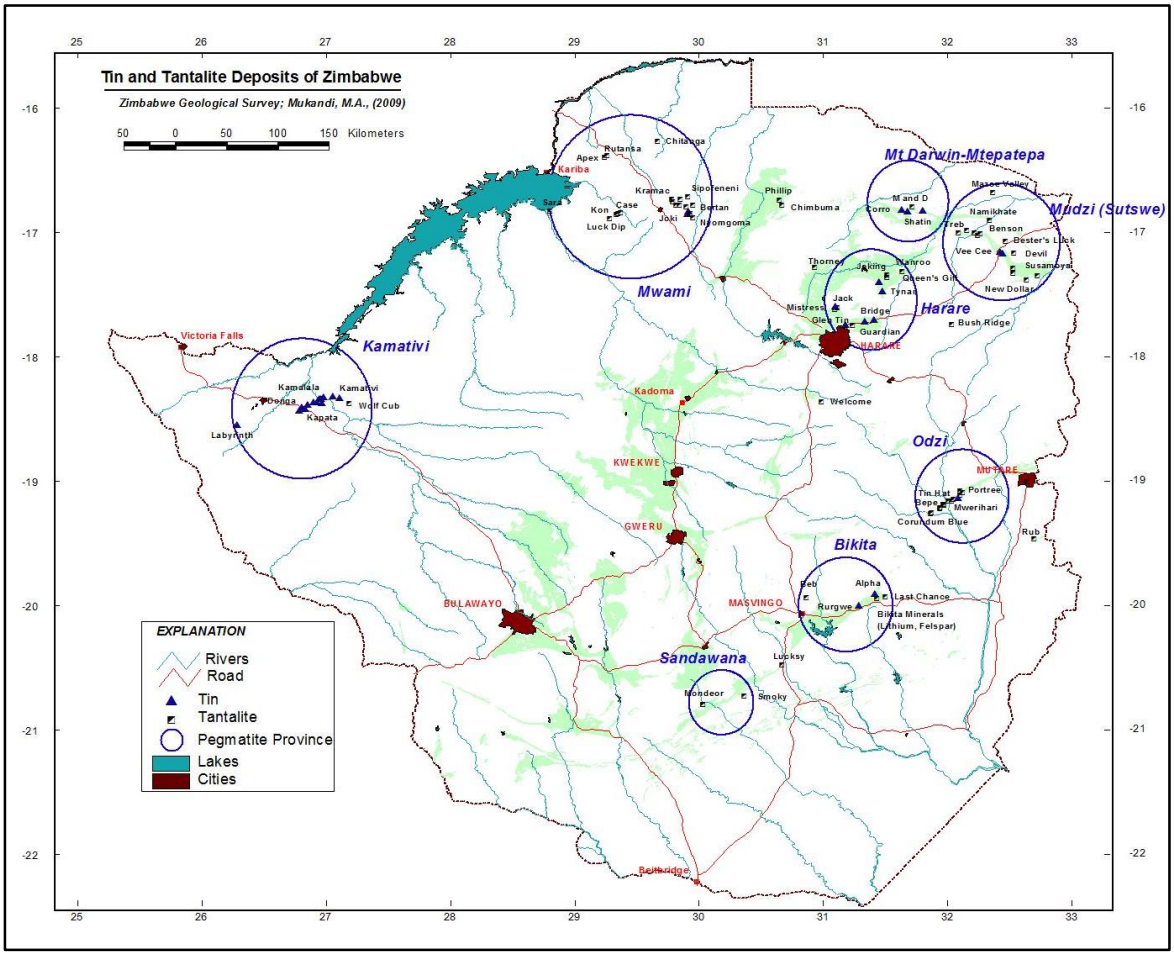


Figure 1. 1: Map showing the pegmatite deposits in Zimbabwe. (Zimbabwe Geological Survey, Mukandi, M.A., 2009)

The main lithium minerals mined from these pegmatites are petalite, lepidolite, spodumene, eucryptite, and amblygonite (Sitando, 2012). All of these five minerals are found at Bikita (Sitando, 2012). All the areas mentioned above are of Archaean age (Robb, 2005) except for the Proterozoic

pegmatites in the Zambezi metamorphic belts around the Kamativi area in the northwest of Zimbabwe.

Robb (2005) describes pegmatites as very coarse-grained granitic rocks formed by extreme fractionation of the magma during crystallisation. They can also be formed as a result of small degrees of partial melting to form dykes and segregations in high grade metamorphic terrains (Robb, 2005). Pegmatites may be zoned usually with a quartz-rich core. They show variable textures, large grain sizes and are highly fractionated. Large crystals of quartz, muscovite and feldspar make up the bulk of the rocks and these can be used for industrial purposes. Beryl, tourmaline and topaz are semi-precious stones which may also occur in minor amounts.

Concentrations of elements such as B, Be, Cs, Ce, Li, Nb, Sn, Ta, Tho, U, W, Zr may be found in pegmatites (Robb, 2005). There are two groups or families of pegmatites that are recognised:

I. Nb-Y-F (NYF) group which is associated with sub-alkaline to metaluminous (mostly I-type) granites and
II. Li-Cs-Ta (LCT) group which is associated with the peraluminous (largely S-type) granites (Cerny, 1991a).

1.2 Location

The Mbeta pegmatites are located approximately 50km in a direct line southwest of Gwanda (Figure 1.2) in the Matabeleland South province. Access by road however is less direct (90km) when driving from the town of Gwanda, first for 10km along the road to Beitbridge, then right onto the Ntepe road for 42km and finally right onto a gravel road to Mbeta for another 30km.

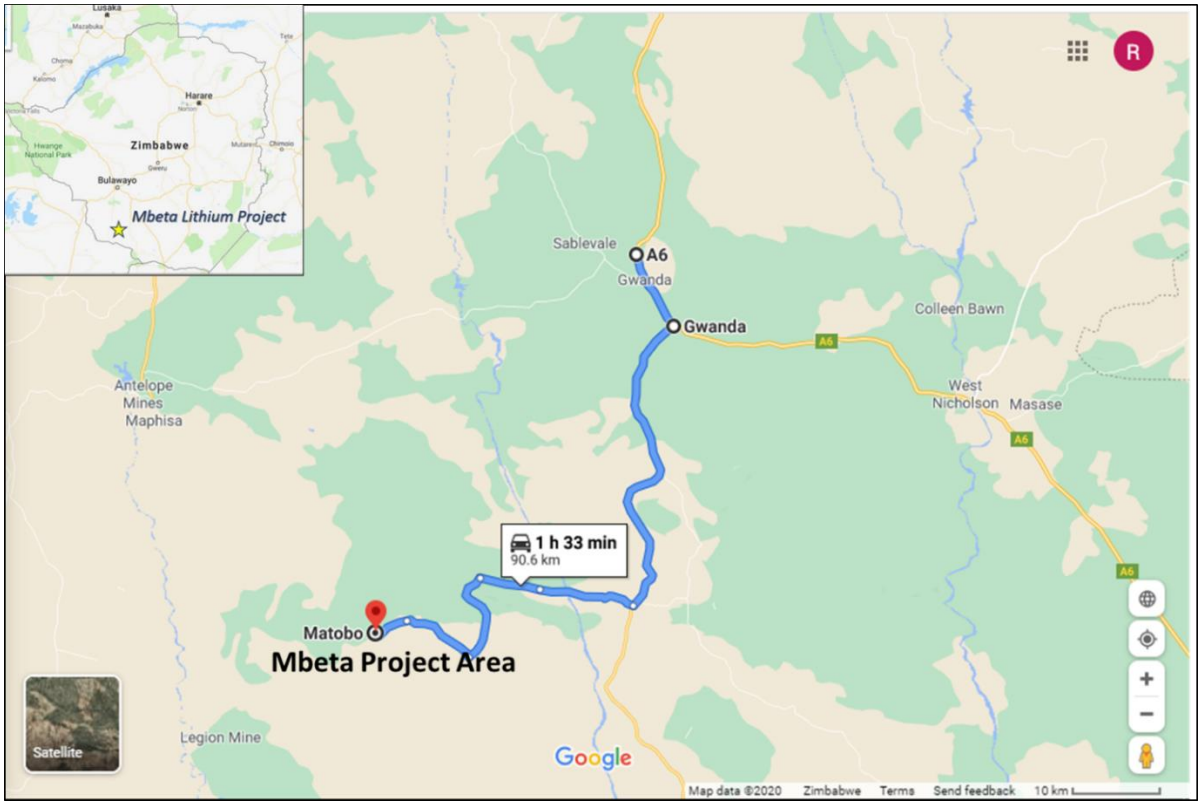


Figure 1. 2: Mbeta Project Location Map. (Adapted from Google Map).

1.3 Regional Geology

The Lower Gwanda greenstone belt is one of the smaller and lesser-known belts of the Archean basement outcropping in the Matopo district and Gwanda districts of SW Zimbabwe. Phaup (1983) describes the belt as consisting of schists surrounded by younger granites. In the west of the belt the sequence consists of metamorphosed and folded lavas, banded ironstones and other sediments, while hornblende schists dominate in the east. Sill- like intrusive occur in the west as lenses of serpentinite and actinolite schist and thus are difficult to distinguish from their host rocks. While the granites are interpreted to be younger, they share much of the deformation present in the Gwanda schists, incorporating them into two roof pendants represented by the Antelope and Lower Gwanda gold belts.

1.4 Local Geology

The Mbeta area is in the Lower Gwanda greenstone belt. The only papers that documented the pegmatites in the area show that only lepidolite, then known as lithia mica, was found in this area (Goldberg, 1933). According to Bartholomew (1990, p. 76), “the pegmatites are identified as dykes

cutting within a shear zone across a narrow greenstone belt". These pegmatites are close to the transition zone between the local greenstone belt and the surrounding granites and gneisses (Figure 1.3).

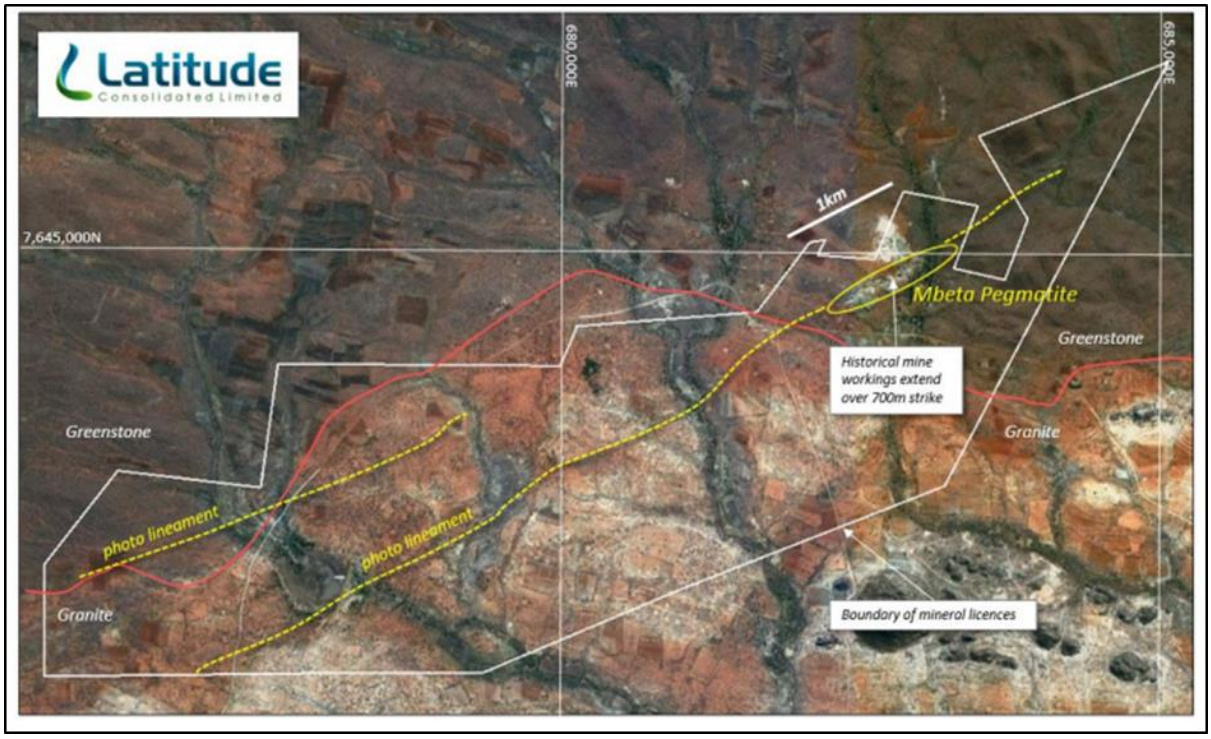


Figure 1. 3: Google image of the Mbeta area showing boundary permits, geological contacts and the location of the historical lithium pegmatite workings and associated photo lineament. (Adapted from the ASX Announcement Report. Burns, 2018)

The greenstones are epidiorites and amphibolites that are fine-textured. Information found from a Zimbabwe Geological Survey report (Reference GS8/ 268/ 63, p. 2) describes these pegmatites as being coarsely crystalline and weakly zoned. They dip to the northwest about 45^0- 60^0 within the shear zone (Figure 1.4). The pegmatites consist of quartz, lepidolite, sodic-feldspar, and massive topaz. The pegmatite core is composed of massive feldspar with small white quartz inclusions. Feldspar and white quartz on the northwestern side of the core make up the footwall. There is abundant medium- grained lepidolite with irregular quartz inclusions to the southeast of the core.

Historically the pegmatites have been worked and shallow open pits (as shown in Figure 1.4) are found in the area which shows a pegmatite body striking 40^0 northeast with a dip of 60^0 northwest. The pegmatite has a central core of quartz and on the contacts, there is pink and white feldspar, abundant lepidolite, glassy white quartz, and white topaz.

Information from the Geological Survey report (Reference GS8/ 268/ 63) shows that several assay results from lepidolite-bearing ore samples ranged from 2.60% to 6.20% Li_2O with an average of 4.5% Li_2O. In 1958, Barclays Bank Bulawayo detected 70.76% combined pentoxides of tantalum and niobium in a heavy mineral concentrate.

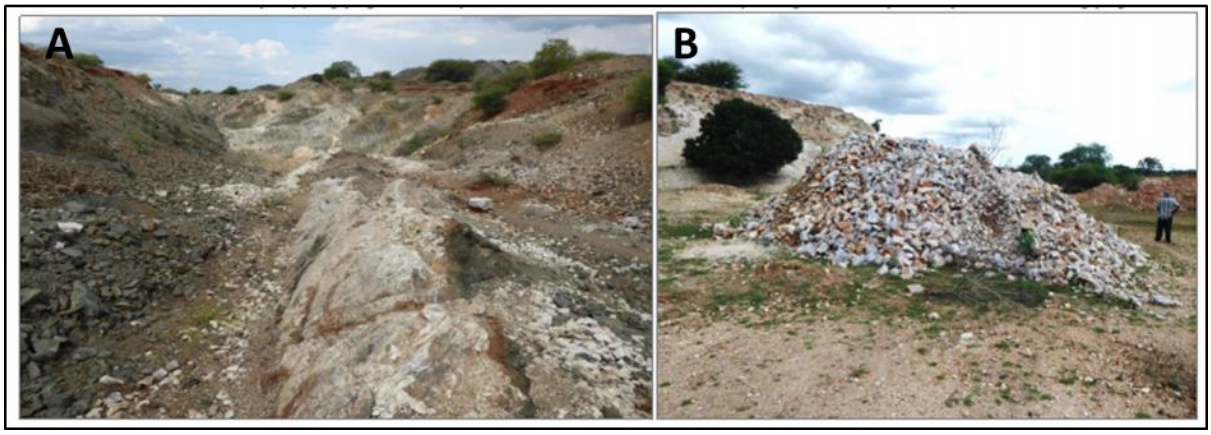


Figure 1. 4: Photographs showing the exposed pegmatites at Mbeta. (A) Moderately dipping pegmatite exposed in the floor of a historical pit. (B) Stockpiled lepidolite-bearing pegmatite. (Adapted from the ASX Announcement Report. Burns, 2018)

1.5 Project Justification

The Zimbabwe Geological Survey has performed limited research or exploration for the last three decades due to a lack of resources and funding by the government. Consequently the deposits at Mbeta are long overdue for further exploration and documentation, thereby realising their potential for lithium, tantalum and associated commodities.

Existing records cite assay results of lepidolite-bearing ores taken from the open pits at Mbeta which are documented in the Geological Survey report (Reference GS8/ 268/ 63) which shows a respectable average of 4-4.5% of Li_2O, attesting to the potential of an economic reserve if further exploration is done. These analyses were carried out in the 1950s and the analytical methods then were not as advanced as they are now. It was also noted that no standards, blanks or duplicates were reported in the evaluation of the samples, therefore there is a need for verification of these results. The sampling technique used in the collection of the samples was also not mentioned in the report. No drilling to delineate the pegmatite body has been carried out.

Therefore, there is a need for thorough geological prospecting to be undertaken in the area to ascertain the potential mineral resource, since there has been a rush for lithium by many miners in this area. Lithium is an important component of lithium-ion batteries which is a major source of power for the electric vehicles. The area seems to be a potential lithium resource because of the lepidolite found in the area, so there is a need for surface mapping and for samples to be taken for both

mineralogy and geochemical analysis to increase the confidence of the deposit to investors interested in the area.

1.6 Problem Statement

In recent years, there has been a much increased demand for lithium due to its uses and technological advances in the developed countries. The Mbeta area has been ignored or forgotten but it has the potential to be one of the producers of lithium and tantalum in Zimbabwe. The area is under-explored so there is a need for a thorough study of the pegmatites that will be able to assist the holders of claims in that area and the government of Zimbabwe.

1.7 Aims and Objectives

The main aim of the study is to use geological and geochemical approaches to understand the occurrence of pegmatites at Mbeta.

The objective is to investigate the geology, petrography and geochemical signature of the pegmatites.

The principal objectives of the investigation are as follows;

- To map the pegmatites and study their zoning and structure.
- To create a geological map of the pegmatites of the Mbeta area.
- To analyse the mineralogy of selected lithologies found in the Mbeta pegmatites.
- To analyse the relationship of the pegmatites with the local geology.

1.8 Methodology

- ***Project stages and data sources***
  The investigation of the pegmatites of the Mbeta area has been carried out using the following stages.

Stage 1: Geological Mapping

This included the geological surface mapping of all the rock units found in the Mbeta area at a scale of 1cm to 3.6m. Mapping provided information about the pegmatite zoning, lithology, texture, mineralogy and degree of alteration. Digital map production made use of ArcGIS 10.2 and Google Maps.



Stage 2: Collecting samples for mineralogy, petrology and XRD analysis

Eleven samples were collected for laboratory analysis and these were collected from the different pegmatite zones that were identified. A systematic investigation was made of major constituent minerals such as microcline, quartz, sodic plagioclase, muscovite and biotite, as well as important accessory minerals such as beryl, spodumene, garnet, magnetite, phosphate minerals, and Nb-Ta oxides.

The information search made use of the following databases and web search engines: Science Direct, Google, Research gate and Academia. A patent search was done using Google Scholar. The keywords used were 'pegmatites', 'pegmatite genesis', 'pegmatite classification', 'lepidolite', 'Mbeta pegmatites' and 'Bikita minerals'.

WITS
UNIVERSITY

CHAPTER 2

LITERATURE REVIEW

2.1 Definition of Pegmatites

Simmons and Webber (2008), Robb (2005) and London (2008) all state that pegmatites are igneous rocks which are coarse-grained and are characterised by granitic rock-forming minerals. Dominant minerals comprise quartz and alkali feldspars that typically occur as large discrete crystals but occasionally show graphic intergrowths (see Figure 2.1) typically enhanced in the rare elements, for example, Li, Ta, Be.

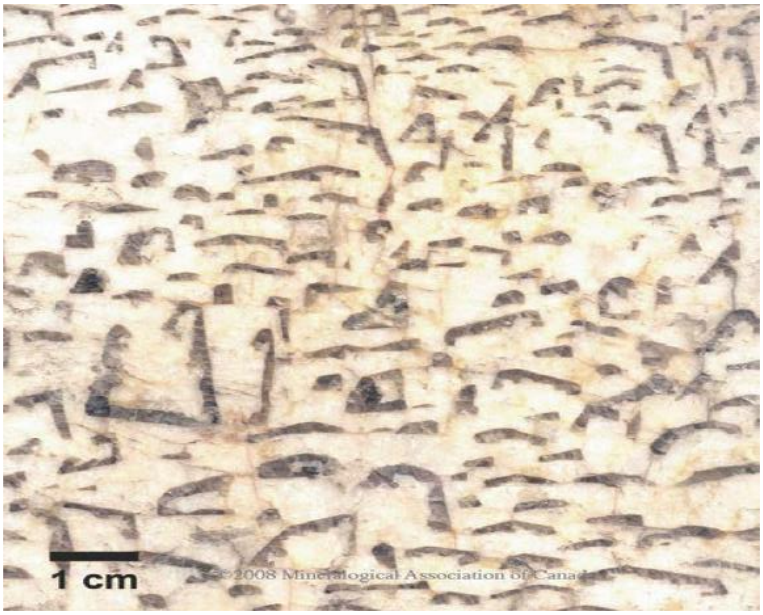


Figure 2. 1: Image showing the graphic texture of pegmatites (Harraz and Aly, 2004).

2.2 Origin

As suggested by Steiner (2019), pegmatite-forming magma can be formed by partial melting of metasedimentary and meta-igneous rocks whereby the felsic melt is isolated from its source by channel flow and deformation-induced migration to higher crustal levels. Crystallisation occurs under extreme hydrous conditions with or without separation of a fluid phase (Dill, 2015). Pegmatites formed by low degrees of partial melting in medium- high grade metamorphic terranes are termed anatectic by these authors but there has been much historical support for a residual origin.

London (2005) agrees with the model developed by Jahns (1955; 1982) and Jahns and Burnham (1969) for the development of pegmatites by the fractionation of large volume granitic magmas, thereby concentrating volatiles and incompatible elements. In the Jahns model, the formation of pegmatites is intimately associated with fluid saturation in the magma. The presence of a discrete fluid phase is regarded as fundamental to pegmatite development and was also used as explanation for the extremely coarse grain size in pegmatites. While modifications to this model (London 2008; London and Morgan 2017) question whether the presence of a hydrous phase is essential to the formation of pegmatitic textures, the Jahns is still widely accepted a milestone contribution to the understanding of pegmatites.

2.3 Classification of Pegmatites

Cerny and Ercit (2005) give credit to Ginsburg and Rodionov (1960), and particularly to Ginsburg et al. (1979) who introduced a modern era of pegmatite classification. They classified the pegmatites based on crustal environment, the depth of the intrusion and the relationship to metamorphism and granitic plutons (refer to Table 2.1). The four geological classes of the classification are the abyssal, muscovite, rare-element and miarolitic types (Cerny and Ercit, 2005). Cerny (1990; 1991a) also added to the classification three petrogenetic groups which were based on additional petrological, paragenetic and geochemical criteria and referred to as the NYF, LCT and mixed.

Cerny and Ercit (2005) later relooked at the REE- bearing pegmatites in which three classes were presented, which include the muscovite- rare element class, and modified the subdivision of the miarolitic pegmatites and their links to the rare- element class.

Simmons and Webber (2007) recommended that depth-zone classification of granitic rocks introduced by Buddington (1959), Ginsburg and Rodionov (1960) and Ginsburg et al. (1979) affects the modern pegmatite classification schemes. This classification categorised pegmatites according to the depth of emplacement and relationship to metamorphism and granitic plutons.

Four classes (see Table 2.1) of granitic pegmatites were recognised and Cerny and Ercit, (2005) proposed that they were inferred from the depth-related “formation” of Ginsburg et al (1979) which were based on the pressure conditions that characterise their host- rock suites (Cerny and Ercit, 2005). The four different categories that were identified by Cerny (1991a) were:-

(i) **Abyssal class**. Pegmatites of this class are found in rocks of high metamorphic grade (amphibolite to granulite facies). Their textures are variable and may include some of the complex pegmatitic textures (e.g. graphic granite)

(ii**) Muscovite class**. Pegmatites of this class are typical for rocks with slightly lower P-T conditions than the abyssal class. Other than that, it is not quite clear what should be the clear separating point

between the two classes. Pegmatites of this class are conformable with the host rocks and are thought to be generated locally by the anatexis (partial melting) of the high-grade metamorphic rocks.

(iii) **Muscovite–rare-element class**. The pegmatites of this class are intrusive bodies which form a continuum from granite to rare-element pegmatites.

(iv) **Rare- element class**. These pegmatites intrude host rocks with the peak metamorphic conditions falling in the low-pressure greenschist facies or amphibolite facies. This class is the most diverse in composition and the most important in terms of the economic usage of these rocks.

(v) **Miarolitic class**. This class is characterised by the presence of open cavities in the pegmatite. The cavities may remain open, be filled with clays, or lined with crystals. These pegmatites were probably emplaced at shallow depths.

The environment of formation, metamorphic facies and relationship to parental granites of these four classes and their likely economic minerals, is shown in Table 2.2 (Cerny, 1991a, 1991b).

Pegmatite classes based mainly on depth of formations.

Table 2. 1: Four main categories of pegmatite classification were identified that were based on the depth of formation. (Cerny, 1991a)

THE FOUR CLASSES OF GRANITIC PEGMATITE ČERNÝ, 1991						
Class	**Family**	**Typical Minor Elements**	**Metamorphic Environment**	**Relation to Granite**	**Structural Features**	**Examples**
Abyssal	—	U, Th, Zr, Nb, Ti, Y, REE, Mo poor (to moderate) mineralization	(upper amphibolite to) low- to high-P granulite facies ~4-9 kb ~700-800°C	none (segregations of anatectic leucosome)	conformable to mobilized cross-cutting veins	Rae and Hearne Provinces, Sask. (Tremblay, 1978); Aldan and Anabar Shields, Siberia (Bushev and Koplus, 1980); Eastern Baltic Shield (Kalita, 1965)
Muscovite	—	Li, Be, Y, REE, Ti, U, Th, Nb > Ta poor (to moderate) mineralization, micas and ceramic minerals	high-P, Barrovian amphibolite facies (kyanite-sillimanite) ~5-8 kb ~650-580°C	none (anatectic bodies) to marginal and exterior	quasi-conformable to cross-cutting	White Sea region, USSR (Gorlov, 1975); Appalachian Province (Jahns *et al.*, 1952); Rajahstan, India (Shmakin, 1976)
Rare - Element	**LCT**	Li, Rb, Cs, Be, Ga, Nb <,> Ta, Sn, Hf, B, P, F poor to abundant mineralization, gemstock industrial minerals	low-P, Abukuma amphibolite to upper greeenschist facies (andalusite-sillimanite) ~2-4 kb ~650-500°C	(interior to marginal to) exterior	quasi-conformable to cross-cutting	Yellowknife field, NWT (Meintzer, 1987); Black Hills, South Dakota (Shearer *et al*, 1987); Cat Lake-Winnipeg River field, Manitoba (Černý *et al.*, 1981)
	NYF	Y, REE, Ti, U, Th, Zr, Nb > Ta, F poor to abundant mineralization, ceramic minerals	variable	interior to marginal	interior pods, conformable to cross-cutting exterior bodies	Llano Co., Texas (Landes, 1932); South Platte district, Colorado (Simmons *et al.*, 1987); Western Keivy, Kola, USSR (Beus, 1960)
Miarolitic	**NYF**	Be, Y, REE, Ti, U, Th, Zr, Nb > Ta, F poor mineralization, gemstock	shallow to sub-volcanic ~1-2 kb	interior to marginal	interior pods and cross-cutting dikes	Pikes Peak, Colorado (Foord, 1982); Sawtooth batholith, Idaho (Boggs, 1986); Korosten pluton, Ukraine (Lazarenko *et al.*, 1973)

Table 2. 2: The four classes of granitic pegmatites showing environment of formation, metamorphic facies, relationship to parent granites and their likely economic minerals. (Cerny, 1991a, 1991b).

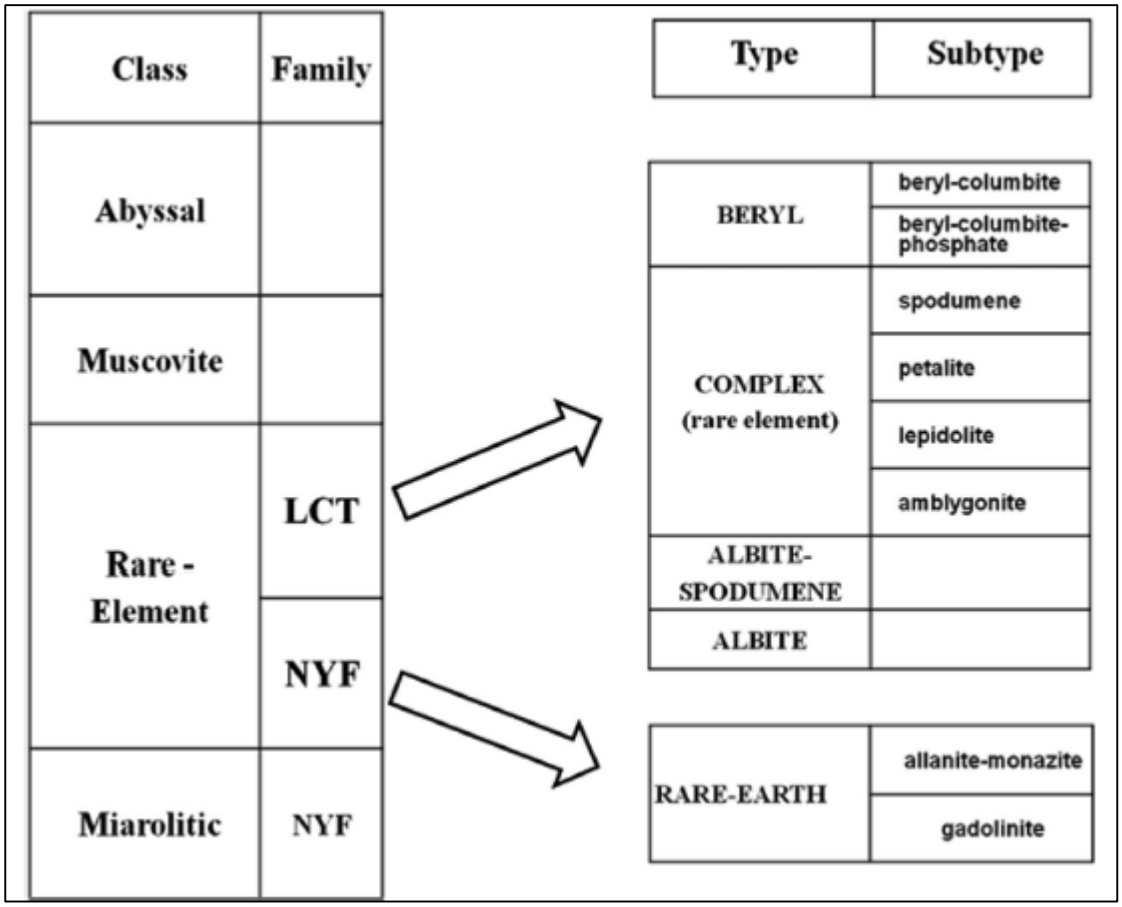
Pegmatite class	Environment of formation	Metamorphic facies of host rocks	Relationship to parent granites	Economic minerals
Miarolitic (gem-bearing)	~1-2 kbar	Greenschist	Within or peripheral to subvolcanic granitic plutons	Quartz crystals, beryl, topaz, tourmaline
Rare-element	~2-4 kbar	Lower amphibolite (Abukuma-type)	Peripheral to granitic intrusions	Spodumene, amblygonite, petalite, lepidolite, pollucite, beryl, columbite-tantalite, microlite, wodginite, uraninite, cassiterite, xenotime, gadolinite
Muscovite	~5-8 kbar	Upper amphibolite (Barrovian-type)	No obvious association with granitic intrusions in many cases	Muscovite, feldspar, uraninite
Abyssal	~4-9 kbar	Granulite (Barrovian- to Abukuma-type)	May be associated with migmatitic granite	Feldspar, quartz

2.3.1 The LCT and NYF Groups of Pegmatites

Furthermore, two pegmatite families are distinguished from the Rare Element Classes (see Table 2.3) the LCT family and NYF family (Bradley et al, 2010). LCT stands for **Lithium**, **Caesium**, and **Tantalum**. This assemblage of elements is found in highly evolved pegmatites derived from S-type granites. S-type granites are thought to originate by melting of sedimentary rocks rich in illite/muscovite. Additional elements which these pegmatites may contain are Be, B, F, P, Mn, Ga, Rb, Nb, Sn, and Hf (Bradley et al, 2010).

The NYF family, where NYF stands for **Niobium**, **Yttrium**, and **Fluorine** are typical pegmatites evolved from A-type granites, which are anorogenic or “within-plate” granites. Additional elements in these pegmatites are the heavy-rare earth elements (Gd- Lu) Be, Ti, Sc, and Zr. A common feature is the occurrence of amazonite, green-coloured Pb-bearing potassium feldspar (Bradley et al, 2010).

Table 2. 3: Relationship between the Cerny's (1991a) pegmatite classes, families, types and subtypes related to LCT and NYF families.



2.4 Types of Pegmatites

In addition to the two groups of NYF and LCT, pegmatites can be zoned (complex) or unzoned (simple) and if zoned have a fairly typical zonation, frequently with a quartz core (Steiner, 2019).

The sequence of crystallisation is thought to occur from the margins inwards (cooling effects) and concentrations of incompatible element-rich minerals frequently occur at the margins of the pegmatite and the quartz core (Steiner, 2019).

2.4.1 Simple Pegmatites (Unzoned)

Simple pegmatites are homogenous pegmatites which can be contrasted with layered granites and zoned pegmatites by having no noticable internal structure (London, 2005). However, they do usually have a fine- grained border zone of a few cms thick (Landes, 1933). They are comprised of similar minerals as zoned pegmatites.

Unzoned pegmatites are situated inside or adjacent to granite cupolas and are characterised by their homogenous textures and coarse grain size, a few cm or bigger (Steiner, 2019). Plagioclase and quartz are typically anhedral and of uniform size, though K- feldspar is porphyritic and shows skeletal or graphic granite intergrowths. Unzoned pegmatites can be a good sources of economic quartz, feldspar, spodumene and mica (Steiner, 2019).

Norton and Redden (1990) depict that the unzoned pegmatites are usually tabular to lenticular sills concodant with the foliation or bedding of the host rock. The majority of them are in the range of 10 and 100m long and with only a few that are more than 300m long (Norton and Redden, 1990).

2.4.2 Complex Pegmatites (Zoned)

The zonal mineral assemblages in complex pegmatites is greatly dependant on the habit and orientation of the crystals, and also the spatial segregation in the internal fabric (Steiner, 2019). A typical zoned pegmatite consists of the border, wall, intermediate and core zones which have unique mineralogical and geochemical properties (Steiner, 2019). This is best illustrated in Table 2.1 and Figure 2.2 below. The border zones comprise 1–3 cm wide cooling margins of fine-grained and granophyric granitic rock at the contact with the host rock. The typical mineralogy comprises plagioclase-quartz-muscovite, with accessory tourmaline, beryl, garnet, cassiterite and columbite. The wall zone consists of inward-orientated K-feldspar, micas, beryl, and tourmaline, with considerably larger crystal sizes. The intermediate zone follows inward from the wall zones and is principally formed of more abundant monophase K-feldspar, quartz, muscovite, sodic plagioclase and lithium aluminosilicates. The centre or core of zoned pegmatites is pure quartz. Historically, it was assumed that the quartz core formed during the last stage of the pegmatite crystallisation process. However, experiments by London and Morgan (2017) demonstrated that in Li-rich melts, albite, and lepidolite can follow the crystallisation of pure quartz.

2.4.3 Mineral Composition of Typical Pegmatite Zones

A typical mineralogical zonation of a pegmatite is shown in Table 2.4

Table 2. 4: Table showing the mineral compositions of typical pegmatite zones (Simmons, 2007).

Zone	Texture	Principal Minerals	Accessory Minerals
Border zone	Fine grained	Plagioclase or microcline, quartz, ± muscovite	Schorl, garnet, magnetite, microcline or plagioclase
Wall zone	Coarser	Quartz, plagioclase, microcline, ± muscovite, ± biotite	Schorl, garnet, beryl, apatite
Outer Intermediate zone	Progressively coarser to giant size crystals; pocket development	Microcline, quartz	Schorl-elbaite, sodic plagioclase, muscovite, phosphates
Inner Intermediate zone (Core-margin)	Both coarse and fine, some giant crystals; pocket development	Quartz, microcline, sodic plagioclase, ± muscovite, ± biotite	Schorl-elbaite, beryl, phosphate minerals, Nb-Ta minerals
Core		Quartz	Beryl, spodumene

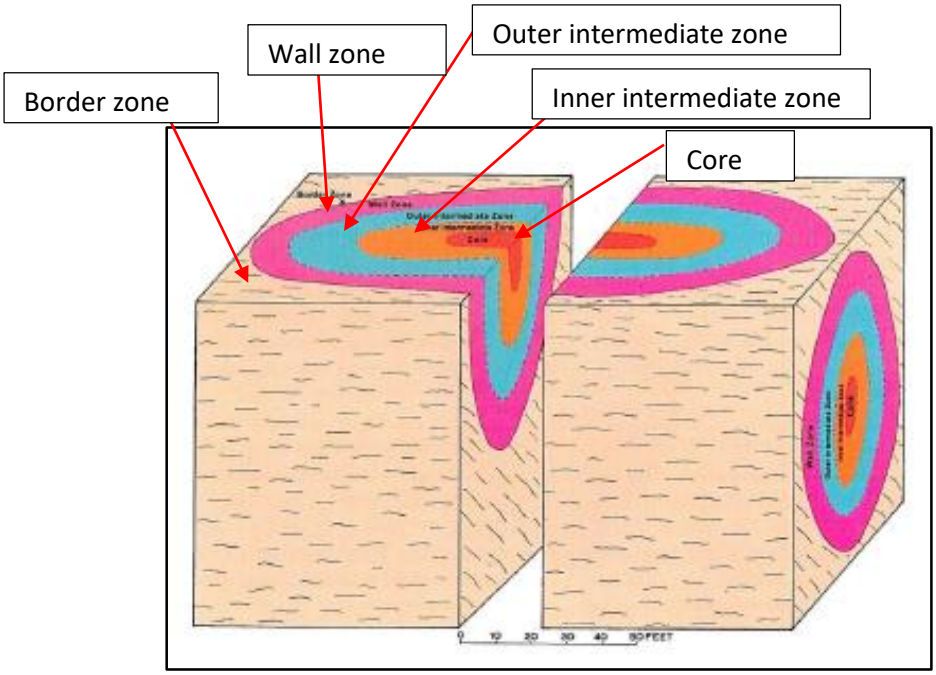


Figure 2. 2: Zoning structure in pegmatites (Steiner, 2019).

Zoned pegmatites usually occur in clusters and the types differ in different clusters (Norton and Redden, 1990). A more subtle regional zonation may occur in which rare-mineral pegmatites are more abundant and muscovite pegmatites are less abundant towards the edges of the pegmatite region. This pattern corresponds to a drop in crystallisation temperatures from more than 660^{o}C in parts of the granite, some of which have primary sillimanite rather than muscovite, to under 600^{o}C in inward zones of a couple of uncommon mineral pegmatites, a significant number of which are below the sillimanite isograd (Norton and Redden, 1990). Zoned pegmatites tend to be less fertile or barren in the core but as fractionation increases, the zonation becomes more complex with enrichments of incompatible elements as shown in Figure 2.3 (Cerny, 1991b).

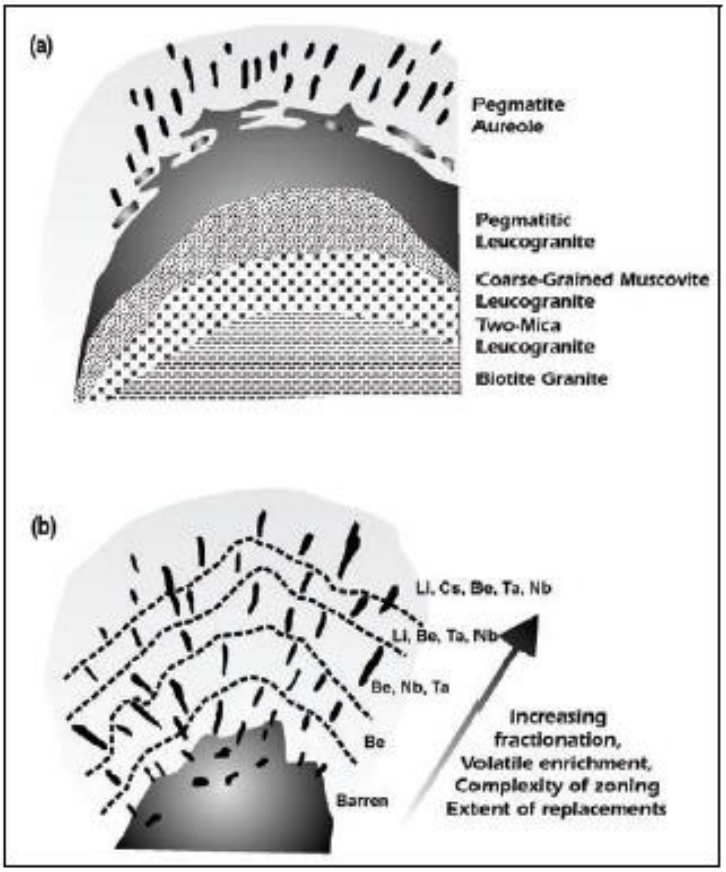


Figure 2. 3: Regional zoning in fertile granites and pegmatites (from Cerny, 1991b): (a) regional zoning of a fertile granite (outwardly fractionated) with an aureole of exterior lithium pegmatites; (b) schematic representation of regional zoning in a cogenetic parent granite + pegmatite group. Pegmatites increase in degree of evolution with increasing distance from the parent granite.

2.5 Age Distribution

LCT pegmatites are identified within orogenic belts, regularly including in high-grade metamorphic terrains and reworked or exhumed deep continental crust (Steiner, 2019). Examples are found the world over, for example, in Palaeoproterozoic granulite belts of northern Scotland (Shaw et. al., 2016),

Archean–Proterozoic greenstone belts of Canada, Africa and Australia and Phanerozoic mountain belts, especially the European Variscides (also called the Hercynian Fold Belt), and its expansion along the Alleghanian Orogen into the New England territory of North America (Dill, 2015). LCT pegmatites prevalently occur in continent-continent collision zones (Cerny, 1991b), although Sn and W bearing deposits can extend to decoupled and happen in post-orogenic extension and continental arc settings (Romer and Knoner, 2016).

Pegmatites occur on all continents, typically where orogenic roots have been brought to the surface by exhumation and erosion. They range in their age from very old, for example, the 3.5 billion years old (Archaean) pegmatites in Kenya-Tanzania-Zimbabwe to young, 147 million years old (Jurassic) pegmatite near San Diego, California, USA.

2.6 Mineralogy of Pegmatites

The primitive granitic pegmatites contain the common rock-forming minerals K-feldspar, plagioclase, quartz, muscovite and/or biotite.

Rarer but economically important pegmatite minerals are listed in Table 2.5. This table has been compiled from the text in London (2008) from a more complete and much longer list of minerals, many of which were also noted by Ginsburg (1984).

Table 2. 5: Economic rare minerals of pegmatites (London, 2008).

Mineral/group	composition
lithium alumosilicates	
spodumene	$LiAlSi_2O_6$
petalite	$LiAlSi_4O_{10}$
tourmaline	
schorl	$NaFe_3Al_6(BO_3)_3(OH)_4Si_6O_{18}$
dravite	$NaMg_3Al_6(BO_3)_3(OH)_4Si_6O_{18}$
elbaite	$NaLi_{1.5}Al_{1.5}Al_6(BO_3)_3(OH)_4Si_6O_{18}$
garnets	
spessartine	$Mn_3Al_2(Sio_4)_3$

beryl	$Be_3Al_2Si_6O_{18}$
pollucite	$CsAlSi_2O_6$
phosphates	
monazite	$CePO_4$
amblygonite	$LiAlPO_4F$
lithiophyllite	$LiMnPO_4$
topaz	$Al_2SiO_4F_2$
oxides	
cassiterite	SnO_2
columbite-tantalite	$(Mn,Fe)(Nb,Ta)_2O_6$
rutile	TiO_2
uranitite	UO_2
zircon	$ZrSiO_4$

2.7 Genetic Model

There are many models that describe the genesis of granitic pegmatites but none seem to satisfactorily describe all the various features of the pegmatites (Simmons and Webber, 2008). The most favoured by many researchers being the genesis from residual melts derived from the crystallisation of granitic plutons so that, the incompatible components such as certain rare elements, fluxes and volatiles are enriched (Simmons and Webber, 2008). Also Ginsburg (1984) published a model which explains that these pegmatites are closely associated with igneous rocks that were formed from the melting of pre-existing sediments and pre-existing igneous rocks. London (2008) discusses in his model of pegmatite evolution that pegmatite crystallisation is due to disequilibrium crystallisation from undercooled, flux-bearing granitic melt. Cerny (1991a) agrees that large crystals are believed to be contributed from the lower temperatures in the crystallisation process which then decreases the nucleation density and growth rates, melt polymerisation and viscosity thereby increasing the diffusion rates and solubility.

2.8 Pegmatite Exploration

Pegmatite exploration tends to follow techniques which range from grassroots to advanced (Selway et.al 2005). Grassroots projects focus on the area or region which has pegmatite bodies and evaluate their mineralisation potential. This will include the examining of the regional zoning of the fertile granites and associated pegmatites using bulk whole-rock, K-feldspar and muscovite compositions. Determining the degree of fractionation of the granite and pegmatite and identifying the presence of the pegmatite minerals is also evaluated (Selway et. al 2005). Grassroots exploration also includes a bulk sampling of metasomatised host rocks, involving chip samples, channel samples, and drill core samples.

Advanced exploration is executed to study the pegmatite in detail. It looks at the specific location of zones of mineralisation within the pegmatite body. This will include metallurgical studies of pegmatite assemblages' minerals using sophisticated laboratory techniques, such as electron microprobe and scanning electron microscope (Selway et.al 2005).

2.9 Case Studies

A number of Archaean and Palaeoproterozoic pegmatite areas occur within Zimbabwe. These are briefly outlined to provide a contextual setting for those at Mbeta.

2.9.1 Bikita Minerals

The pegmatites of the Bikita area have long been known and are noted by pegmatologists for the array of minerals. According to Wilson and Martin (1963), of the 35 pegmatites in the area examined by J Dawson which in the Bikita Tinfield, include the Beadmore Mine and portion of the Main Bikita pegmatite, most of these exhibit some degree of zoning. Dawson noted that the quartz cores are generally developed throughout or over the major part of the course of the pegmatite. The quartz units are asymmetrically sited towards the hangingwall of the pegmatite. The hangingwall and the intermediate hangingwall phases rarely exceeded one-third of the total pegmatite width. The zonation of the pegmatites as defined by Wilson and Martin (1963), focussed particularly on the relative proportions of soda and potash feldspars.

2.9.2 Zoned Pegmatites (Type Na- K) at Bikita

a. *Hanging wall zone*- a well developed zonal unit composed of medium-crystalline albite, quartz, mica, and occasional K-feldspar in many pegmatites. This zone may contain significant values of finely-crystalline beryl (Wilson and Martin, 1963).

b. *Intermediate hanging wall zone*- a poorly defined, narrow and often impersistent zonal unit composed of albite, lamellar albite, mica and some quartz. Where the zone exceeds 20cm in

width, coarse K- feldspar and some beryl may be developed at the quartz unit margin. Tantalite may occur in significant amounts e.g., in the Ebonite West pegmatite, tantalite is sporadically distributed within this zone (Wilson and Martin, 1963).

c. *Intermediate footwall zone*- a persistent unit showing considerable variations in width and modal percentage of minerals present both in-depth and along strike of the pegmatite (Wilson and Martin, 1963). Bodies of massive lepidolite, lamellar albite aggregates, coarse blocky albite, coarse K- feldspar, mica and some quartz may occur in this zone. Beryl crystals of variable size and distribution, occasional crystals of topaz and crystals of tantalite tend to have formed at the margin to the quartz core.

d. *Footwall zone*- a persistent zonal unit, composed of predominantly fine-crystalline albite, with lamellar albite present in many cases, quartz, mica, and rare K- feldspar. The footwalll zone grades into the intermediate footwall zone.

2.9.3 Type (K- Na) at Bikita

In this type, the pegmatites are narrow and contain a prominent centrally placed quartz core. The quartz core margin zones contain coarse K-feldspar some fine albite, quartz, mica and significant amounts of beryl. Footwall and hanging wall zones are very narrow, being composed of fine-crystalline quartz, K-feldspar, mica and albite.

2.9.4 Kamativi Tin Deposits

The pegmatites of the Kamativi Schist belt are divided into three types based on their mineral assemblages and their mode of emplacement and development (Watson, 1962).

a. The Tourmaline- bearing, Non- Mineralised Replacement Pegmatites

Quartz oligoclase rocks are the commonest pegmatites in the Kamativi Schist belt. Microcline is frequently present and muscovite is usually abundant as coarse clusters, but biotite is rare. Small almandine garnets are common. The most characteristic constituents are black schorl in large, scattered, often euhedral crystals up to 15cm in size (Watson, 1962).

The pegmatites are cream-yellow in colour with a roughly equigranular texture and grain size averaging 2.5cm. They vary in size from small stringers to massive bodies. Their strike and direction are always concordant with the planes of schistosity of the quartz-mica-schist host rocks from which they have apparently formed by metasomatic replacement after the manner of the replacement gneisses. These tourmaline-bearing, replacement pegmatites are widely found throughout the Kamativi Schist Belt and its migmatic zones. It is suggested that the tourmalinisation of the tourmaline-bearing pegmatites are all part of a granitisation process whereby large original schistose areas have

been altered to gneiss and that during this process the boron content of the granitised schists have been mobilised and concentrated in the relict schist belt as a sort of 'boron front' (Watson, 1962).

b. Tin- bearing – Intrusive Pegmatites

These are confined to the Kamativi Schist Belt and its migmamite zones. They are found in three forms;

I. Dyke-like pegmatites that are steeply dipping and parallel to the foliation of the schists, e.g, the Kalinda tin-bearing pegmatites and the Lutope west across the Gwai River.
II. Rare pegmatites that are oriented at right angles to the foliation of the schists. They form bodies more than 3m long and 1.2m across and are found in Kamativi.
III. Roughly horizontal sheets are well-developed at Kamativi

The original pegmatite was composed of quartz-microcline-muscovite but it has been heavily albitised and the original microcline-pegmatite is now only found in remnant subsidiary patches. Tantalite, columbite and amblygonite are all found associated with cassiterite in these pegmatites. While the tin-bearing pegmatites at Kamativi, Kalinda and Lutope have accessory fine-grained tourmaline (Watson, 1962).

c. Tourmaline- bearing, Mineralised, Quartz-Pegmatites and Quartz veins

According to Watson (1962), at Kalinda, quartz-pegmatites and quartz veins with accesory fine, black, acicular tourmaline are associated with wolframite mineralisation. At Lutope similar quartz-pegmatites contain wolframite. At Kalinda, the scheelite minerisalisation even permeates the host schist, and at both Lutope and Kalinda it is usually tourmalinised in the contact zones. At Kamativi, the tin-bearing pegmatites frequently cut unmineralised tourmaline-bearing, replacement pegmatites and they are younger than the replacement pegmatites. At Kalinda, the tin-bearing pegmatites are cut by the mineralised, wolframite-bearing, intrusive, tourmaline pegmatites which must then in turn be younger than the tin-bearing pegmatites. Low temperature quartz veins cutting the tin-bearing pegmatites at Kamativi represent the final, hydrothermal phase of the pegmatic intrusions (Watson, 1962) .

2.9.5 Acadia Lithium Project

The project lies 1.5km northwest of the Lonely Park homestead, Arcturus on Thorn Vlei Farm which is 38km east northeast of Harare in the Harare Greenstone belt (Tyler, 2017). The pegmatite is composed of microcline, quartz and muscovite with petalite, eucryptite and smaller amounts of spodumene and amblygonite. It belongs to the Na-Li group and it is a flat-lying body dipping gently northwards (Baldock et al. 1991).

Crude horizontal zoning is evident (Baldock et al. 1991). The border zones which are about 25cm wide are composed of fine-grained microcline, petalite, quartz and muscovite. Inwards from the border zone are the outer wall zones which attain a maximum width of 30cm and are enriched in microcline. Much of the inner portion of the body consists of very coarse, pale-grey petalite containing pods of

eucryptite (Baldock et al. 1991). These minerals contain inclusions of spodumene and amblygonite. (Baldock et al. 1991). Minor albite is widespread in the core but lepidolite is very rare. Fine-grained banded felspathic greisen is mixed with the coarse petalite-rich layers resulting in a decreased Li_2O content (Baldock et al. 1991).

2.10 Conclusions from the review

Bikita is the world's third largest lithium producer and an important caesium source, and although cassiterite-bearing, does not produce tin currently. It is clear from the review, that not only are pegmatites an important source of lithophile elements, but that Zimbabwe has the potential to be one of the world's important potential sources of these much-needed metals.

The Mbeta pegmatites were chosen as a subject of this study because of their potential to host such important lithophile elements. It is, therefore, necessary to study their origin, occurrence and economic mineral viability.

CHAPTER 3

METHODOLOGY

3.1 Introduction

The study followed three general methods and approaches to achieve the general and specific objectives of the proposed research. These include pre-fieldwork, fieldwork and analysis of the data. In pre-fieldwork, data was collated from the literature, the problem statement identified, and based on the objectives decided, relevant topographical maps were obtained for the Mbeta area. During the fieldwork, there was a collection of field data on the structural setting of the pegmatite, representative fresh samples from the outcrops and open pits were collected, lithological descriptions of the samples in hand specimens made and GPS locations were noted for where the samples came from. Following this laboratory analyses and petrographic descriptions were integrated into a synthesis and interpretation of the data and writing of the research report.

I. Pre-fieldwork

Activities included field logistics planning and a literature survey including a collection of hardcopy and digital maps (Figure 3.1) for the purposes of recording geological information, sample localities and other relevant cadastral information (e.g. lease boundaries). It is during this time that suitable training and preparation was carried out to facilitate travel, accommodation, site access and occupational health and safety, daily work plans and schedules and operations of specialised equipment.

II. Fieldwork

Geological mapping was recorded as overlays on to Google Earth satellite view base maps. Sample description, sampling, labelling and packaging of the lithologic samples were completed. Sampling locations were recorded in the Excel sheet for further inputting and processing using QGIS.

III. Analysis

After returning from the field the digital geological and sample location maps were uploaded and finalised. Sample collected included 10 rock specimens and a crush from a dump site next to surface excavations (refer to Table 3.1 for descriptions). Preparation for thin section microscopy involved cutting to an appropriate size with a diamond saw at Wits Geosciences. Additional specialised preparation of the samples for geochemical analysis was also scheduled. Ultimately, the data obtained both in the field and the Wits Geosciences laboratories were subjected to processing, usually with the aid of PC- based applications, for the purposes of interpretation and compiling a research report.

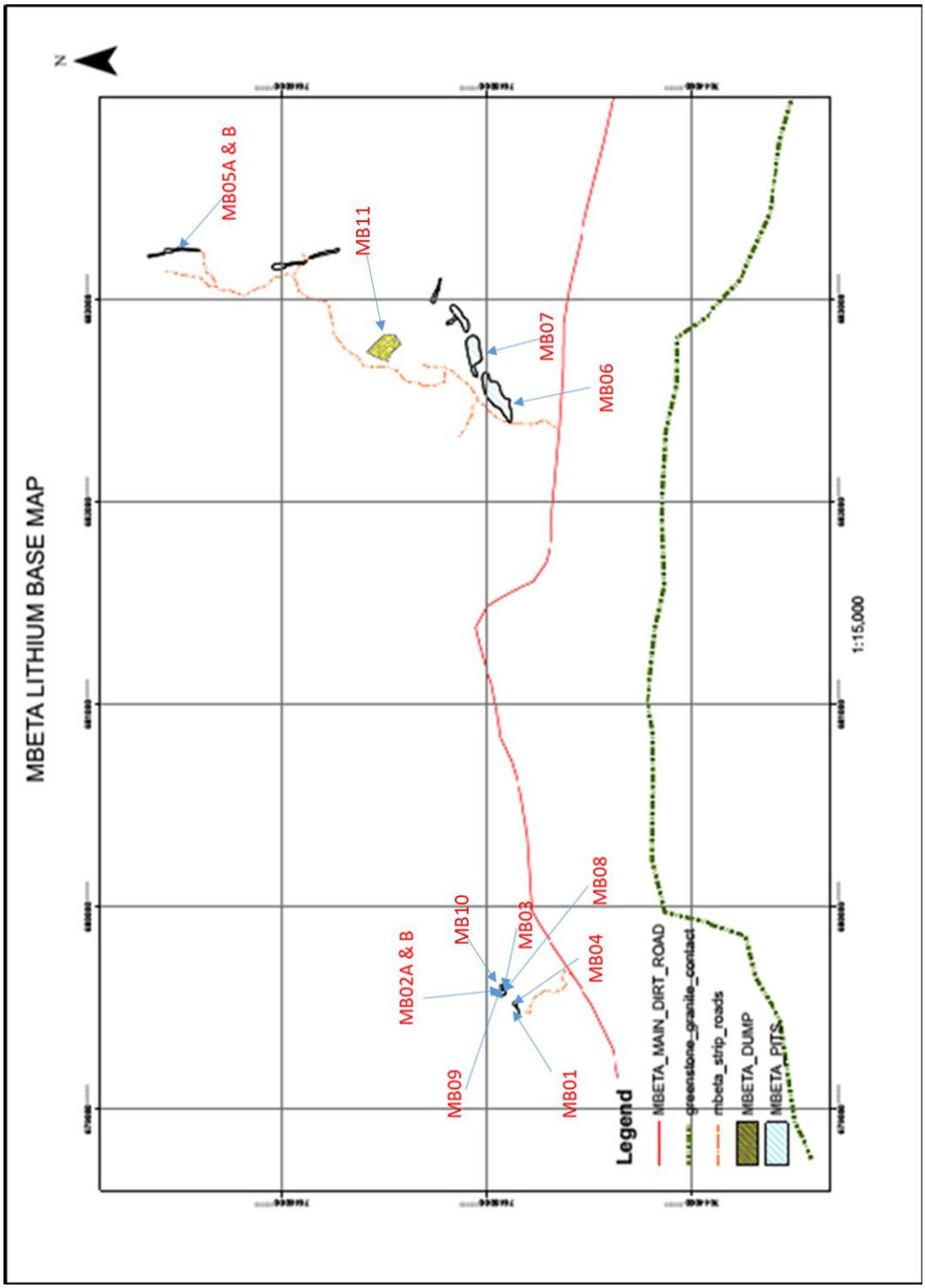


Figure 3. 1: Mbeta Base map showing the Mbeta pits, dump and the greenstone granite contact.

Table 3. 1: Table showing the rock samples collected from the main, western and northern pits at Mbeta.

Sample number	Location	Picture/image	Description	Zone
1	Western pit 35k 679502E 7644801N		The sample from a highly oxidised outcrop outside the pit has large quartz crystals and greenish veins.	From outside the pit. Possibly from the inner intermediate pegmatite zone.
2	Western pit 35k 679463E 7644826N		Large crystals of quartz and dark spots suspected to be of Ta oxide.	From outside the pit Possibly from the inner intermediate pegmatite zone.
3	Western pit 35k 679529E 7644816N		Large crystals of quartz and muscovite with accessory lepidolite.	From inside the pit in the inner inter-mediate pegmatite zone.
4	Western pit 35k 679595E 7644924N		Sample collected from the contact of the pegmatite and greenschist. Sample likely to be feldspar.	From inside the pit in the inner inter-mediate pegmatite zone.
5	Northern pit 35k 683167E 7645983N		Sample has large crystals of quartz with accessory purple lepidolite.	From inside the pit and is in the inner intermediate zone of the pegmatite.
6	Main pit 35k 682449E 7644906N		Sample has pinkish quartz crystals.	From a pegmatite dyke in the main pit.
7	Main pit 35k 682438E 7644906N		Sample with greenish tinted micas.	From the inner intermediate zone of the pegmatite.
8	Western pit 35k 679562E 7644921N		Sample is pure quartz	From inside the pit. In the core of the pegmatite
9	Western pit 35k 679567E 7644921N		Sample shows crystals of purplish lepidolite	From inside the pit. Inner intermediate zone.

10	Western pit 35k 679595E 7644924N		Sample of greenschist with a schistose texture	Host rock.

Thin sections were studied using a binocular petrographic microscope (Olympus BX 53m) equipped with a DP 74 digital camera linked to a PC running the imaging software cellSens. Written notes were recorded, photomicrographs taken that could be stitched to provide whole section coverage and modal percentages of the minerals were determined by point counting.

The ten rocks and dump samples were split, crushed and milled to a fine powder at Wits Geosciences suitable for qualitative and quantitative XRD analysis by an outside Consulting Laboratory. These powders were also used to prepare fusion disks and analysed by XRF at the Wits Geosciences Earth laboratory.

The analytical data (petrography, XRD and XRF) were collected, collated and integrated with field observations for the purpose of interpretation and discussion.

Other software packages used to synthesise the data were Microsoft PowerPoint, Microsoft Word, Microsoft Excel and Gimp for the petrographic conversion of images.

During the different phases, a variety of additional software was used for the production and analysis of topographic, satellites and geological maps, including QGIS and Google Earth.

More details of the research methodology in each stage are presented below.

3.2 Field mapping

Fieldwork was undertaken to conduct a superficial mineral prospection of the Mbeta pegmatites to gain a better understanding of geological controls and mineral distribution, given the geological and economic importance of the pegmatites, especially in the study area (Genuino et al, 2016). In addition, a representative suite of fresh rock samples for petrographic, XRD and XRF analysis was collected. Mapping was undertaken on a scale of 1cm to 3.6m.The GPS coordinates of the locations were taken and plotted on the base map (Figure 3.1).

3.3 Sample preparation and XRD analysis

Samples for XRD and XRF analysis were prepared and tested using methods described in Wilson (2012). Selected and cleaned rock chips were passed through a carbon- steel jaw crusher, the approximately 100g was further ground in a carbon- steel swing mill. Portions of the powder were subject to qualitative and quantitative XRD analysis at XRD Analytical and Consulting CC by Dr. Sabine

Verryn. The samples were prepared for XRD analysis using a back-loading preparation method. Each sample was scanned using a PANalytical Aeris diffractometer with PIXcel detection and fixed slits with Fe filtered Co-Kα radiation. The phases were identified using X' Pert Highscore plus software. The relative phase amounts of the minerals (weight %) were estimated using the Rietveld method.

3.4 X-Ray Fluorescence (XRF) analysis

Powdered samples were mixed with Johnson Matthey Spectrolflux 105, fused at 1100 °C and cast into a glass disk for analysis using a PANalytical PW2404 X-ray fluorescence (XRF) spectrometer at the Witwatersrand University Earth Lab in Johannesburg. Generic calibrations were made using mixtures of synthetic oxide and international standard rocks, as well as internal controls. The main International Reference Materials series USGS (USA) and series NIM (South Africa) were used as calibration standards.

Although the material was also prepared for trace element analysis, the trace data was not provided because of a long delay of faulty equipment in the Earth Lab.

3.5 Petrographic analysis

Fresh representative samples were collected from Mbeta to encompass the observed mineralogical and textural variations. Eleven thin sections were prepared at the University of the Witwatersrand with a preferred thickness of 30µm. The thin sections were examined using the petrographic microscope (Olympus BX 53m/DP 74 and the Olympus SC50) at the Petrography Laboratory at the School of Geosciences, University of the Witwatersrand.

Each thin section was scanned with the DP 74 to provide an easy overview of the entirety of the thin section and studied to determine the mineralogy, texture, composition, grain size, grain shape, structure and modal percentage of the minerals in the rock. The minerals were studied in plane and cross-polarised light henceforth referred to as PPL and XPL respectively. The images are included in the Appendix A. The naming convention used for samples, both thin sections, XRD and XRF were in the form of MB01, MB for Mbeta and 01 for sample number.

3.6 Modal mineral composition analysis (point counting)

A modal mineral composition analysis (point counting) was carried out in the Petrography Laboratory at the School of Geosciences, University of the Witwatersrand (refer to Figure 3.1). Point counting made use of a digital image of the entire thin section (XPL as described in section 3.5) following (Larrea et al., 2010).

Point counting was undertaken on all the eleven thin sections and >400 points were counted for each thin section, based upon a grid system with data point intercepts evenly spaced along parallel traverse lines across the view. Line spacing of 0.5mm and 0.25mm point stops were adopted as an acceptable balance between mineral grain resolution and sufficient counts. Minerals counted were quartz, plagioclase (albite), micas (muscovite and lepidolite) and accessory minerals (rutile, topaz and garnets).

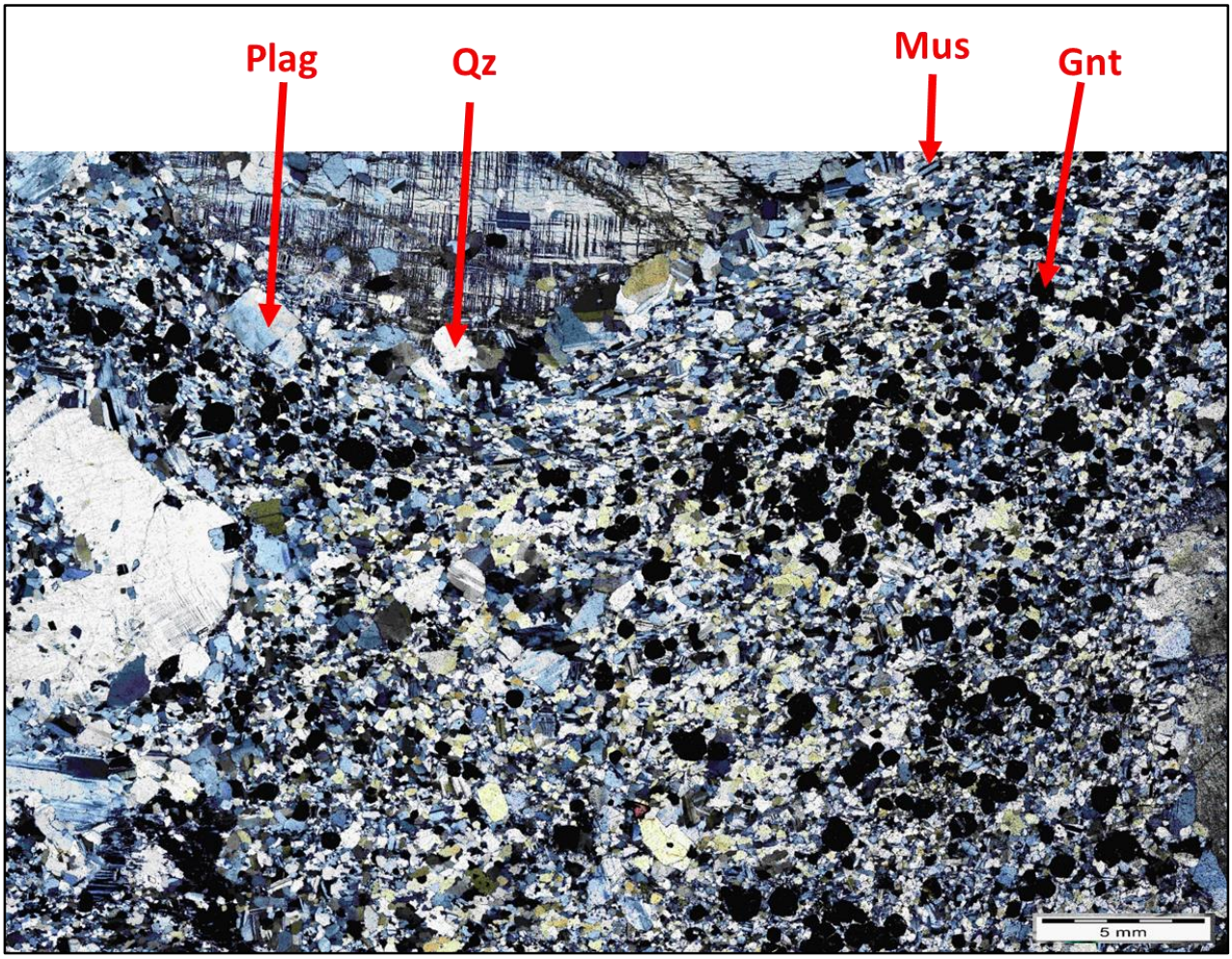


Figure 3. 2: Image of MB02A showing point counting of minerals (Qz) quartz, (Plag) plagioclase/ albite, (Mus) muscovite and (Gnt) garnets.

CHAPTER 4

FIELD MAPPING

4.1 Introduction

The results of the field mapping at Mbeta are presented in this chapter. The purpose of the field mapping was to determine the lithological units found in the area, any zonation noted in the pegmatites and relationship with the surrounding units. The Mbeta area is dominated by thorny bushes and a few mopani trees. The soil cover is red soils which change to red-brown soils as it transitions from the greenstones to the pegmatite zone.



Figure 4. 1: Google Earth extract showing the exact localities where samples were collected at Mbeta.

4.2 Geology

The rocks into which the Mbeta pegmatites are emplaced are greenschists and serpentinite of the Lower Gwanda greenstone belt. Serpentinite occurs as narrow, lenticular masses, enclosed within the easterly-trending foliation of the greenschists and have been interpreted as pre-tectonic sheet-like intrusives (Phaup, 1983). The greenstone outcrops are characterised by fine-textured epidiorites and

amphibolites (Figure 4.2). They display variably developed fracturing and schistose foliation that strikes N80^{0}E and dip south at between 45^0- 60^0. A regional contact with gneissic granite occurs within a kilometre south of the principal pegmatite workings (Figure 1.4).

A swarm of approximately parallel coarsely-crystalline pegmatite veins and dykes occur in the area. They occur in a zone of apparent shearing measuring more than 400m in width and are traceable along strike for a distance of at least 1.8 km. The pegmatite belt strikes N70^{0}E and the individual pegmatites dip at varying angles.



Figure 4. 2: Image showing the greenstone walls and the massive feldspar outcrops within pegmatite from the Main Pit at Mbeta.

Main Pit

The main pegmatite which has been extensively trenched, dips either steeply towards the southeast or is near-vertical. A 4m pegmatite dyke which is dominated by lepidolite (refer to Figure 4.2 and 4.3) has been exposed in the main quarry. It strikes N67^{0}E and dips steeply towards the southeast, although a flatter dip is suggested on the floor of the quarry. The bounding greenstone walls have been well fractured, these rocks strike N80^{0}E and the dip is towards the south generally at about 45^0.



Figure 4. 3: Image showing the massive lepidolite exposure in the main pit. (GPS location: 35K 682449E 7644906N).

The pegmatite that has been worked consists chiefly of quartz, sodic feldspar, lepidolite and massive topaz. There is an apparent zonal arrangement of these minerals, the 1.5m central 'core' of the pegmatite is composed almost wholly of massive feldspar having small lenticular inclusions and stringers of white glassy quartz, although it should be noted that the various zones are somewhat indistinct and appear to be gradational.

Intergrowths of feldspar and white quartz make up the northwestern zone that is up to 0.5m or 1m wide. Abundant medium to fine-grained lepidolite occurs as massive irregular inclusions in a quartz core that is about 1m wide immediately southeast of the core. This grades into massive crystalline white topaz which grades finally into a 0.3m marginal zone of massive feldspar.

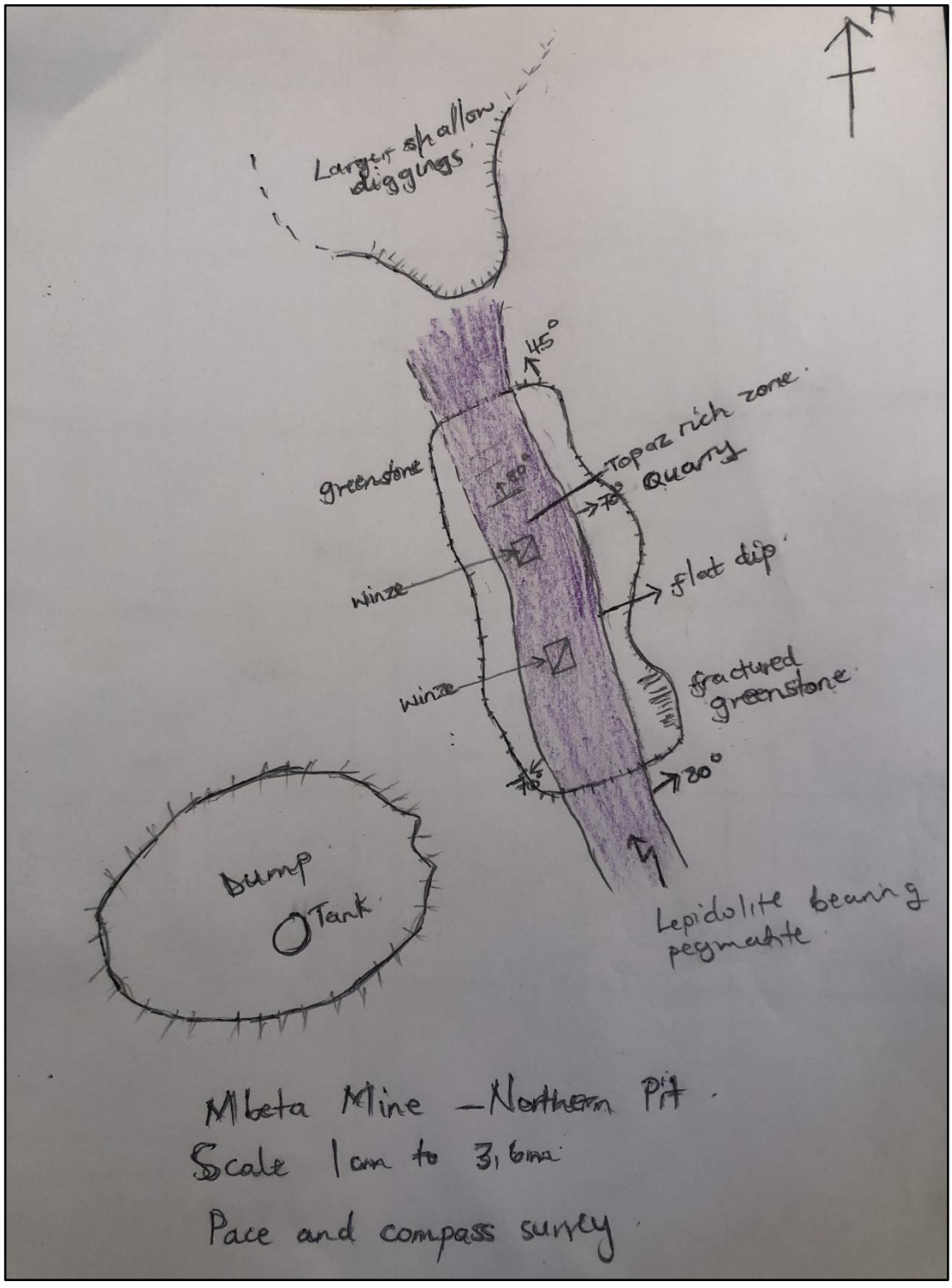


Figure 4. 4: Geological map of the Main Pit showing the lepidolite bearing pegmatite intruding into the greenstone.

The topaz-rich zone shown in Figure 4.5, contains a streak of bluish quartz as well as small books of mica. Elsewhere on the claims, small shattered blebs of pale-blue topaz as shown in Figure 4.5, embedded in quartz were noted.

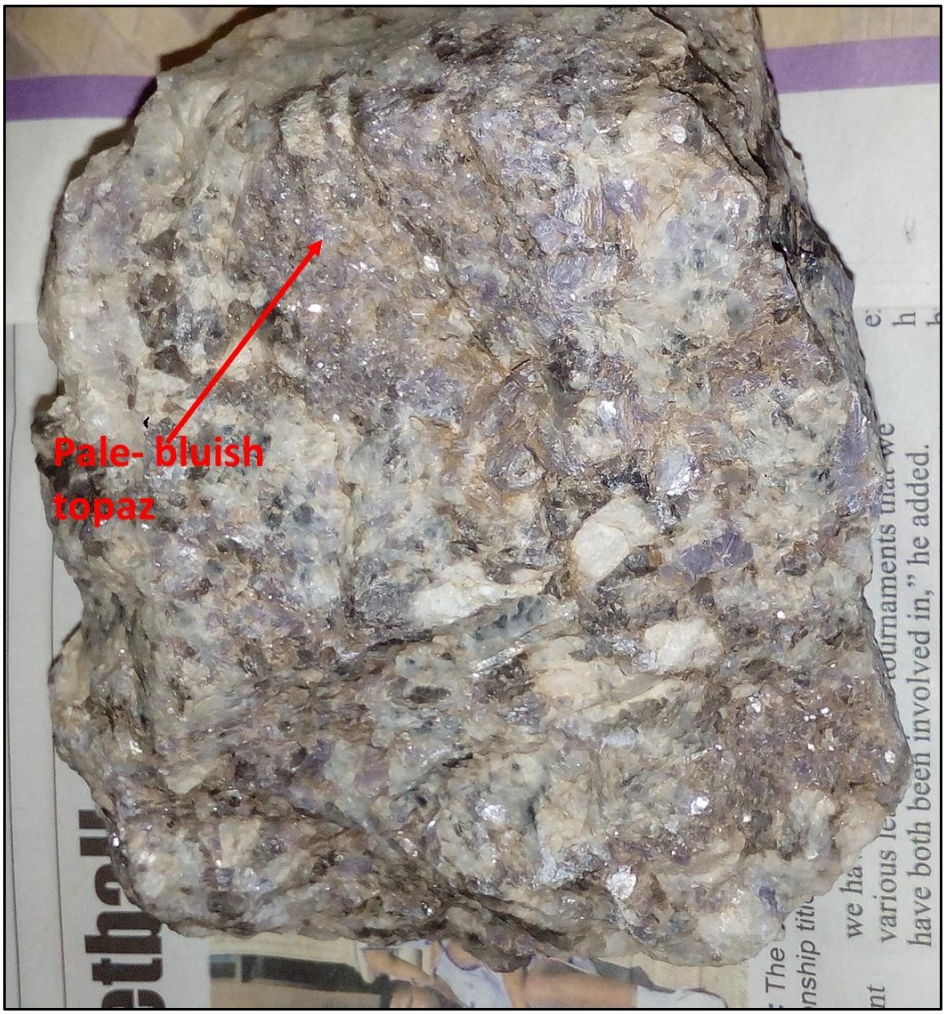


Figure 4. 5: Image of sample showing the topaz with bluish quartz from the western pit but it gives a true representation of how the topaz occurs in the Mbeta pits. Sample number MB03. (GPS Location: 35K 679529 E 7644 816N).

Northern Pit

About 200m northeast of the main quarry is a shallow open-cast pit that is about 30m in length. In it is exposed a 3m, coarsely-crystalline pegmatite body composed almost wholly of white quartz and sodic feldspar. It strikes N62^{0}W and dips towards the southwest at about 5^0. Only sparse lepidolite and a little tantalite have been found in this locality.

There are a series of shallow workings about 300m north of the main quarry. These workings have exposed a 2m wide pegmatite body which strikes N40^{0}E and dips north-west at 60^0. The wallrocks are serpentinite. The pegmatite is composed of a 0.6m central core of quartz flanked on either side by zones composed of pink and white feldspar, abundant lepidolite, glassy white quartz and white topaz.

Western Pit

About 2km to the west of the main quarry is another open cast pit. These workings have exposed a 6m wide pegmatite body that is almost 80m in length. It strikes N60^{0}E and dips northwest at 65^0. The pegmatite consists chiefly of quartz (as illustrated in Figure 4.6), sodic feldspar, lepidolite and massive topaz. There is an apparent zonal arrangement of these minerals, the 2m central 'core' of the pegmatite is composed almost wholly of massive feldspar having small lenticular inclusions and stringers of white glassy quartz.

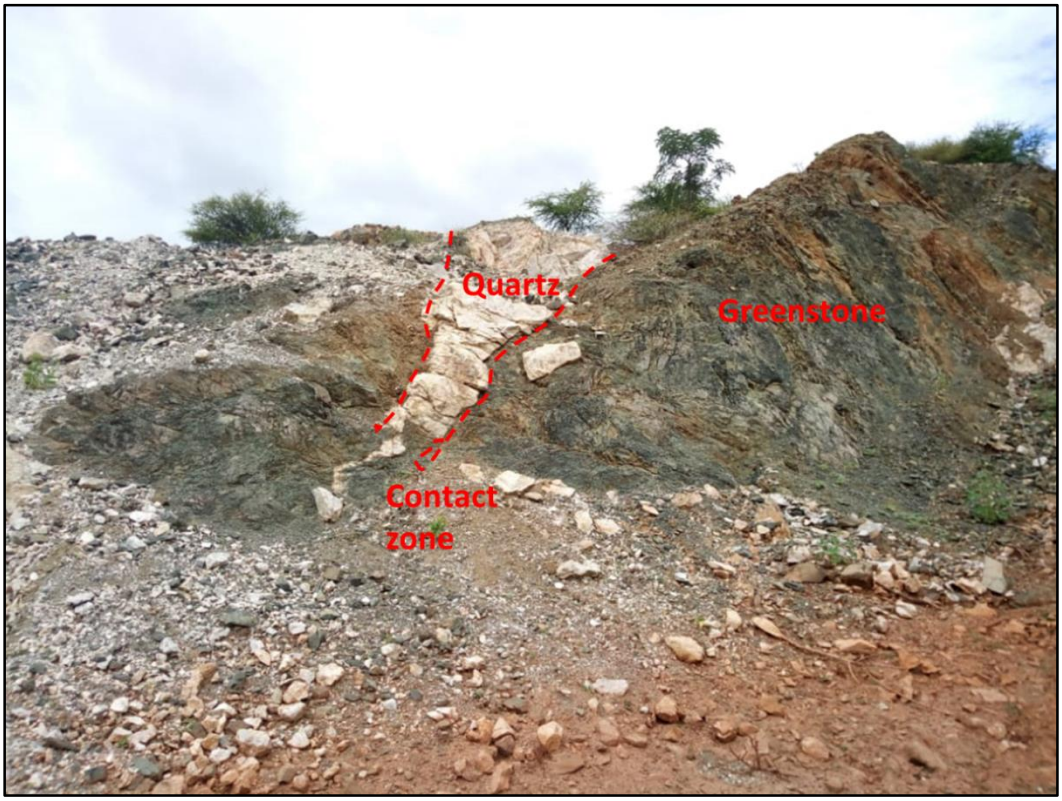


Figure 4. 6: Sharp contact of quartz with the greenstones at the Western pit at Mbeta. (GPS location: 35K 679463E 7644826N).

The petrography of the various samples taken from the pegmatite belt is described in the next chapter.

About 7m southwest of the western pit quarry, there are extensive very shallow open workings. The pegmatite in this locality has been strongly fractured, the fractures striking E20^{0}S and dipping

southwards at 50^0. There appears to be a 1.5m central core of quartz and feldspar with fairly abundant lepidolite. This core is flanked on either side by zones up to 2.7m wide of sodic feldspar (Figure 4.7), minor quartz and occasional lepidolite.



Figure 4. 7: Image showing the core of feldspar with minor quartz and lepidolite illustrating the sharp contact with the greenstone. (GPS location: 35K 679463E 7644826N).

Quartz that is generally white, but occasionally bluish, occurs on the margins of the pegmatite dyke. This pegmatite has been further exposed by a series of shallow trenches dug at intervals of several hundreds of metres, for some considerable distance in a south westerly direction.

WITS
UNIVERSITY

CHAPTER 5

PETROGRAPHY

5.1 Introduction

Results derived from thin section observations, modal and bulk rock compositional analysis are presented in this chapter. The petrography encompasses the mineral compositions, textures, petrogenetic relationships and classifications. It embraces not only the systematic description of the rocks but also the origin of the pegmatites and relation to host rocks. The account is limited to the samples that were collected from the Mbeta area.

5.2 Modal Composition Analysis

The comparative abundance of main mineral components determined from counting a minimum of 400 points in each thin section was based on the Terry and Chillingar (1955) method. The principal minerals were quartz, albite and muscovite as shown in Table 5.1 and in Table 5.2 expressed as percentage.

Table 5. 1: Point counting was undertaken on 11 samples and this table shows the actual grains of minerals counted.

Sample	Quartz	Albite	Muscovite	Rutile	Topaz	Lepidolite	Garnet	Points
MB01	73	343	5	0	0	0		421
MB02A	83	331	7	0	0	0	16	437
MB02B	120	275	6	1	0	0		402
MB03	203	210	33	0	13	22		481
MB04	2	451	21	0	2	0		476
MB05A	148	175	126	0	0	4		453
MB05B	117	246	47	0	0	1		411
MB06	121	361	20	1	15	3		521
MBO7	50	343	30	0	0	0		423
MB08	444	8	1	0	0	0		453
MB09	136	151	117	0	0	10		414

Table 5. 2: Table showing modal composition expressed as a percentage from the results of point counting.

Sample	Quartz	Albite	Muscovite	Rutile	Topaz	Lepidolite	Garnet	Points
MB01	17.3	81.5	1.2	0	0	0		421
MB02A	18.9	75.8	1.5	0	0	0	3.8	437
MB02B	29.9	68.4	1.5	0.2	0	0		402
MB03	42.2	43.7	6.8	0	2.8	4.5		481
MB04	0.4	94.8	4.4	0	0.4	0		476
MB05A	32.7	38.6	27.9	0	0	0.8		453
MB05B	28.5	59.8	11.5	0	0	0.2		411
MB06	23.2	69.2	3.9	0.2	2.9	0.6		521
MBO7	11.8	81.2	7	0	0	0		423
MB08	98.1	1.7	0.2	0	0	0		453
MB09	32.7	36.4	28.6	0	0	2.3		414

Figure 5.1 shows the graphical representative of the modal composition analysis of the Mbeta samples. The analysis shows that quartz occurs in all the samples and is one the principal mineral averaging 11-43% and is highest in sample MB08 from the core of the pegmatite in the western pit, where it constitutes 98%.

Albite is dominant in all other samples ranging between 38-95%. Of note is sample MB04 which has 94.8% of plagioclase which was collected from the western pit of the Mbeta area and was from the contact of the pegmatite with the greenschist host rock. Outcrops of albite rich lithologies (“albitite”) are very common in both the western and northern Mbeta pits.

Muscovite also occurs in all the samples ranging from 1-27.9% with the highest percentage in sample MB05B.

Lepidolite occurs in sample MB03 and MB09 from the western pit, and MB05A, MB05B and MB06 from the northern pit. The highest proportion of lepidolite occurs in sample MB03 with 4.5%. Lepidolite is characteristic of the LCT family of pegmatites and is regarded as a complex type (rare element) according to the classification of Cerny (1991a).

Topaz occurs in samples MB03 and MB04 from the western pit and MB06 from the northern pit where it usually occurs in the core of the pegmatite. Garnets are only observed in sample MB02A from the western pit. Accessory garnets in pegmatites generally occur in the intermediate zone according to Whitworth and Rankin (1989) and Whitworth, (1992). Rutile occurs in MB02B (western pit) and MB06 (northern pit). From the modal composition analysis it is evident that all the pegmatite pits were represented and shows similarities in occurrence.

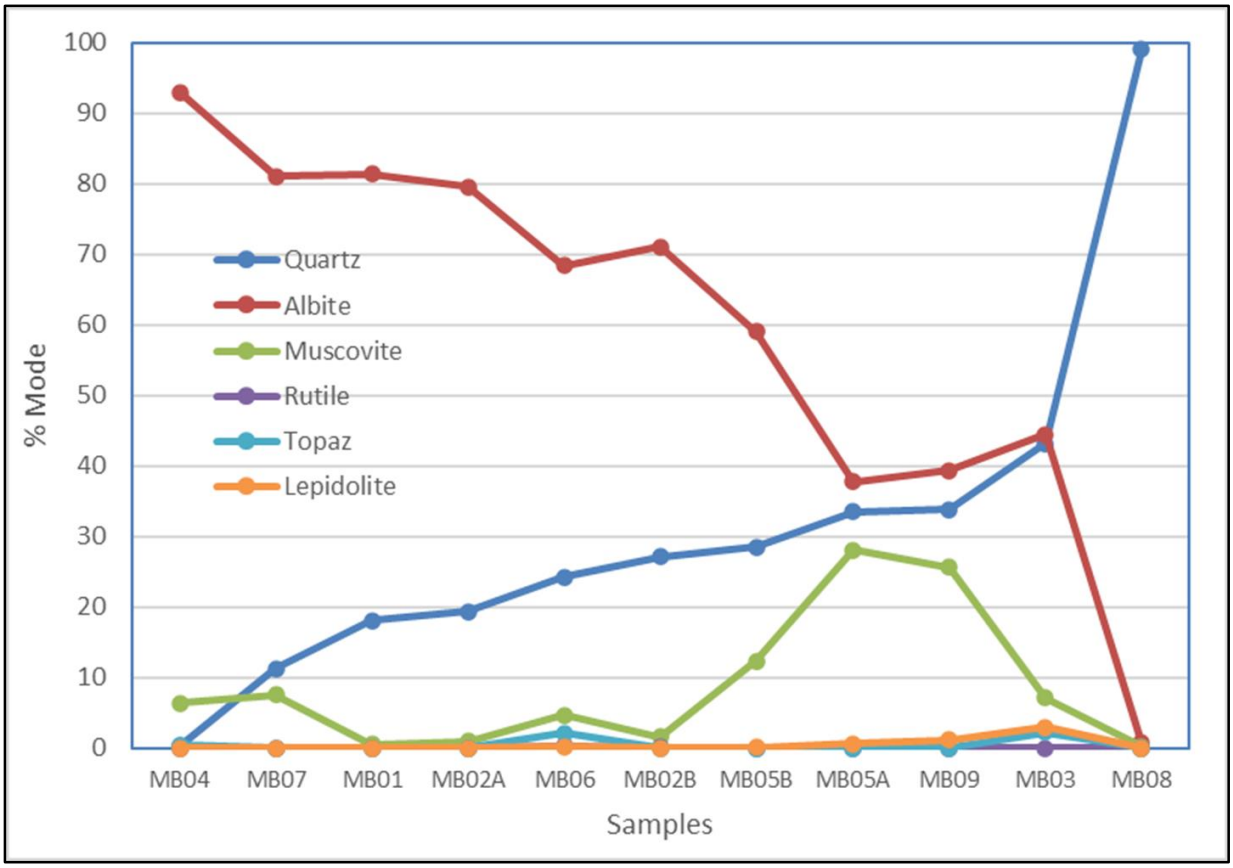


Figure 5. 1: The graphical representative of the modal composition analysis of the Mbeta samples.

5.3 Petrographic descriptions

In this section observations from the thin sections have been recorded together with photographs. Examination of rock thin sections provides useful detail regarding mineral identity, their generalised compositions, textures, distributions, structural setting and occurrence throughout the Mbeta pegmatites. Transmitted light microscopy makes use of both plane-polarised light (PPL) and cross-polarised light (XPL). The likely protoliths for the different lithologies will also be established, as well as a closer look at the ore minerals and how they are distributed throughout the samples.

The thin sections were grouped based on the mineralogical association. Details and descriptions of the samples are shown in Table 3.1 and the position from which the thin sections were taken is shown in Appendix B.

5.3.1 Mineralogy

Quartz

Quartz occurs in all the samples collected at Mbeta in the range 10-40%, except for albitite MB04 (<1% in Table 5.2) and the quartz core sample MB08 (99% in Figure 5.2). The quartz occurs as subhedral grains of approximately 5mm in size. They display 1st order greys in XPL with undulose extinction. Sample MB08 represents the core of the pegmatite in the western pit. According to Steiner (2019), it is assumed that this quartz core formed during the last stage of the pegmatite crystallisation process. Experiments by London and Morgan (2017) also demonstrate that the Li-rich melts, albite and lepidolite can follow the crystallisation of this pure quartz. The observation by London and Morgan (2017) is exhibited in the western pit where this quartz sample was collected, where zonation of quartz, feldspar and lepidolite is seen.

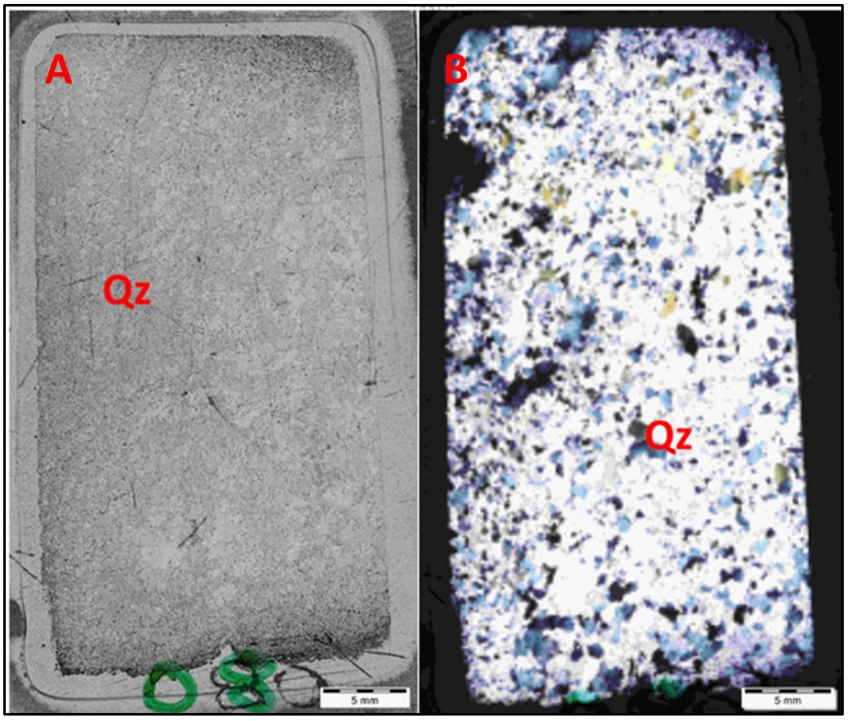


Figure 5. 2: Image showing the scanned thin sections of MB08 (western pit). (A) Is a plane polarised light showing quartz grains. (B) Is in cross polarised light showing the even granular texture of the grains.

Albite

Albite occurs in all the non-monomineralic samples ranging 36-82% (Table 5.2), to the virtual exclusion of K-Feldspar. Distinguishing features in thin section are typified by MB01 (Figure 5.3), where subhedral grains of albite show a cloudy turbid appearance in PPL and 1st order grey interferences shades in XPL, with polysynthetic albite twinning. Perfect cleavage is observed and extinction is oblique with cross-hatch twinning. The feldspar is porphyritic and sometimes displays skeletal or graphic intergrowths (Figure 5.3).

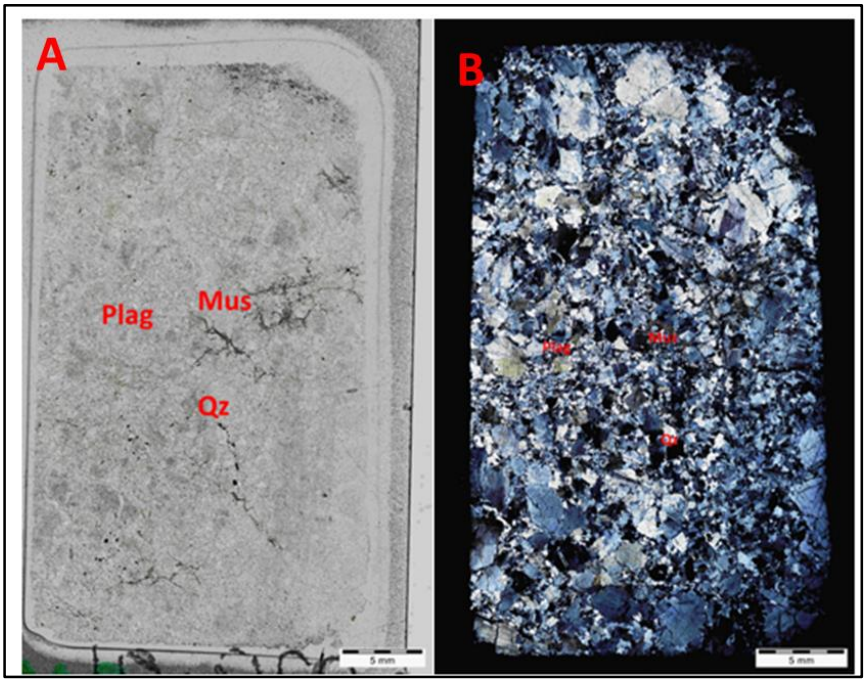


Figure 5. 3: Image showing the scanned thin section image that is rich in plagioclase, muscovite and quartz in thin section in MB01 (western pit). (A) Plane- polarised light (B) Cross- polarised light.

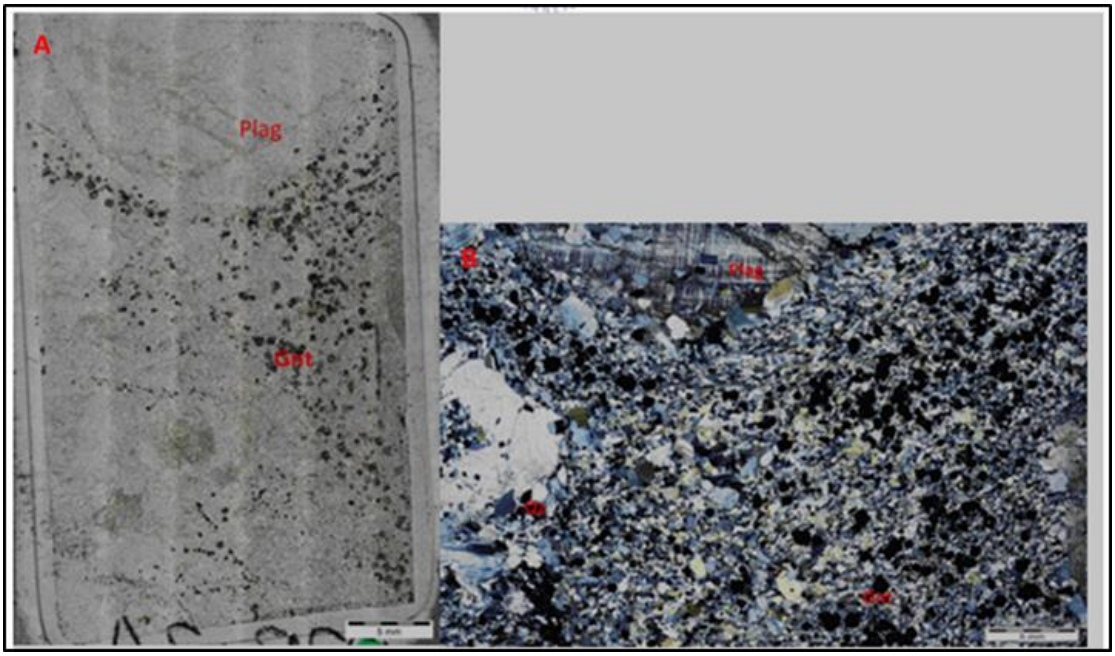


Figure 5. 4: Image of MB02A (collected from the western pit) showing albite exhibiting a wide range in grain size, shape, as well as skeletal and graphic intergrowths. (A) Plane polarised light (B) Cross- polarised light. Garnet also occurs in this sample and a grain showing isotropism is labelled.

Muscovite

Muscovite occurs in all the samples and shows a range of 1-30%. The muscovite is highly visible in samples such as MB04 (Figure 5.5), MB05A, MB05B, MB07 and MB09. In PPL muscovite is usually colourless but sometimes appears very pale green to light-brown. It displays 3rd order interference colours and thus has a birefringence which is very distinctive in XPL. At extinction the grains display the characteristic speckled pattern. Apart from massive patches of coarse flakes, muscovite also occurs as medium grained disseminations with quartz and albite. The muscovite is highly weathered in some parts especially the western pit and forms books. In the Cerny (1991a) classification which is based on depth of formation it states that elements such as Li, Be, V, REE, Ti, U, Th, Nb and Ta can enter the muscovite structure and/ or occur as discrete mineral species associated with muscovite-rich zones.

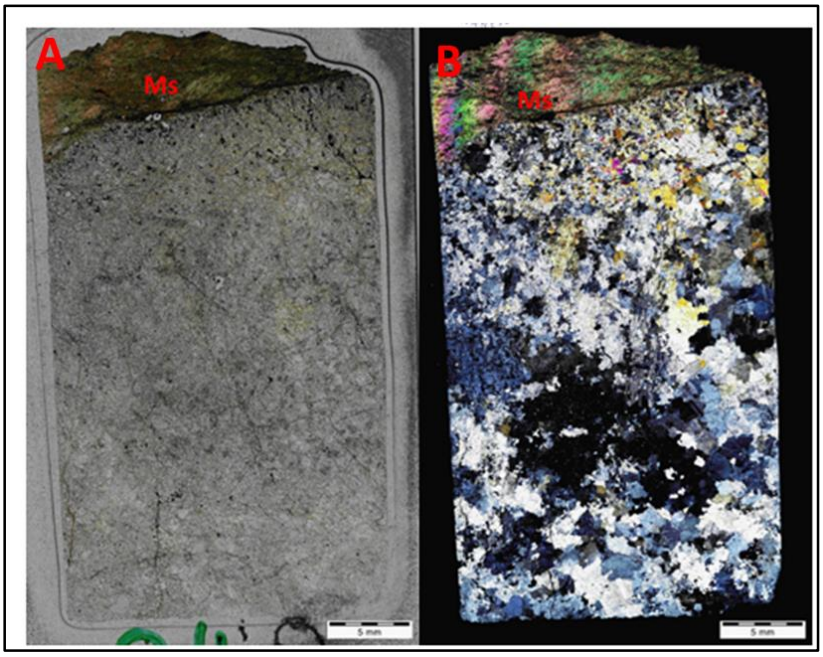


Figure 5. 5: Image showing scanned thin sections that include muscovite in MB04. (A) Plane polarised light. Note that muscovite is restricted to a massive lens at the top of the photo. (B) Cross- polarised light.

Lepidolite

Lepidolite is observed in sections MB03 (western pit), MB05A & MB05B (northern pit) and MB09 (western pit). Lepidolite is recognizable as having a lower birefringence in XPL than muscovite although it is difficult to differentiate between the two in PPL, as both are colourless. Modal analysis of the samples yielded an estimate of 0.2-4.5% lepidolite in the pegmatites. Lepidolite is the only ore mineral of Li observed in the samples. In hand specimens it is purplish. In the western pit, it is distinctive in that it is seen on the margins with quartz core and the greenschist. The presence of lepidolite in the pegmatites classifies the pegmatites to be of the LCT family of the complex type (Cerny, 1991)

Garnet

In MB02A from the western pit (refer to Figure 5.4), garnets are visible with the largest grain of 2mm. They occur as isometric grains with very high relief. They occur as inclusions in graphic intergrowth with quartz, muscovite, or feldspar. Garnets occur as accessory minerals in peraluminous granites and granitic pegmatites (Whitworth, 1992). They are indicators of physicochemical conditions of pegmatite formation (Sokolov and Khlestov, 1990). Garnets usually occur with quartz-feldspar associations just as in the Mbeta pegmatites. According to Whitworth (1992) and Whitworth and

Ranking (1989), garnetiferous pegmatites occur within the intermediate zone of the pegmatite dyke. Petrological observations indicate that the garnet-bearing pegmatites are affected by post magmatic deformation and metasomatism which is often is restricted to micro shear zones and fracture sets associated with them (Gharib, 2012).

Topaz

Topaz is observed in sections MB03 (western pit), MB04 (western pit) and MB06 (main pit). Topaz occurs as anhedral crystals (Figure 5.6) with perfect cleavage. It has a low birefringence (grey-white-yellow interference colours of the 1st order. Texturally, the Mbeta topaz appears intergrown with quartz and albite, a setting different from that reported by Simmons and Webber (2008) involving crystallisation in open or clay-filled voids in the cores of miarolitic pegmatites.

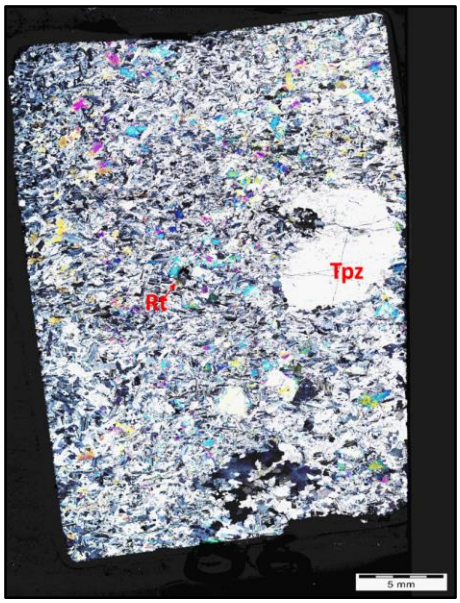


Figure 5. 6: Image showing scanned thin sections with large crystals of topaz in MB06 (main pit) in XPL.

Rutile

Rutile is observed in sample MB02B (western pit) and MB06 (main pit) (refer to Figure 5.6). Rutile exhibits high relief in PPL and straight extinction in XPL (Figure 5.6). While occurring at Mbeta as simple discrete grains, it can also appear as tiny rod-like inclusions in quartz. It occurs as an accessory mineral in trace amounts in the intermediate zone of the pegmatite dykes. Rutile occurs as euhedral to anhedral crystal associated with the alteration of microcline to quartz and muscovite.

5.4 Mineralogy using X-Ray Diffraction (XRD) analysis

X-ray diffraction (XRD) is a critical method in rock or soil mineralogical analysis. It is an analytical technique mostly used on a crystalline material to identify the phases present and can provide details on the unit cell dimensions (Lutterotti, 2009). It is used mainly to classify unknown crystalline materials (e.g., crystals, inorganic compounds). It is also possible to quantify the degree of crystallisation, as well as to distinguish different phases with similar compositions (Lutterotti, 2009).

XRD analysis was conducted by XRD Analytical and Consulting on 11 samples. The analysis identifies quantitative weight per cent of minerals in each sample. The weight per cent of minerals from XRD provide an alternative estimate to thin section modal analysis (area or volume per cent).

The bulk rock samples were crushed and milled into powder samples for analysis. The samples confirmed the presence of quartz, plagioclase (albite), muscovite, topaz, rutile and lepidolite as observed in the petrographic studies. A summary of the mineralogical composition of the samples from the XRD analysis is given in Table 5.3. The XRD scans of the Mbeta samples are presented on a diffractogram in Figure 5.7.

Table 5. 3: Percentage mineralogical abundances (%) of the Mbeta Pegmatites by XRD.

Sample No	Quartz	Albite	Muscovite	Rutile	Topaz	Lepidolite
MB01	18.1	81.4	0.5	0	0	0
MB02A	19.4	79.6	1	0	0	0
MB02B	27.1	71.1	1.6	0.1	0	0
MB03	43.2	44.5	7.1	0	2.2	3
MB04	0.3	93	6.4	0	0.4	0
MB05A	33.5	37.8	28.1	0	0	0.6
MB05B	28.5	59	12.3	0	0	0.1
MB06	24.3	68.4	4.7	0.3	2.1	0.2
MBO7	11.3	81.1	7.6	0	0	0
MB08	99.1	0.8	0.2	0	0	0
MB09	33.8	39.4	25.6	0	0	1.2

0=n.d. - not detected above the detection limit of 0.5-3 weight per cent.

From the analysis, it can be noted that albite is the most abundant mineral followed by quartz then muscovite. Rutile, topaz and lepidolite occur in minor amounts.

5.5 X-RAY Fluorescence (XRF) analysis

Upon excitation, by primary X-rays, chemical elements in a prepared sample will fluoresce secondary X-rays with characteristic energies and intensities proportional to their abundance (Verma, 2007).

The major element compositions of the Mbeta pegmatite samples are presented in Table 5.4. The LOI content of the samples shows a range of 0.08-2.24 wt. % and is consistent with the proportion of hydrous minerals (muscovite and lepidolite) present. No sample has an anomalously high LOI due to alteration of feldspar.

All samples are rich in SiO_2 and Al_2O_3 reflecting the mineralogy (quartz and feldspar) with the compositional ranges controlled by the modes. The contents of Na_2O, K_2O and CaO are particularly instructive in that they define the principal feldspar present in the Mbeta pegmatites. Generally Na_2O is much more abundant than K_2O and CaO suggesting that the principal feldspar is very sodic. Where K_2O is highest the samples concerned contain substantial mica (XRD results in Table 5.3), so assuming this mineral to contain 10% by weight K_2O, a correction results in an inferred feldspar composition of >80% albite component. It follows that the Mbeta pegmatites are distinctly albitic, with little or no K-feldspar present, at least in the samples so far collected and analysed.

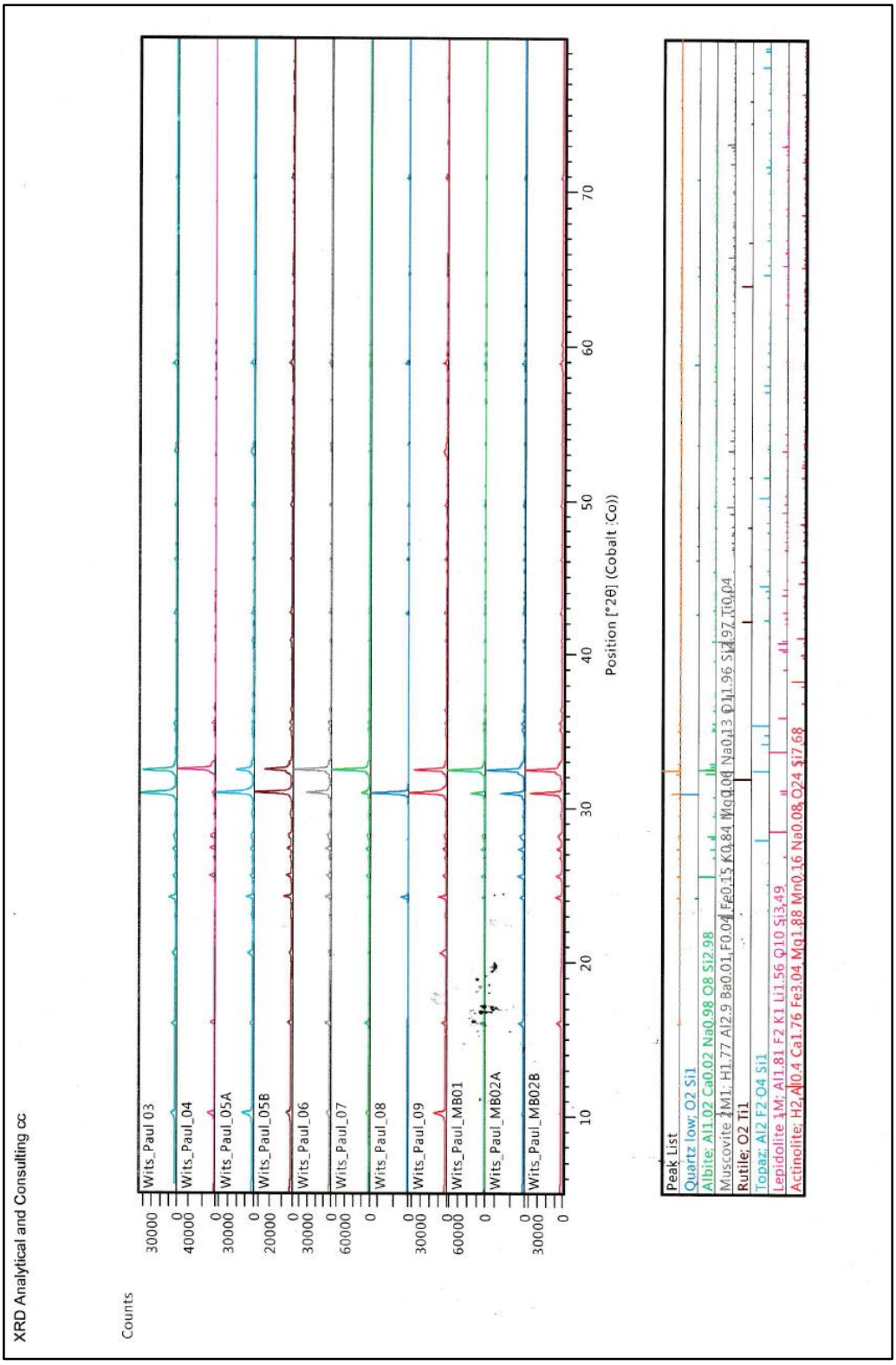


Figure 5. 7: Consolidated XRD scans of the Mbeta samples together with reference diffractogram of the principal minerals.

Table 5. 4: Table showing the major element (wt. % oxides) analysis of the Mbeta pegmatites.

Sample	**wt. %**	**MB01**	**MB02A**	**MB02B**	**MB03**	**MB04**	**MB05A**	**MB05B**	**MB06**	**MB07**	**MB08**	**MB09**
SiO_2	%	74.99	73.72	76.04	75.11	63.50	69.23	71.11	70.88	69.10	97.93	70.96
Al_2O_3	%	15.18	15.49	14.01	15.48	20.64	18.90	17.49	17.67	18.59	0.15	17.02
Fe_2O_3	%	0.50	1.07	1.49	0.36	1.46	0.25	0.53	0.71	0.76	0.89	0.28
MnO	%	0.01	0.26	0.52	0.05	0.04	0.23	0.10	0.25	0.48	0.01	0.25
MgO	%	0.14	0.04	0.05	0.03	1.30	0.04	0.04	0.02	0.03	0.00	0.05
CaO	%	0.27	0.42	0.36	0.09	1.61	0.04	0.09	0.12	0.12	0.02	0.04
Na_2O	%	8.83	8.61	7.39	4.23	9.57	3.84	5.81	6.32	8.77	0.01	3.50
K_2O	%	0.04	0.14	0.48	2.20	1.12	4.31	2.65	2.04	1.31	0.02	3.92
TiO_2	%	0.01	0.01	0.02	0.01	0.06	0.01	0.01	0.01	0.02	0.01	0.01
P_2O_5	%	0.02	0.03	0.03	0.02	0.05	0.01	0.02	0.04	0.04	0.01	0.02
Cr_2O_3	%	0.00	0.00	0.01	0.01	0.01	0.01	0.00	0.00	0.01	0.00	0.01
NiO	%	0.00	0.00	0.00	0.00	0.01	0.00	0.00	0.00	0.00	0.00	0.00
LOI	%	0.52	0.38	0.28	1.37	0.86	2.24	1.72	1.23	0.86	0.08	2.13
Total	**%**	**100.52**	**100.16**	**100.66**	**98.96**	**100.23**	**99.12**	**99.58**	**99.30**	**100.09**	**99.13**	**98.20**

CHAPTER 6

DISCUSSION

6.1 Introduction

Based on the field mapping, the Mbeta pegmatites appear to be emplaced into a photo lineament interpreted as a regional shear zone that traverses both the Lower Gwanda greenstones and the granitic gneisses (Figure 6.1). This setting fits with Selway et al (2005), in that rare-element pegmatites occur along large regional-scale faults in greenschist and amphibolite facies metamorphic terrains. The pegmatites intruded as veins and dykes into the greenstones and serpentinite but none have yet to be located in the granitic terrain to the south of the regional contact.

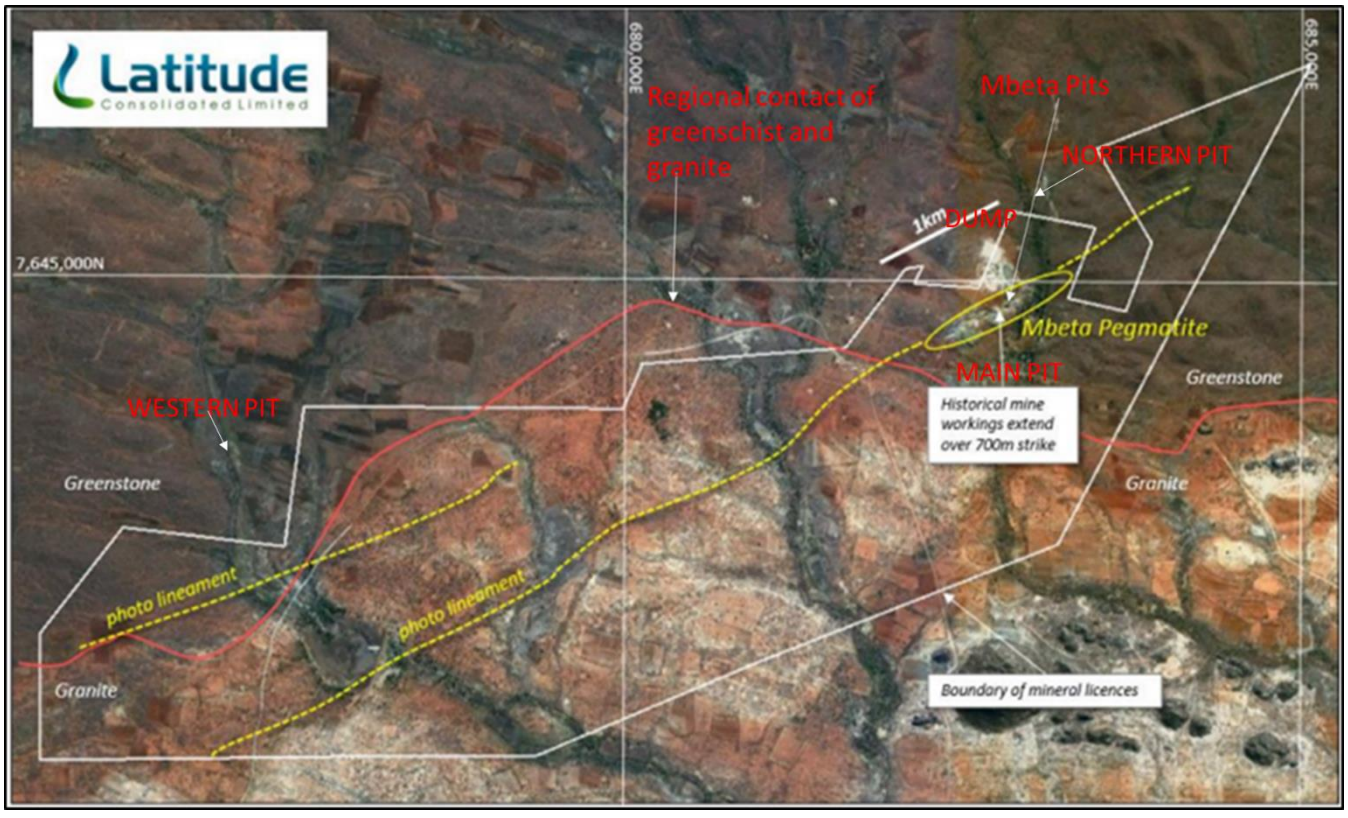


Figure 6. 1: Modified Mbeta photo showing boundary of mineral licences in which the samples were collected from, geological contacts and the location of the historical lithium pegmatite workings and associated photo lineament. (Adapted from the ASX Announcement Report. Burns, 2018)

The Mbeta pegmatites occur along the contacts of greenschist and amphibolite facies metamorphic terrains. The pegmatites consist of plagioclase and green muscovite (Figure 6.1) and this is fairly represented by the samples that were collected from both the northern pits and the western pits.

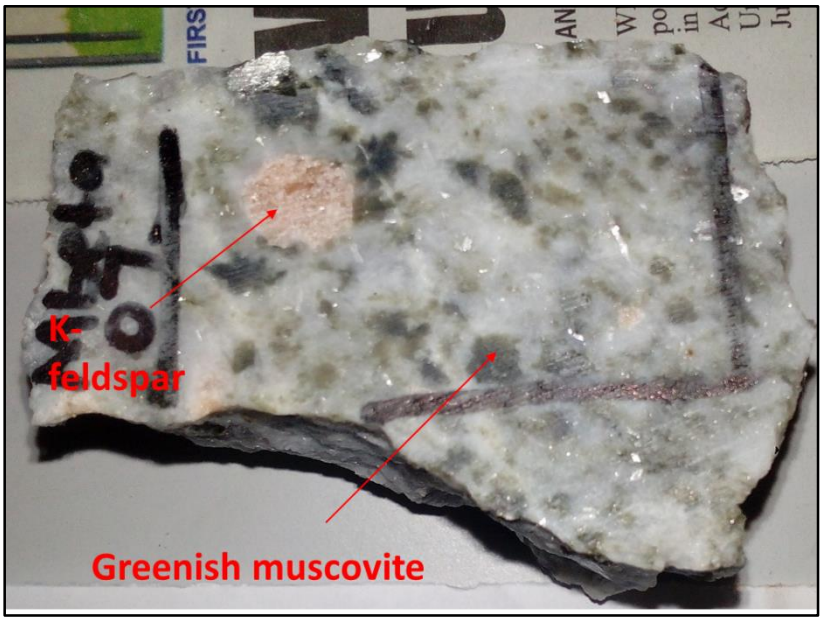


Figure 6. 2: Sample (MB07) from the main pit showing greenish tinted muscovite and K-feldspar. (GPS location: 35K 682438E 7644906N)

Rare-element enriched pegmatites contain one or more rare-element-bearing minerals, such as spodumene, petalite, lepidolite, tourmaline, Cs-bearing beryl, Ta-oxide minerals or pollucite. (Selway et al, 2005). The Mbeta pegmatites samples displayed evidence of lepidolite although the XRD and modal analysis only noted it as minor in abundance with the highest of 3% in sample MB03 (western pit) and 0.2% in sample MB06 (northern pit) according to the XRD analyses.

6.2 Mineralogy

6.2.1 Significance of Albite

The mineralogy of the Mbeta pegmatites is fairly typical for granitic pegmatites with dominantly plagioclase and quartz and accessory muscovite and minor lepidolite. Plagioclase feldspar is almost always albite, and K-feldspar, when present, is identified as microcline, and is locally interstitial to quartz.

With the exception of two near monomineralic samples MB04 (albitite) and MB08 (massive quartz) all the Mbeta pegmatites analysed are quartz- albite- mica assemblages with little or no K-feldspar present. Hand specimen examination alone rarely provides enough information for positive feldspar identification. Thin section microscopy and even quantitative XRD allows more detail but still ambiguity remains concerning the distinction between certain alkali feldspars. As reported in section 5.5 the Mbeta samples all have very low K_2O, and what is there needs to be included in the mica content before allocation to feldspar.

Albite pegmatites such as those established at Mbeta are an integral component of many associations, featuring in most published classification schemes cited in Chapter 2. In particular, they represent the main ore- bearing zone of Bikita (Gallagher, 1975). The XRD mineralogy and major oxide data can be used to compare pegmatite compositions in terms of their quartz and feldspar contents (Figure 6.2). Mbeta all plot close to the Quartz- Albite (Qz- Ab) boundary, with very low contribution from K-Feldspar (Or). Bikita and other Zimbabwean pegmatite localities show a different distribution, some with appreciable Or component that allows the bulk compositions to plot in the granite minimum zone and would be equivalent to true granitic magmas. Notably the Bikita samples have no feldspar at all and these represent the Li- rich ore zone hosts.

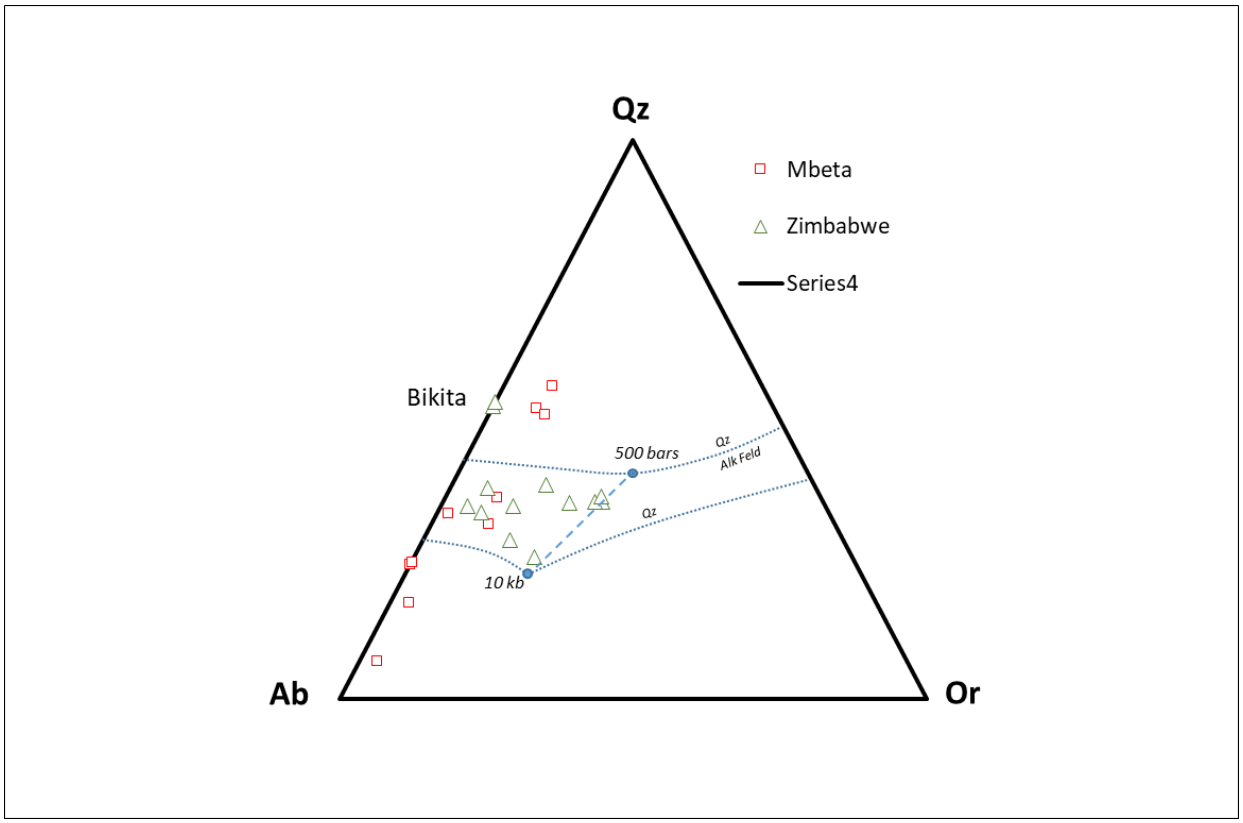


Figure 6. 3: Manipulation of the modal, XRD and XRF tables, together with data from the Bikita literature. The data as a ternary plot showing the Ab rich nature of Mbeta compared with published data from Bikita and other sites in Zimbabwe.

Since albite pegmatites (and albitite granites/ aplites for that matter) cannot represent crystallised magmas, they have been subjected to much attention in the petrological literature. There have been three main models suggested for their origin, including (1) fractional crystallisation and accumulation of sodic plagioclase within certain zones of pegmatite bodies; (2) post- magmatic replacement of two feldspar granite assemblages by Na- rich hydrothermal solutions (Albitisation); and (3) loss of K preferentially into a separated vapour phase during pegmatite crystallisation (Barros et al, 2020; Steiner, 2019; Simmons and Webber, 2008). Albite replacement processes seem to be favoured in many pegmatite descriptions, and considered essential for ore deposit concentration, most significantly at Bikita.

6.2.2 Ore minerals

Lepidolite is rare in the Mbeta pegmatite with a percentage ranging from 0.1-3% from the XRD analyses of representative samples. The mineral occurs mostly in the granular forms though some curved and globular crystals have been found. In both the western pit and the northern pits, zones with lepidolite have been exposed and are highly visible by naked eye for mining and further collection of samples for further analysis.

The colour of lepidolite varies from lavender to purple in the western pit (refer to Appendix A sample MB03) to pinkish especially in the northern pits (refer to Appendix A sample MB06). The granular varieties commonly show some admixture of quartz and muscovite.

Garnets were seen under the microscope in sample MB02A (refer to Appendix C sample MB02A) but were not detected in the XRD analysis. The presence of garnets indicates that the garnet bearing pegmatites are affected by post magmatic deformation and metasomatism which is often is restricted to micro shear zones and fracture sets associated with them (Gharib, 2012) and this can be supported by the Mbeta pegmatites occurring along large regional-scale faults in greenschist and amphibolite facies metamorphic terrains.

Topaz was detected in all the analysis, i.e. XRD, modal composition analysis and petrography. Topaz is usually found in the core of the pegmatite.

6.3 Economic Aspect

In the 1950s, investigations were undertaken to determine the lithium content in the Mbeta pegmatites and the following data was supplied by Mr Young (Goldberg, 1963);

A trial lot analysis by Jan de Poorter is presented in Table 6.1.

Table 6. 1: Table showing analyses and assays by Jan de Poorter (Goldberg, 1963).

Li_2O	4.54%
Fe_2O_3	0.42%
MnO	0.12%
Cr_2O_3	Nil
K_2O	8.96%
F	6.80%
SnO	Nil

Poote Minerals Co. Philedelphia USA carried out an assay on 100 tonnes lot of cobbled lepidolite and the result was 4.34 Li_2O% (Goldberg, 1963). In 1959, the Mines department assayed a lepidolite concentrate and the result was 4.70% Li_2O (Goldberg, 1963). In 1957, Booth et al., analysed of a sample of the ore as shown in Table 6.2;

Table 6. 2: Table showing analysis by Booth, Garnett and Blair (Goldberg, 1963).

Li_2O	4.86%
Fe	0.04%
Mn	0.3%
Sn	Less than 0.01%
Cr	0.01%

Poote Minerals of Philadelphia carried out a number of tests on the ore in 1957/1958. The results were are shown in Table 6.3, 6.4 and 6.5;

Table 6. 3: Table showing analysis by Messrs, Poote Minerals, Philadelphia, on a sample of 115.5 tonnes

Sample Number	Tonnage	Li_2O %
1	115.5	4.8

Table 6. 4: Table showing analysis by Messrs, Poote Minerals, Philadelphia on three samples.

	Sample 1	Sample 2	Sample 3
Li_2O%	5.33	4.8	2.77

Table 6. 5: Table showing analysis by Messrs, Poote Minerals, Philadelphia on a sample of 115.5 tonnes.

Fe	0.05%
Mn	0.33%
Sn	0.01%
Cr	0.002%

A sample sent to Booth et al., in 1958 gave 50.01% Ta_2O_5.

In 1958, Barclay Bank Bulawayo detected 70.76% combined pentoxides of tantalum and niobium in a sample of concentrate. Aliquots of the sample were forwarded to Daniel Griffiths of Benedict, Kitto and Sons, London and the following were the results in Table 6.6.

Table 6. 6: Analyses by Daniel Griffiths, London, Bennedict Kitto and Sons (Goldberg, 1963).

	Kitto	**Griffiths**
Ta_2O_5	54.80%	56.50%
N_2O_5	10.57%	8.9%
TiO_2	1.36%	1.36%
SnO_2	9.14%	8.50%

A chemical analysis by the Government Chemical Laboratory in Harare in 1995 (Dube, 1995) of bulk samples collected from Mbeta showed very low percentages of LiO_2 ranging from 0.23%-0.32%. The tantalum and tin results also were very low as compared to the percentages that were reported by Benedict Kitto and Sons.

Table 6. 7: Results of the chemical analyses on bulk samples at Mbeta in May 1995. (Dube, 1995).

	Sample No 1247	**Sample No 1248**	**Sample No 1249**	**Sample No 1250**
Li_2O	0.29	0.32	0.23	0.23
Ta_20_5	0.98	1.22	1.34	0.90
$Sn0_2$	0.39	0.60	0.54	0.44
Mg0	0.09	0.05	0.06	0.55
K	0.76	0.16	0.20	?
Fe	Trace	Trace	Trace	Trace

Bulk samples collected by Dube and sent to the Government Chemical Laboratory in Harare for assaying had the following results; Li_2O 0.8% and Ta_2O_5 2.19%.

Although the Mbeta claims are believed to be good reserves of lepidolite, results of the current study on the ore are poor and far below the 4-5% of Li_2O specified by Minerals Marketing Cooperation of Zimbabwe (Dube, 1995). This is also contrary to the results of analyses done in the past where Li_2O ranged from 2.5%-6.2% with most in the region of 4.5%.

From the analyses, interesting amounts of Ta_2O_5 of up to 70.76% in the concentrate samples are obtained which could mean that if the pegmatites are studied further, there might be a possibility of a good deposit for tantalum though the analysis done at Mbeta for this study did not show any Ta_2O_5 enrichments.

However, the Mbeta pegmatites could be a source for mining feldspar because of the high plagioclase content, although this would only be a viable proposition if there is a local ceramics industry for the production of white products such as sinks and toilet basins.

CHAPTER 7

CONCLUSIONS AND RECOMMENDATIONS

The present study shows that the pegmatites at Mbeta are broadly granitic but albite-rich and were intruded into the basement greenstone-granite gneiss terranes underlying SW Zimbabwe. The pegmatites occur as veins and dykes in a well-defined $N60^0$ E trending belt.

The petrology and mineralogy studies revealed that the Mbeta pegmatites are dominated by quartz and albite-plagioclase with minor muscovite, lepidolite and accessory minerals such as garnets, topaz and rutile. This albite-rich signature is probably a response to late stage post-magmatic replacement processes, that was associated with the development of rare-element mineralisation (lepidolite), reminiscent of the Li-rich ore zones known at Bikita.

The XRD analyses also corresponded to the petrological interpretation except for the inability to detect the garnets which were noted in hand specimens and thin sections. This was because of overlapping intensity peaks with the peaks of the main minerals (Husebo and Sorensen, 2012). The lepidolite was detected in the samples and it is a good indicator that incompatible elements that are of economic significance such as Li, Ta and Nb may be present. From the previous analyses and assays done on the deposit in the 1950s and 1995, the Mbeta deposit shows potential to host such rare earth elements.

The following recommendation is worth considering;

> Geochemical analyses of more samples from the Mbeta pegmatites should be made in a systematic manner with samples representing different pegmatite zones so that mineral occurrences can be related to each location. In particular a more systematic approach for tantalum should be undertaken as the lepidolite content appears too low to be of economic significance by itself. Similarities with certain albite pegmatites at Bikita suggest that Mbeta is a potential target.

WITS
UNIVERSITY

REFERENCES

Baldock, J. W., Styles, M. T., Kalbskopf, S., Muchimwe, E., 1991. The Geology of the Harare Greenstone Belt and the Surrounding Granitic Terrain. Zimbabwe Geological Survey Bulletin 94.

Bartholomew, D.S., 1990. Base Metal and Industrial Mineral Deposits of Zimbabwe. Mineral Resources Series. 22, 1-157.

Bastin, E. S., 1911. Geology of the pegmatites and associated rocks of the Maine including Feldspar, Quartz, Mica and gem deposits. Departmet of Interior United States Geological Survey, Bulletin 445.

Bradley, D.C., McCauley, A. D., Stillings, L. M., 2010. Mineral Deposit Model for Lithium- Cesium-Tantalum Pegmatites. Departmet of Interior United States Geological Survey.

Brown, G. E. Jr., 1982. The mineralogy of pegmatites. American Mineralogist, Volume 67, pg 180- 189.

Brown, G. E., Ewing, R. C., 1986. Introduction to the Jahn Memorial Issue. American Mineralogist. Vol 71. 233- 238.

Bruker, 2011. Rietveld Method for Quantitative Phase Analysis. Advanced XRD workshop.

Burns, S., 2018. Latitude to Acquire Mbeta Lithium Project in Zimbabwe. ASX Anouncement.

Cerny, P., 1991. Rare-element Granitic Pegmatites. Part 1: Anatomy and Internal Evolution of Prgmatite Deposits. Geoscience Canada Vol 18 No. 2. 49-67.

Cerny, P. Fertile granites of Precambrian rare-element pegmatite fields: Is geochemistry controlled by tectonic setting or source lithologies? Precambrian Res. 1991, 51, 429–468.

Cerny, P., Anderson, A. J., Tomascak, P. B., Chapman, R., 2003. Geochemical and Morphological features of Beryl from the Bikita Granitic Pegmatite, Zimbabwe. The Canadian Mineralogist Vol 41 pp 1003- 1011.

Cerny, P., Ercit, T. S., 2005. The classification of granitic pegmatites revisited. The Canadian Mineralogist, Volume 43, 2005- 2026.

Cerny, P., Ferguson, R, B., 1972. The Tanco pegmatite at Bernic lake, Manitoba IV. Petalite and spodumene relations. Canadian Mineralogist. Vol II, 660- 678.

Chayes, F. 1949. A simple point counter for thin section analysis. American Mineralogist, 34, 1–11.

Dill, H.G., 2015. Pegmatites and aplites: Their genetic and applied ore geology. Ore Geol. 69, 417–561.

Djerdj, 2019. Rietveld Refinement in the Characterisation of Crystalline Minerals.

Dobelin, N., 2015. XRD and Rietveld Refinement. RMS Foundation. Lession 1.

Dube, 1995. Geological Report Note on the Mbeta 2 Mine. Geological Survey of Zimbabwe. Unpublished.

Goldberg, I., 1963. Notes on the Mbeta Mine, Gwanda Native Reserve, Gwanda District. Geological Survey report. 8, 1-3. Unpublished.

Genuino, V. A., Santos, L. C. M. L., Vieira, F. F., Sales, E. D. G., Vidal, F. W. H., 2016. 24th World Mining Congress, 99-107.

Harraz, H. Z., Aly, A. M., 2004. Graphic quartz-feldspar intergrowths in pegmatites: Diffusion and growth kinetics Migif- Hafafit Area, South Eastern Desert Egypt. Al- Azhar Bull. Sci. Volume 15, No 1 (June), 83- 98.

Kinnaird, J., 2018. Lecture 6. Pegmatites and IOCG, 1-20.

Landes, K. K., 1933. Origin and Classification of Pegmatites (Concluded), 95-103.

Larrea, M. L., Martig, S. R., Castro, S. M., Aliana, P.A., Bjerg, E. A., 2010. A Point Counting application for Petrographic Thin Sections.

Linnen, R. L., Lichtervelde, M. V., Cerny, P., 2012. Granitic pegmatites as sources of strategic metals. Elements, Volume 8, 275-280.

Locket, N. H., 1979. The Geology of the around Dett. Rhodesia Geological Survey Bulletin No. 85.

London, D., 2005. Granitic pegmatites: An assessment of current concepts and directions for the future. Lithos 80, 281–303.

London, D., 2008. Pegmatites. Can. Mineral. 10, 368.

London, D.; Morgan, G.B., VI. Experimental Crystallization of the Macusani Obsidian, with Applications to Lithium-rich Granitic Pegmatites. J. Petrol. 2017, 58, 1005–1030.

London, D., 2018. Ore–forming processes within granitic pegmatites. Ore Geol. Rev., 101, 349–383.

Lutterotti, 2009. Introduction to Rietveld Refinements.

McKeough, M. A., Lentz, D. R., McFarlane, C. R. M., Brown, J., 2013. Geology and evolution of pegmatite- hosted U- Tho± REE –Y-Nb mineralisation. Kulyk, Eagle and Karin Lakes region, Wollaston Domain, northern Saskatchewan, Canada; examples of dual role of extreme fractionation and hybridisation processes. Journal of Geosciences, 58 (2013), 321- 346.

Müller A., Simmons W., Wise M., Thomas R., Martin R., Beurlen H., Ihlen M.P., 2014. Initiative of anew classification of pegmatites – a review of initial thoughts. Abstract Volume of the 21st General Meeting of the International Mineralogical Association 1 to 5 September 2014, Johannesburg, South Africa, p. 260

Müller, A.; Simmons, W.; Beurlen, H.; Thomas, R.; Ihlen, P.M.; Wise, M.; Roda-Robles, E.; Neiva, A.M.R.; Zagorsky, V., 2018. A proposed new mineralogical classification system for granitic pegmatites; Part I, History and the need for a new classification. Can. Mineral. 56, 1–25.

Mukandi, M. A., 2009. Tin and Tantalite deposits of Zimbabwe.

Norton, J.J., Redden, J. A., 1990. Relations of zoned pegmatites to other pegmatites, granite, and metamorphic rocks in the Southern Black Hills, South Dakota, 631-655.

O'Connor, B., Raven, M., 1988. Application of the Rietveld Refinement Procedure in Assaying Powdered Mixtures. Power Diffraction. Vol 3.

Partington, G.A, 1995. McNaughton, N.J.; Williams, I.S. A review of the geology, mineralization, and geochronology of the Greenbushes Pegmatite, Western Australia. Econ. Geol. 90, 616–635.

Phaup, A.E., 1932. The Geology of the Lower Gwanda Gold Belt. Geological Survey Bulletin Number 24.

Robb, L., 2005. Introduction to Ore- Forming Processes, 93- 95.

Romer, R.L.; Kroner, U. Phanerozoic tin and tungsten mineralization—Tectonic controls on the distribution of enriched protoliths and heat sources for crustal melting. Gondwana Res. 2016, 31, 60–95.

Selway, J.B., 2005. Breaks, F.W.; Tindle, A.G. A Review of Rare–Element (Li–Cs–Ta) Pegmatite Exploration Techniques for the Superior Province, Canada, and Large Worldwide Tantalum Deposits. Explor. Min. Geol. 14, 1–30.

Shaw, R.A.; Goodenough, K.M.; Roberts, N.M.W.; Horstwood, M.S.A.; Chenery, S.R.; Gunn, A.G. Petrogenesis of rare-metal pegmatites in high-grade metamorphic terranes: A case study from the Lewisian Gneiss Complex of north-west Scotland. Precambrian Res. 2016, 281, 338–362.

Simmons, W. B. S., Webber, K. L., 2007. Granitic Pegmatites: State of the art.

Sitando (2012). Beneficiation of Zimbabwe Petalite: Extraction, Purification and Compound Synthesis.

Steiner, B. M., 2019. Tools and Workflows for Grassroots Li-Cs- Ta (LCT) Pegmatite Exploration.

Stewart, D. B., 1978. Petrogenesis of lithium- rich pegmatites. American Mineralogist, Volume 63, 970-980.

Swanson, S. E., Veal, W. B., 2010. Mineralogy and petrogenesis of pegmatites in the Spruce Pine District, North Caroline, USA. Journal of Geosciences, 55, 27-42.

Sweetapple, M.T., 2017. Granitic pegmatites as mineral systems: Examples from the Archaean. NGF Abstract. Proc, 2, 139–142.

Tyler, R., 2017. Development of the Arcadia Lithium Project. Prospect Resources Limited. Investor Presentation.

Verma, H.R, 2007. Atomic and Nuclear Analytical Methods. XRF, Mossbauer, XPS, NAA and B63lon-Beam Spectroscopic Techniques.

Watson, R. L. A., 1962. The Geology of the Kamativi and Lubimbi Areas. Southern Rhodesia Geological Survey Bulletin No. 57.

Whitworth, M., 1992. Petrogenetic implications of garnets associated with lithium pegmatites from SE Ireland. Mineralogical Magazine. Vol 56, 75- 83.

Wilson, A.H. A chill sequence to the Bushveld complex: Insight into the first stage of emplacement and implications for the parental magmas. J. Petrol. 2012, 53, 1123–1168.

Wilson, J. F., Martin, H. J., 1963. The Geology of the Country around Fort Victoria. Southern Rhodesia Geological Survey Bulletin No. 58.

APPENDIX A

SAMPLING

This appendix shows the sample images that were taken and their descriptions showing the location in which they were collected from. Samples were collected based on lithological and textural differences.

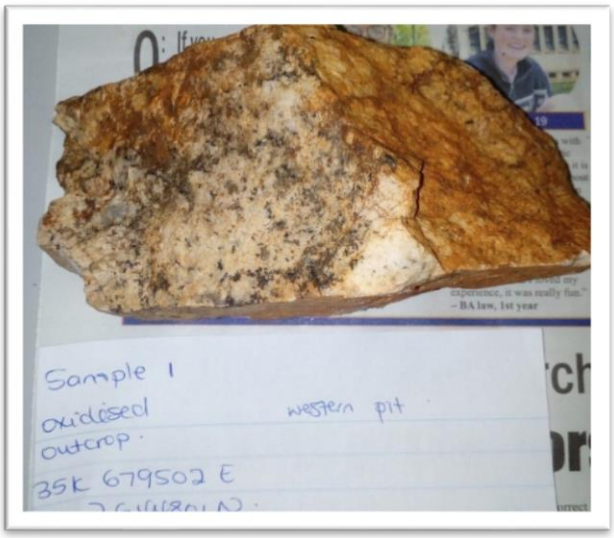


Figure A. 1: Image (MB01) showing oxidised outcrop from Western Pit. (GPS Location: 35K 679502E 7644801)

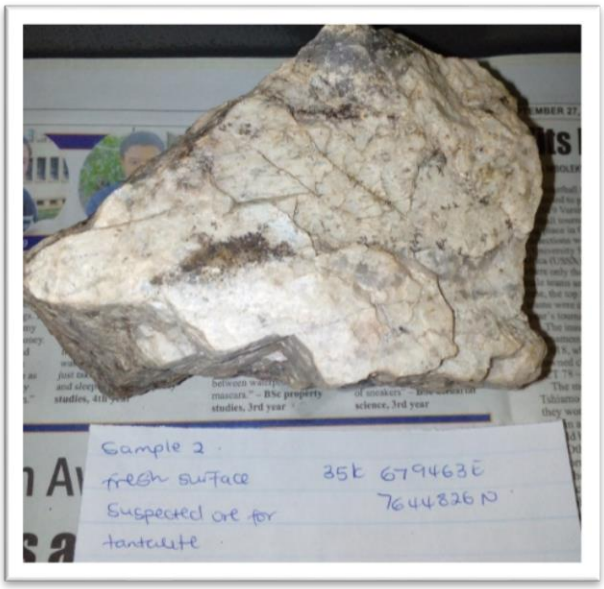


Figure A. 2: Image (MB02) showing fresh sample of pegmatite from the Western pit (GPS Location: 35K 679463E 7644826N)



Figure A. 3: Image (MB03) showing lepidolite from the Western pit. The lepidolite sample exhibits greenish micas. (GPS Location: 35K 679529 E 7644 816N).

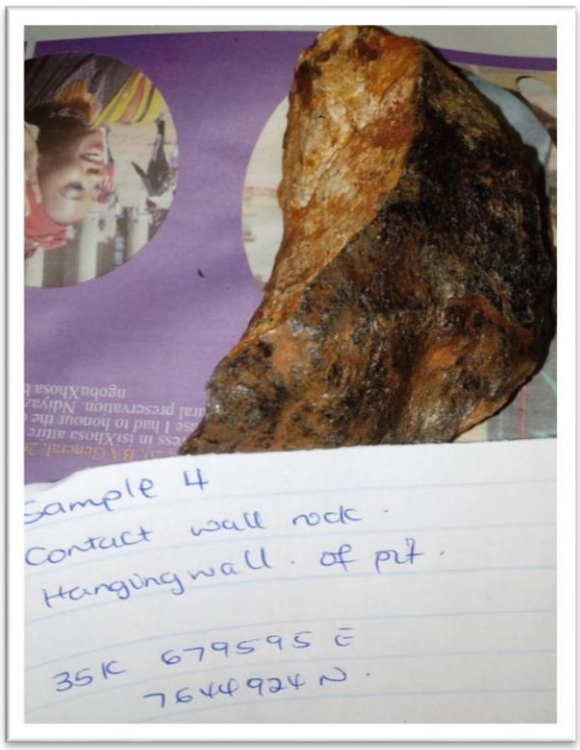


Figure A. 4: Image (MB04) showing the contact of the pegmatite zone and the greenschist zone in the western pit. (GPS Location: 35K 679595E 7644924N).

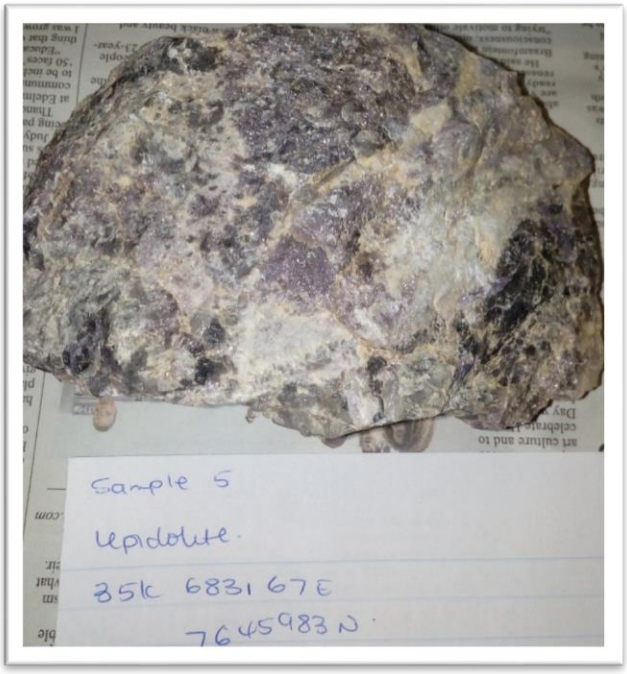


Figure A. 5: Image (MB05) showing the lepidolite sample from the northern pit. (GPS Location: 35K 683167E 7645983N).

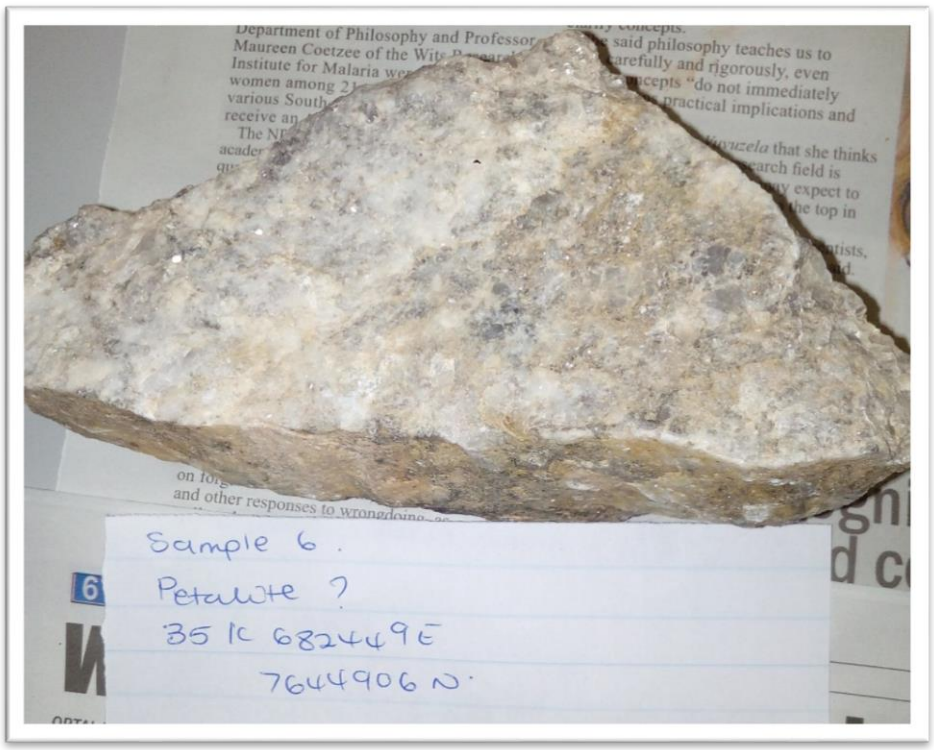


Figure A. 6: Image (MB06) showing a lepidolite sample from the main pit. (GPS Location: 35K 682449E 7644906N).

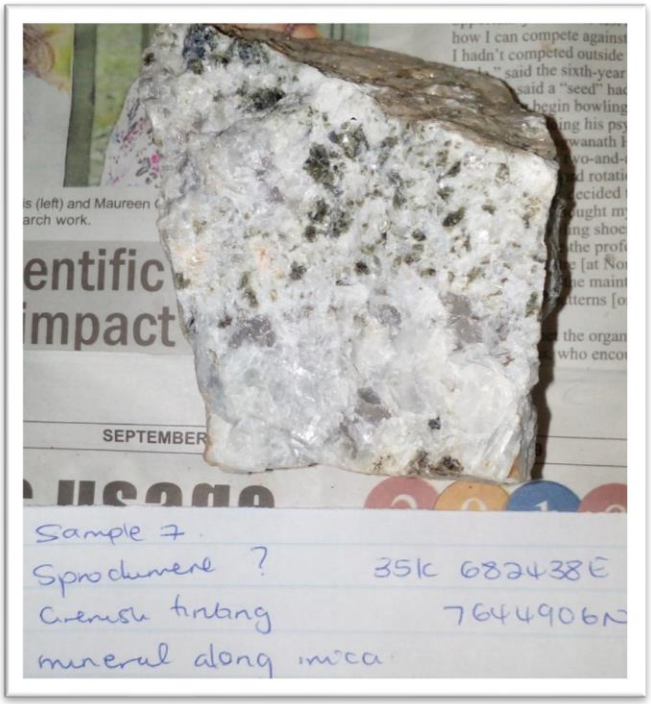


Figure A. 7: Image (MB07) showing a pegmatite sample with greenish micas from the main pit. (GPS Location: 35K 682438E 7644906N).

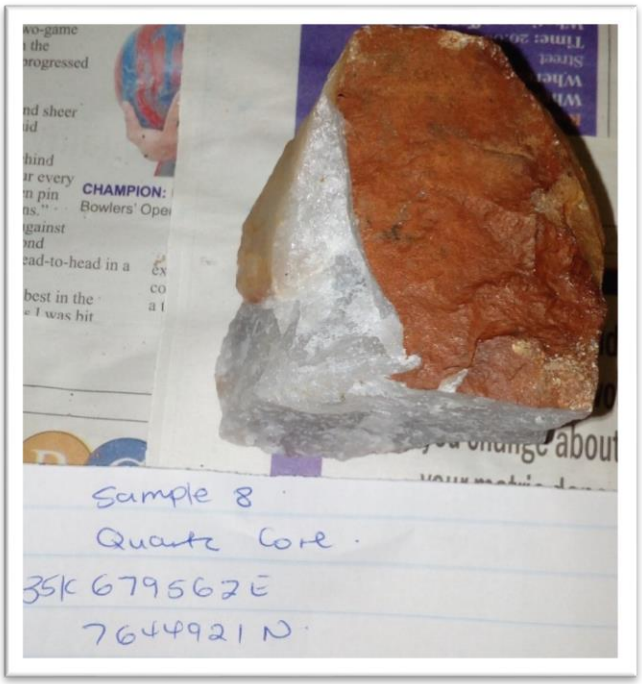


Figure A. 8: Image (MB08) showing the quartz core from the northern pit. (GPS Location: 35K 679562E 7644921N).

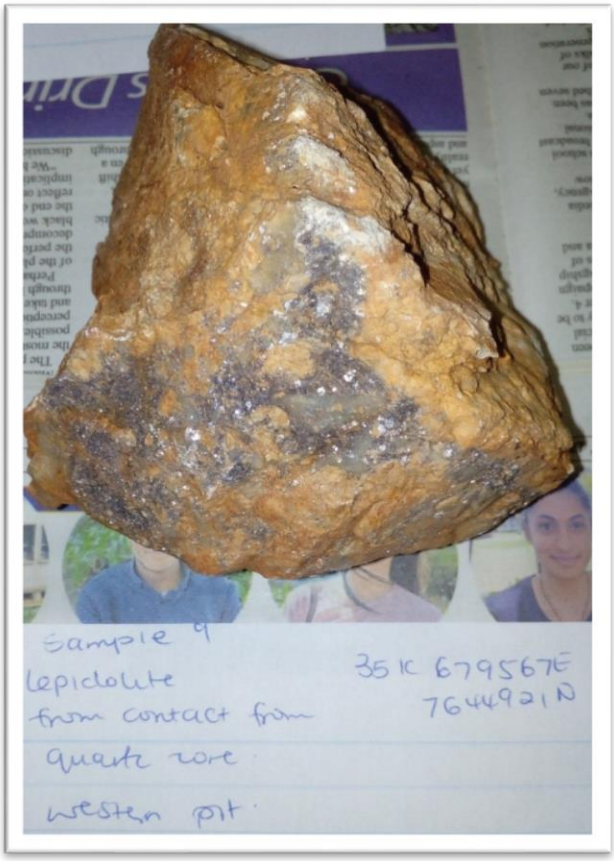


Figure A. 9: Image (MB09) showing the lepidolite quartz contact from the western pit (GPS Location: 35K 679567E 7644921N).

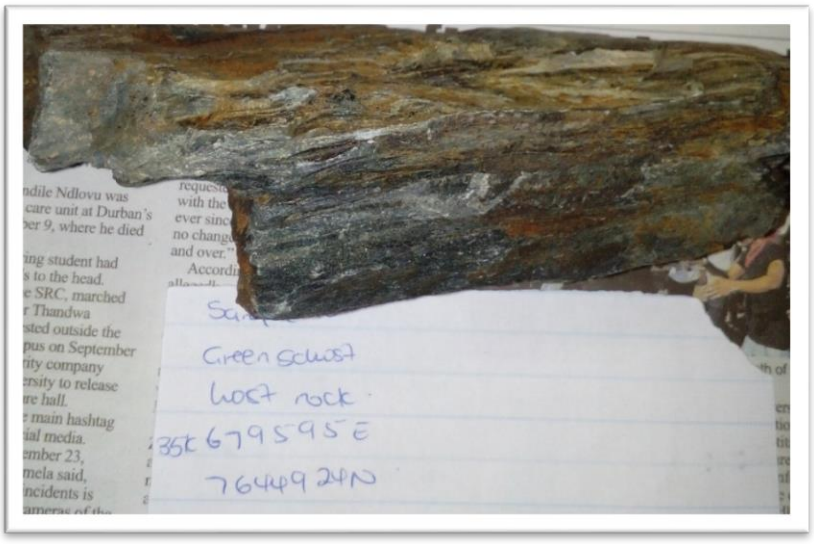


Figure A. 10: Image (MB10) showing the green schist host rock form the western pit. (GPS Location: 35K 679595E 7644924N)



Figure A. 11: Image (MB11) showing sands from the dump north of the northern pits.

WITS
UNIVERSITY

APPENDIX B

SAMPLE PREPARATION FOR THIN SECTIONS

This appendix shows the samples that were collected from Mbeta and being cut for thin sectioning on areas that are petrological and mineralogical exciting.

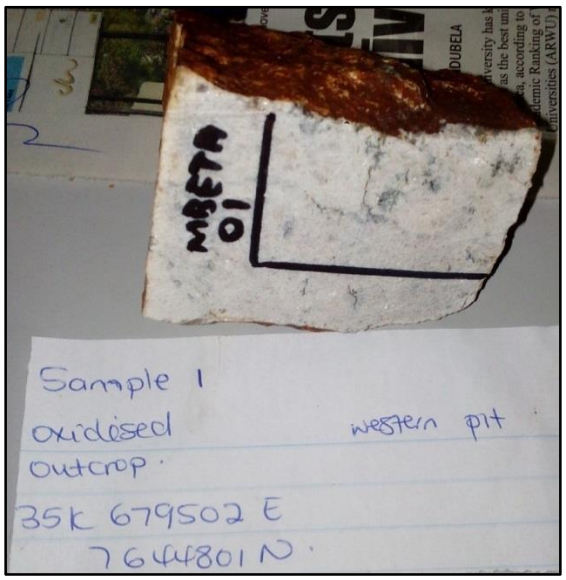


Figure B. 1: Sample number MB01.

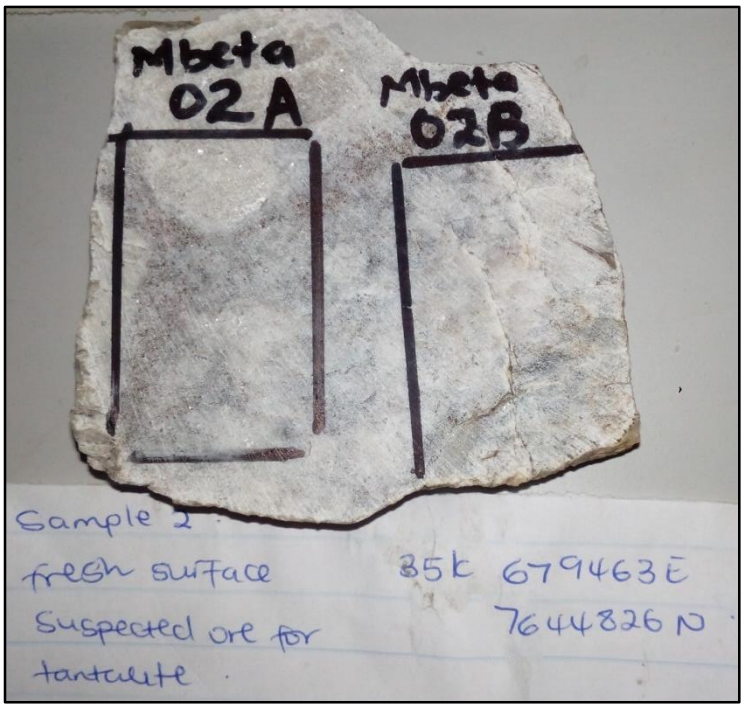


Figure B. 2: Sample number MB02A and MB02B

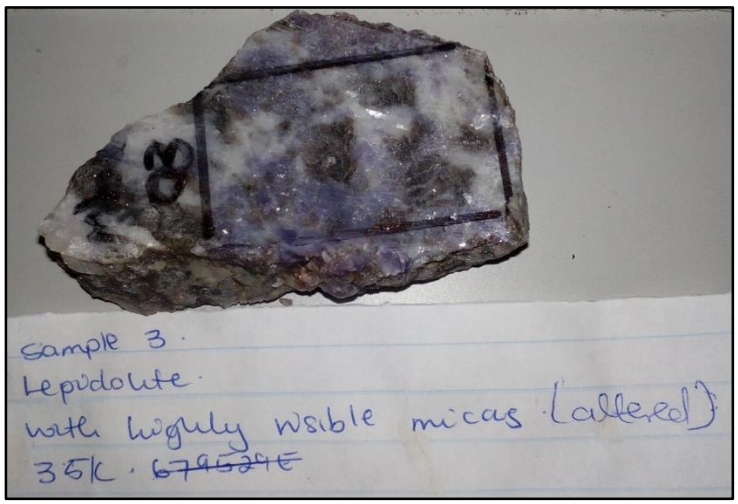


Figure B. 3: Sample number MB03.

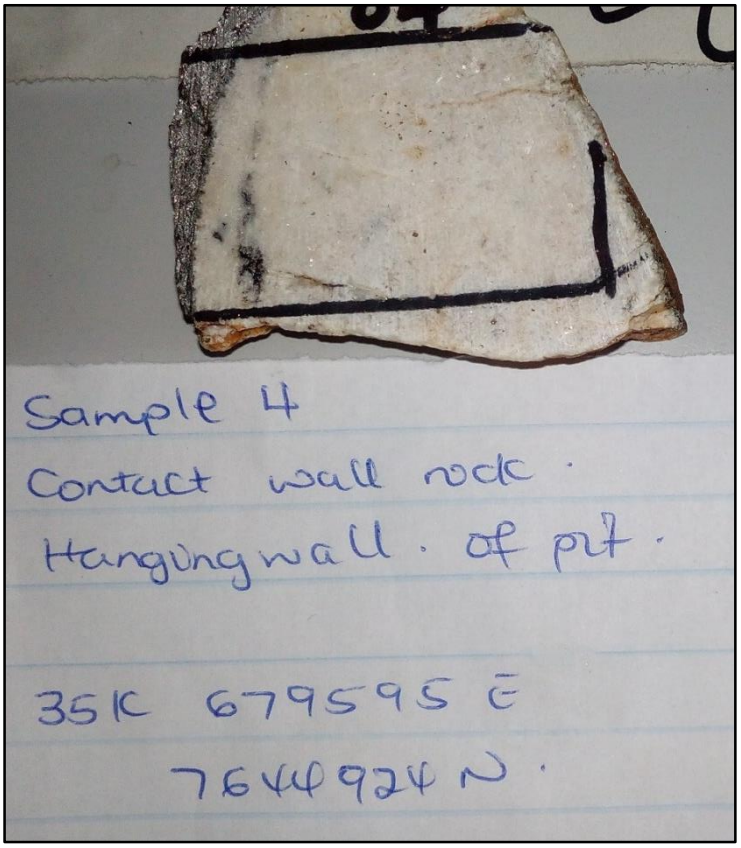


Figure B. 4: Sample number MB04.

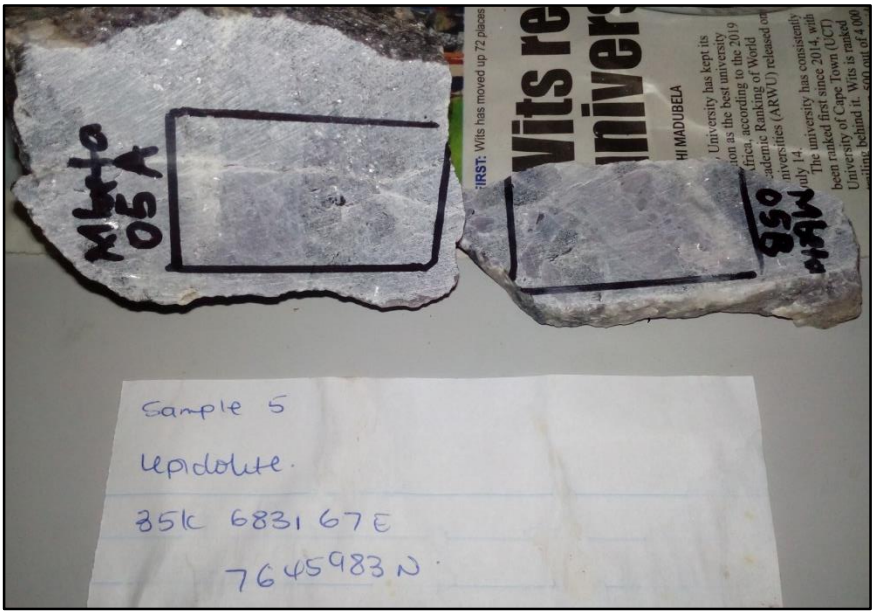


Figure B. 5: Sample number MB05A and MB05B.

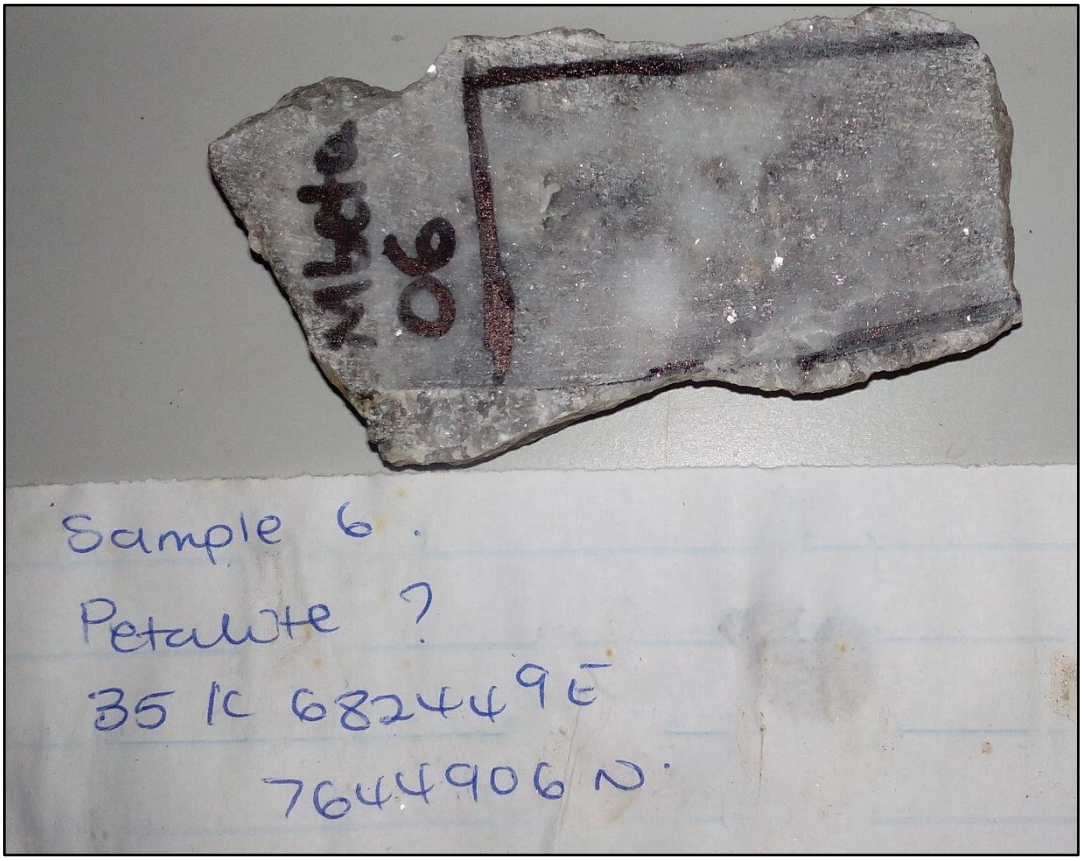


Figure B. 6: Sample number MB06.

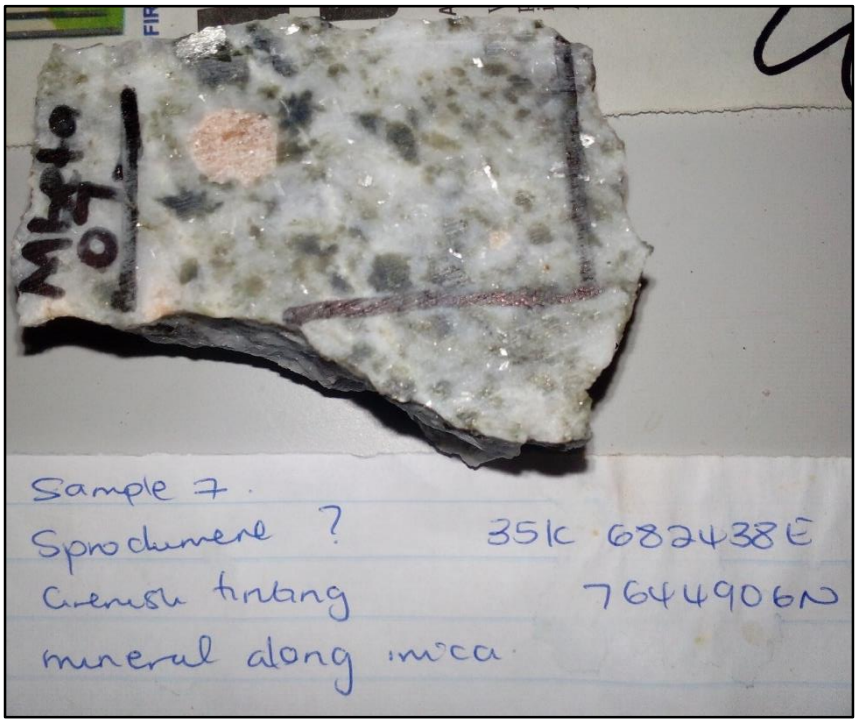


Figure B. 7: Sample number MB07.

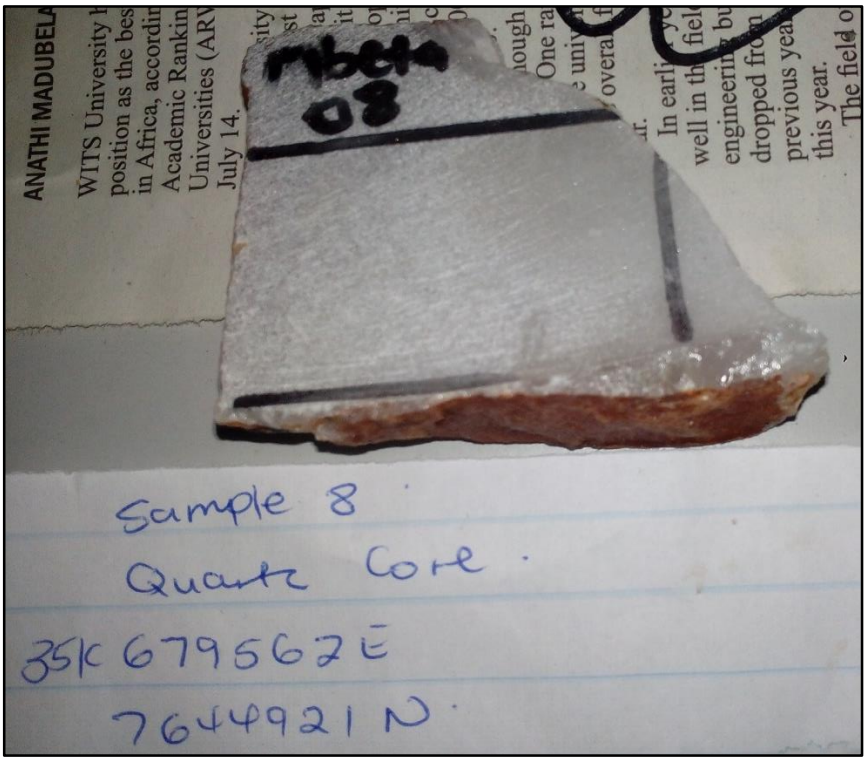


Figure B. 8: Sample number MB08.

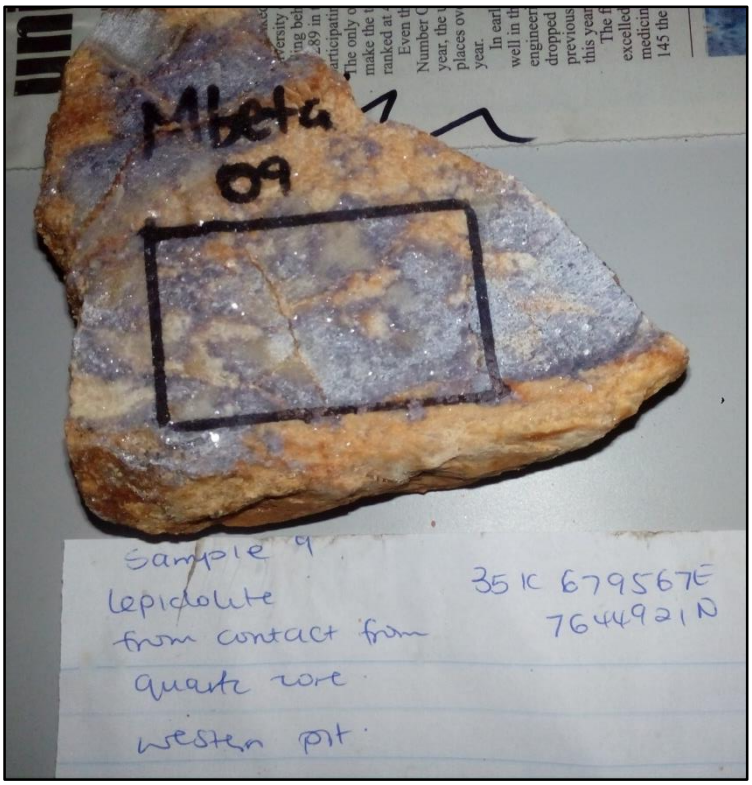


Figure B. 9: Sample number MB09.

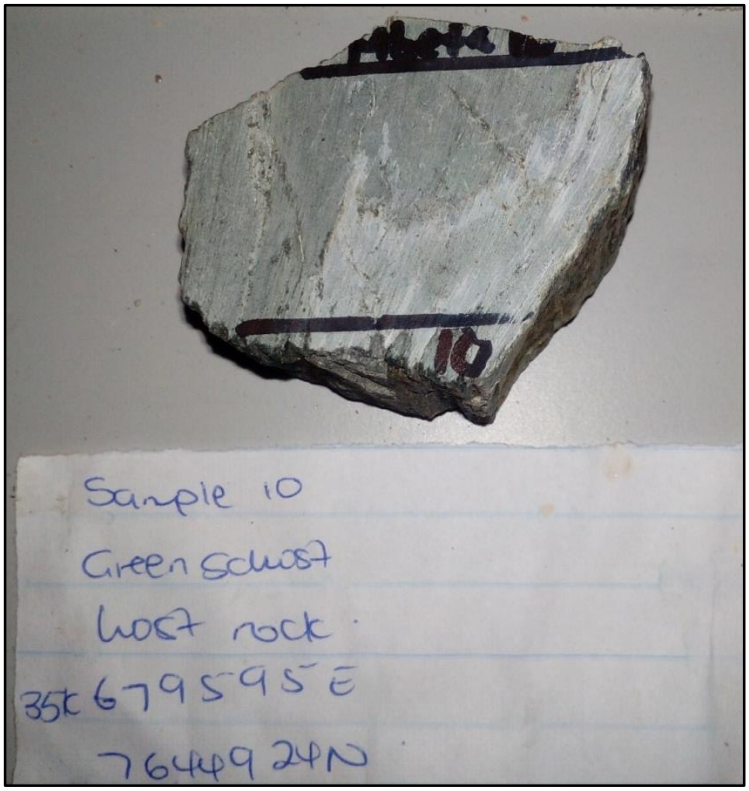


Figure B. 10: Sample number MB10.

APPENDIX C

THIN SECTIONS

This appendix shows the thin section images that were scanned using the Petrological microscope (Olympus BX 53m/DP 74) at the School of Geosciences at the University of the Witwatersrand, Johannesburg, South Africa.

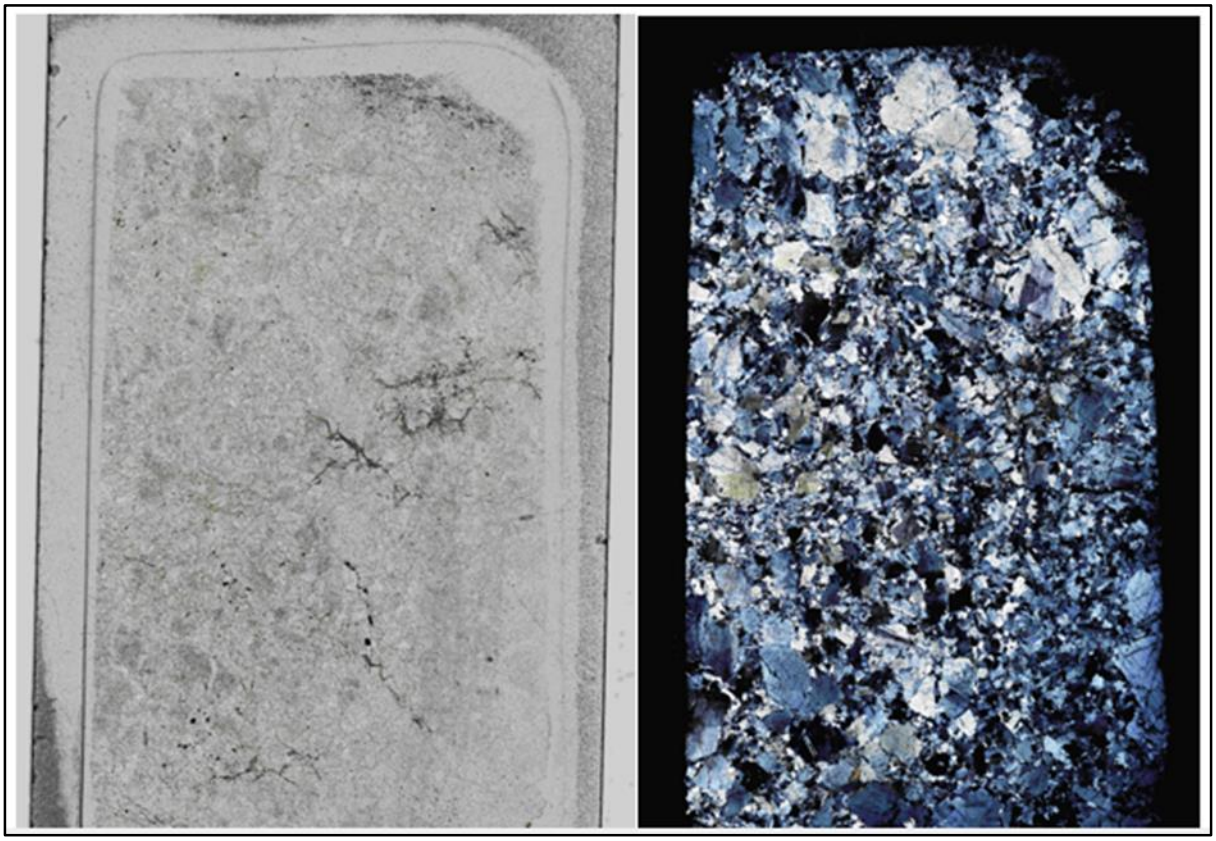


Figure C. 1: MB01 scanned image of the thin section in (PPL) plane polarised light to the left and (XPL) cross polarised light to the right.

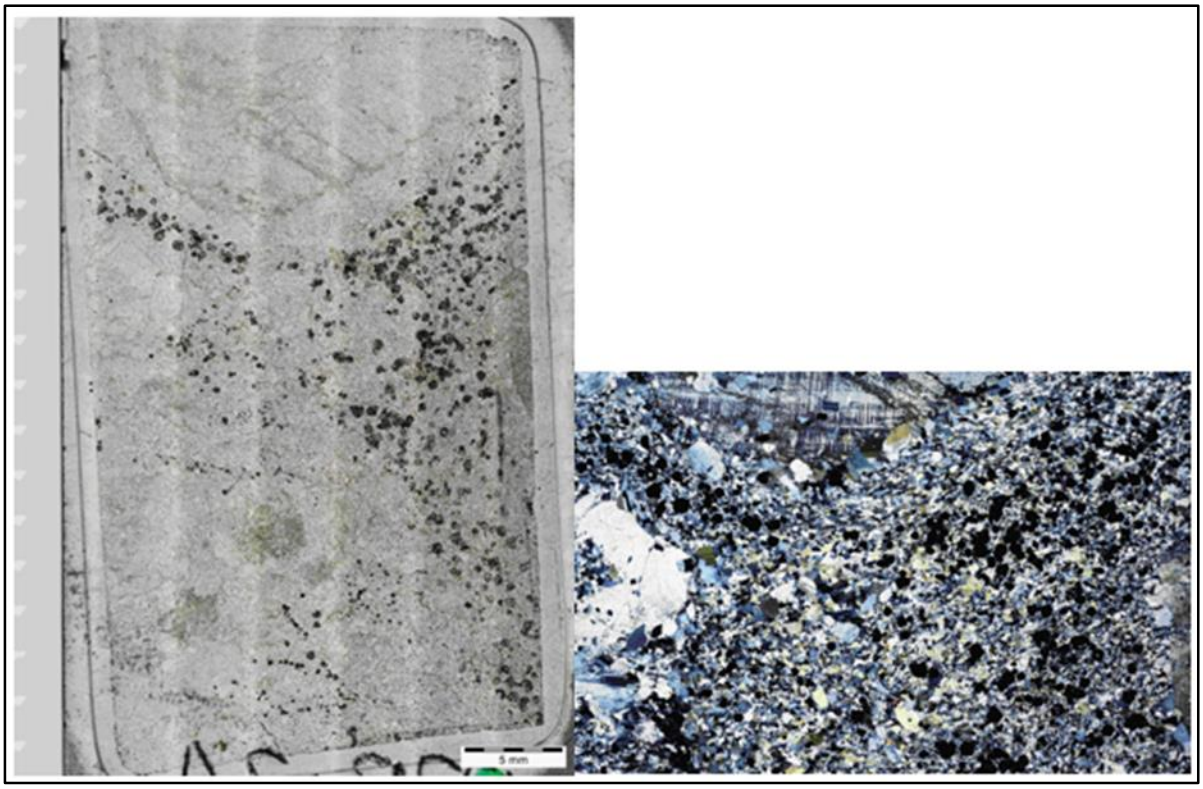


Figure C. 2: MB02A scanned image of the thin section in (PPL) plane polarised light to the left and (XPL) cross polarised light to the right.

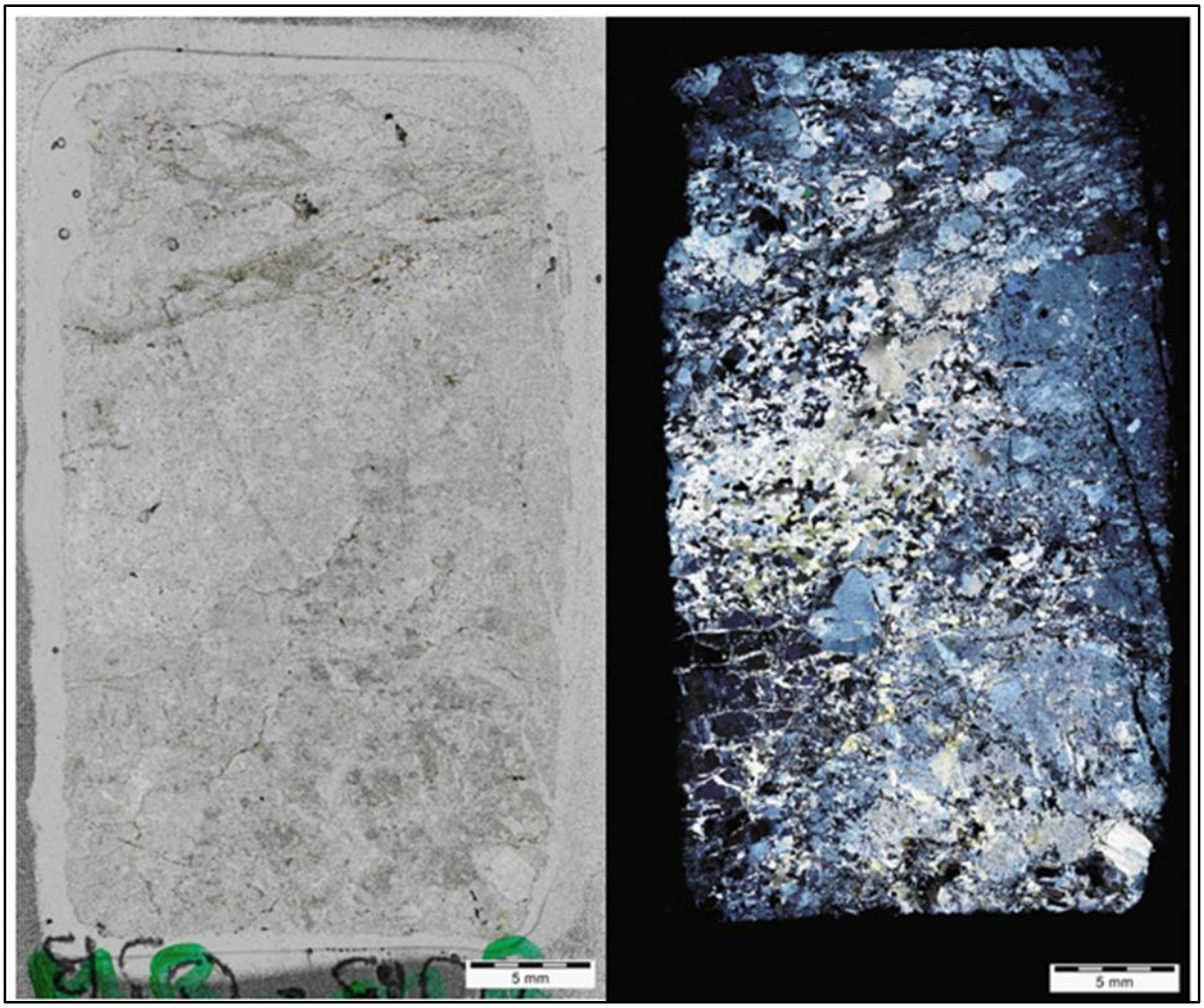


Figure C. 3: MB02B scanned image of the thin section in (PPL) plane polarised light to the left and (XPL) cross polarised light to the right.

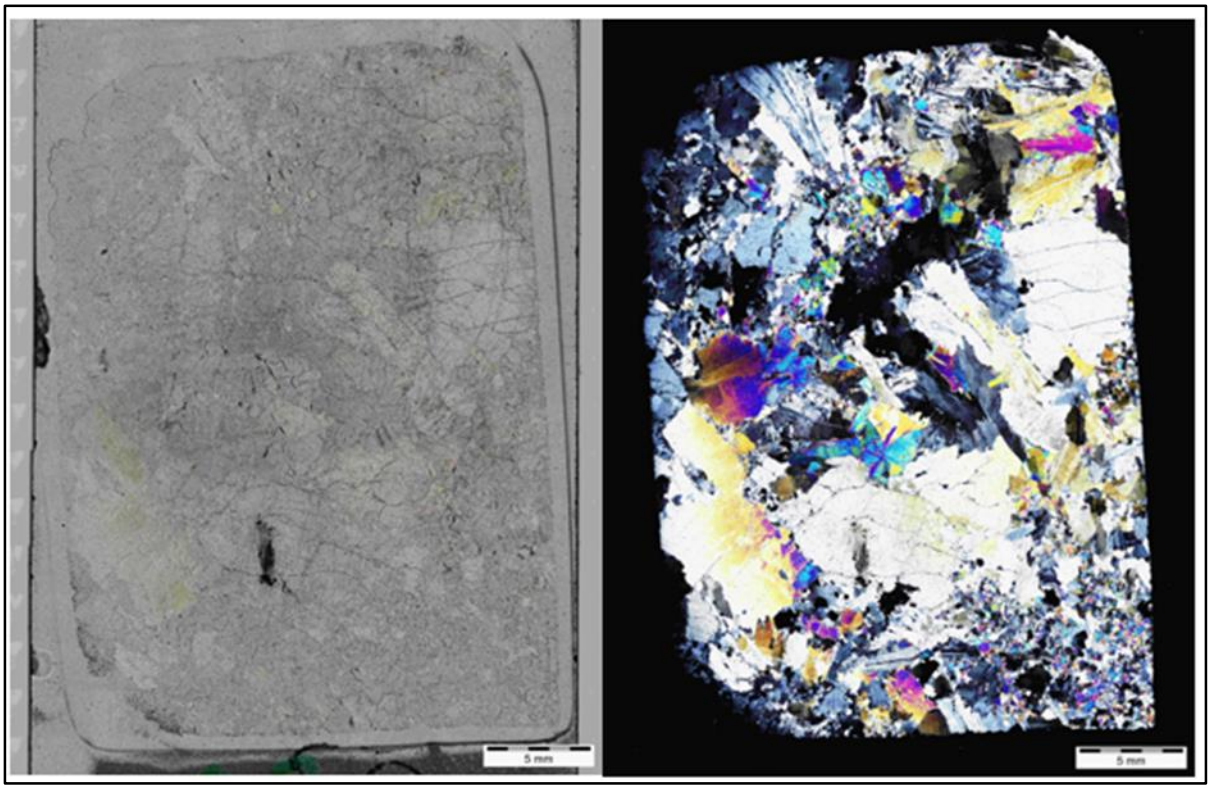


Figure C. 4: MB03 scanned image of the thin section in (PPL) plane polarised light to the left and (XPL) cross polarised light to the right.

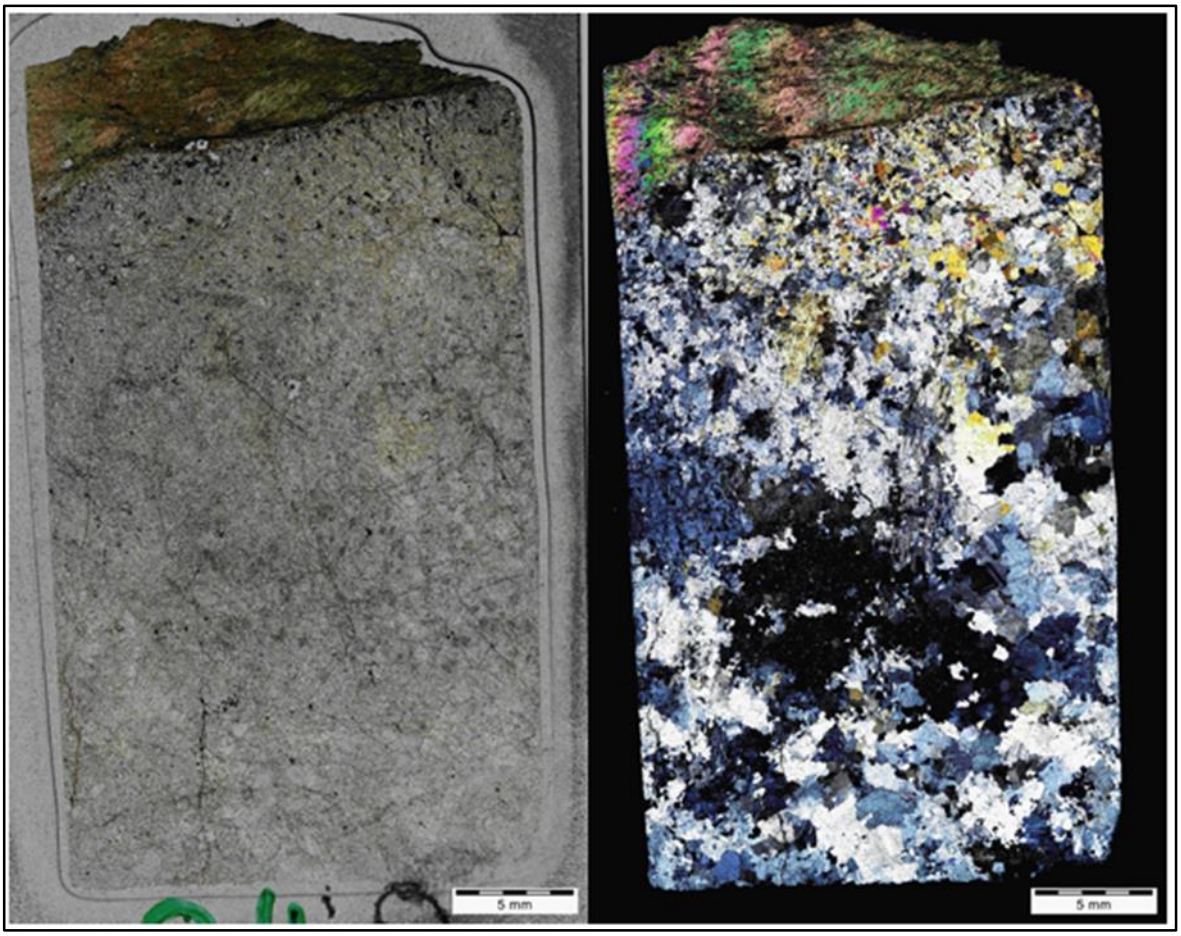


Figure C. 5: MB04 scanned image of the thin section in (PPL) plane polarised light to the left and (XPL) cross polarised light to the right.

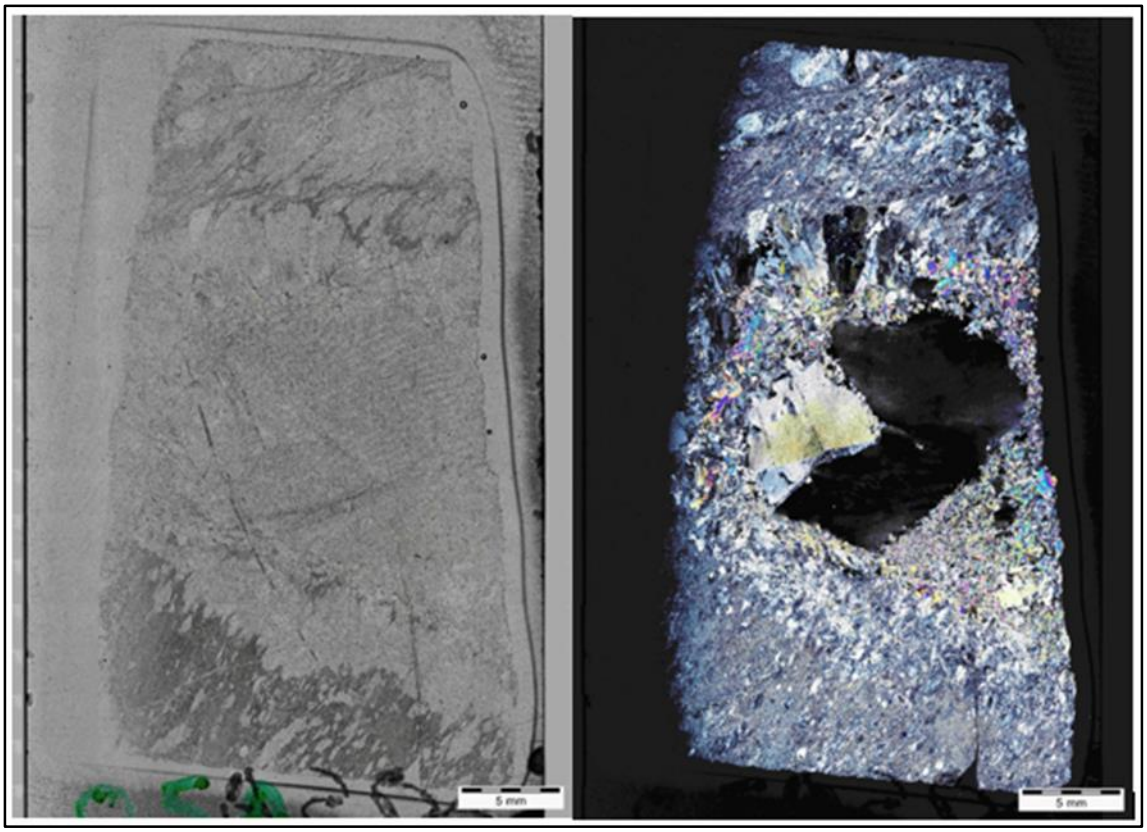


Figure C. 6: MB05A scanned image of the thin section in (PPL) plane polarised light to the left and (XPL) cross polarised light to the right.

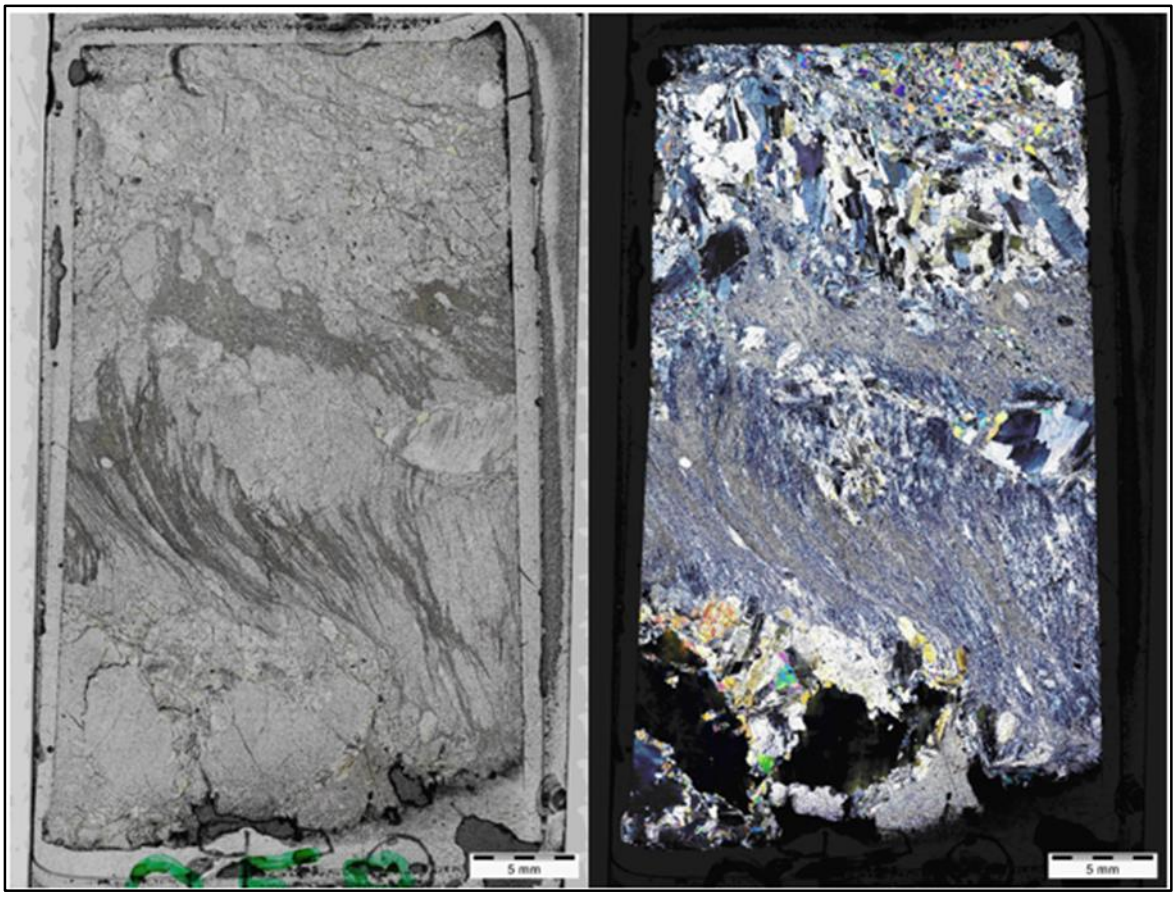


Figure C. 7: MB05B scanned image of the thin section in (PPL) plane polarised light to the left and (XPL) cross polarised light to the right.

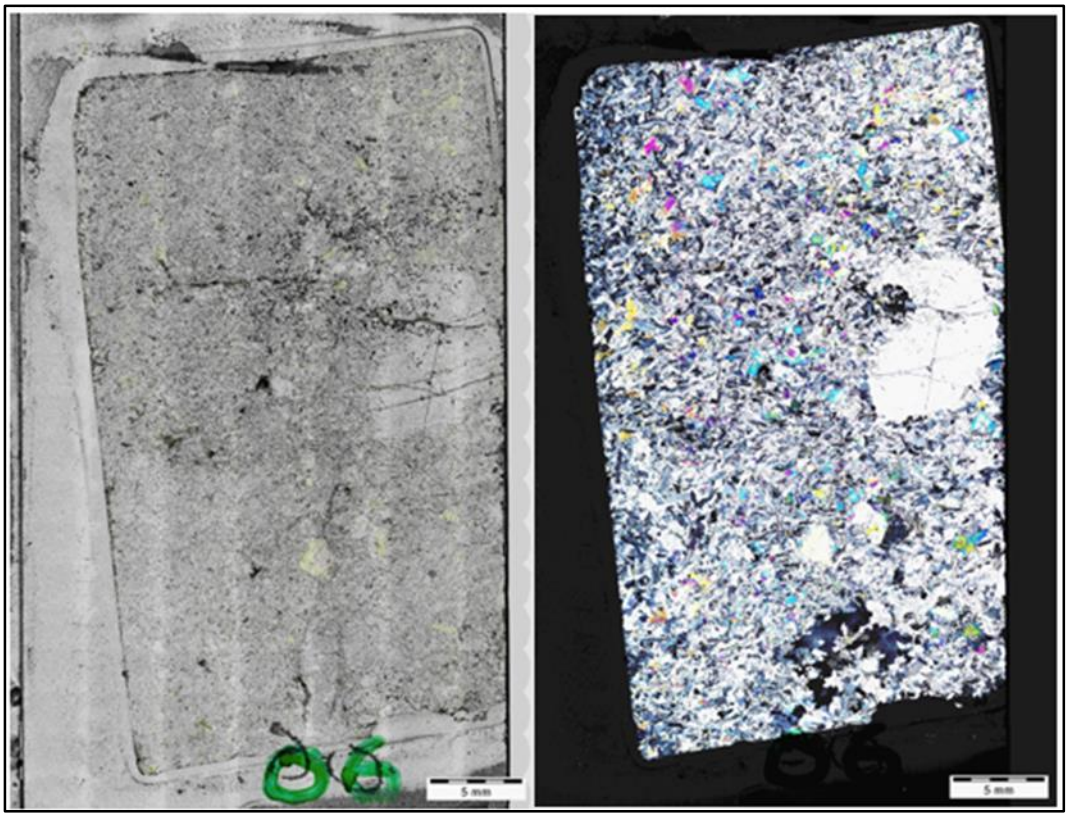


Figure C. 8: MB06 scanned image of the thin section in (PPL) plane polarised light to the left and (XPL) cross polarised light to the right.

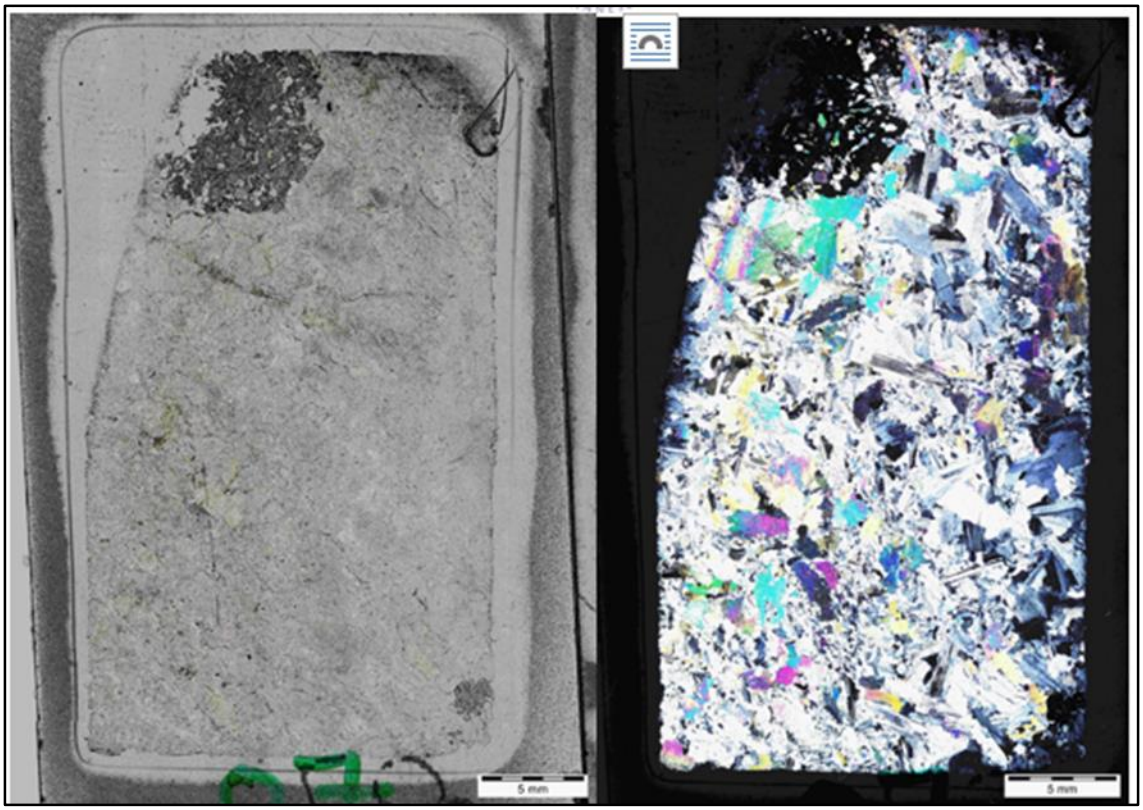


Figure C. 9: MB07 scanned image of the thin section in (PPL) plane polarised light to the left and (XPL) cross polarised light to the right.

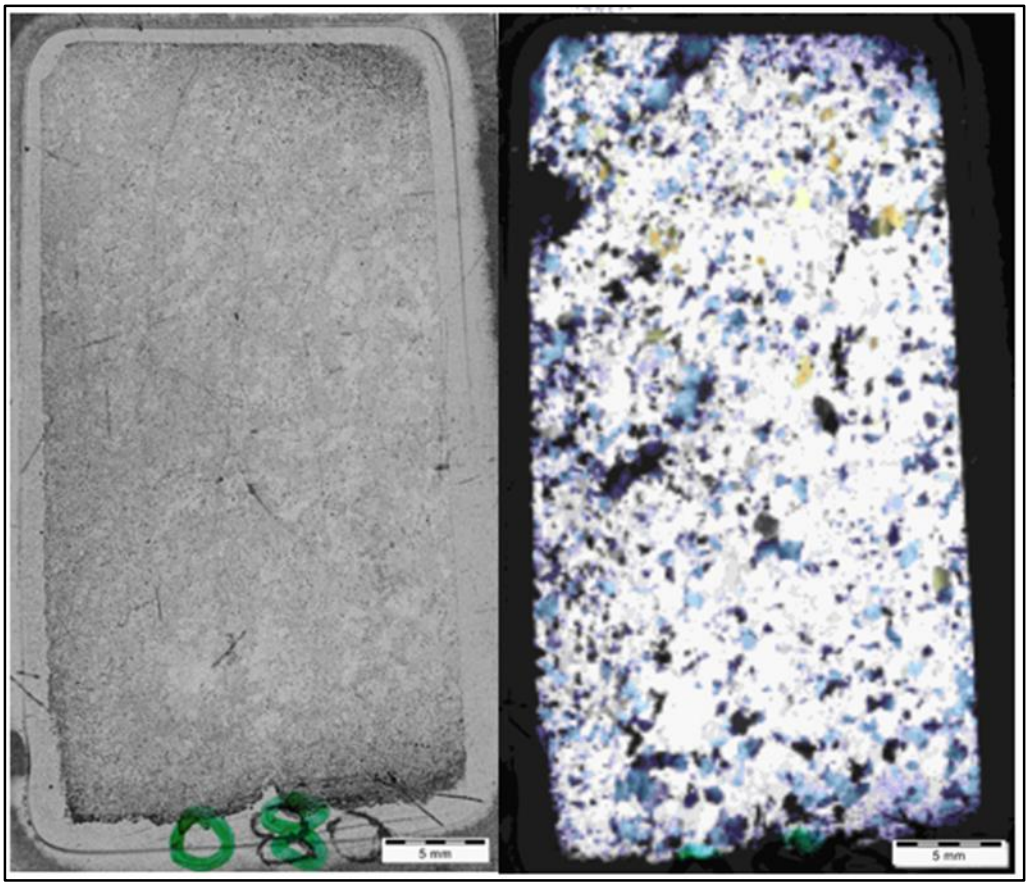


Figure C. 10: MB08 scanned image of the thin section in (PPL) plane polarised light to the left and (XPL) cross polarised light to the right.

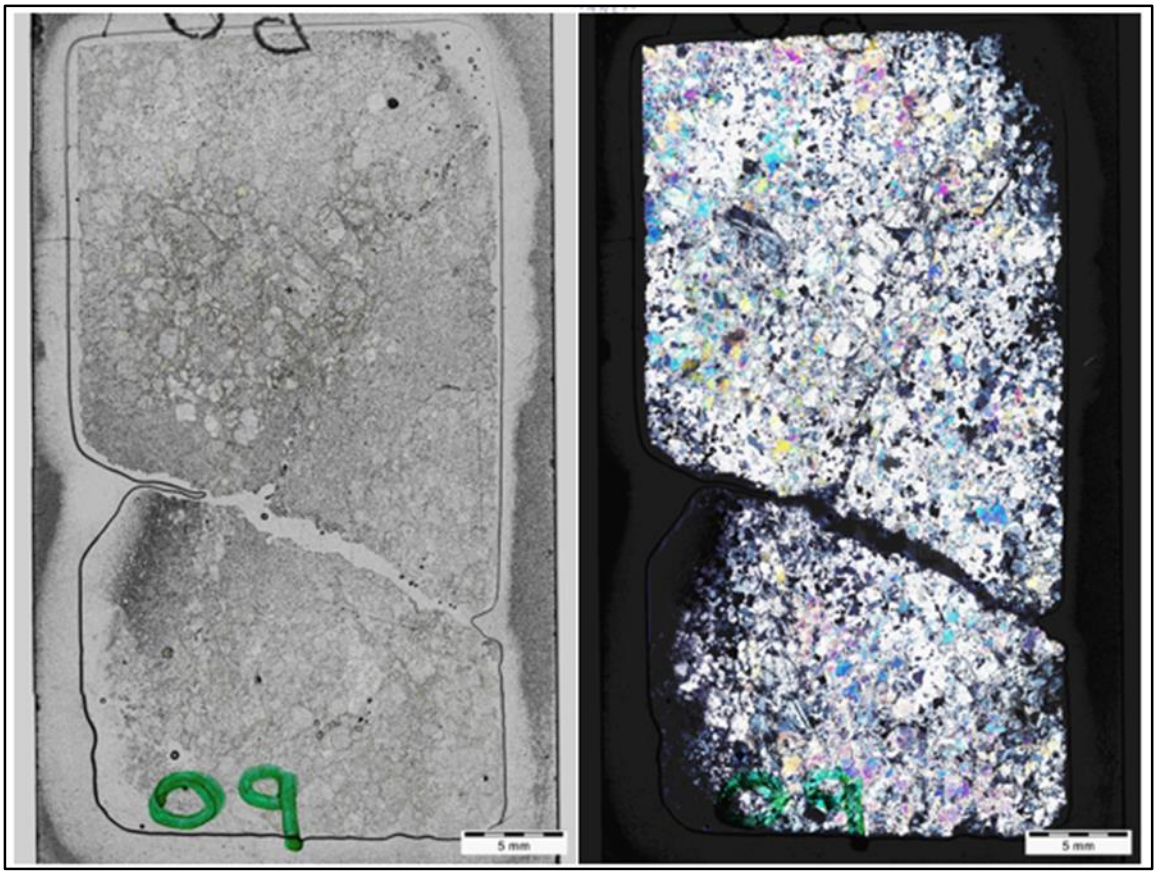


Figure C. 11: MB09 scanned image of the thin section in (PPL) plane polarised light to the left and (XPL) cross polarised light to the right.